

**University of Alberta**

High-Speed Ion Chromatography

by

Panos Hatsis

A thesis submitted to the Faculty of Graduate Studies and Research in partial fulfillment  
of the requirements for the degree of Doctor of Philosophy

Department of Chemistry

Edmonton, Alberta

Spring 2003

National Library  
of Canada

Acquisitions and  
Bibliographic Services

395 Wellington Street  
Ottawa ON K1A 0N4  
Canada

Bibliothèque nationale  
du Canada

Acquisitions et  
services bibliographiques

395, rue Wellington  
Ottawa ON K1A 0N4  
Canada

*Your file* *Votre référence*

*ISBN: 0-612-82114-5*

*Our file* *Notre référence*

*ISBN: 0-612-82114-5*

The author has granted a non-exclusive licence allowing the National Library of Canada to reproduce, loan, distribute or sell copies of this thesis in microform, paper or electronic formats.

The author retains ownership of the copyright in this thesis. Neither the thesis nor substantial extracts from it may be printed or otherwise reproduced without the author's permission.

L'auteur a accordé une licence non exclusive permettant à la Bibliothèque nationale du Canada de reproduire, prêter, distribuer ou vendre des copies de cette thèse sous la forme de microfiche/film, de reproduction sur papier ou sur format électronique.

L'auteur conserve la propriété du droit d'auteur qui protège cette thèse. Ni la thèse ni des extraits substantiels de celle-ci ne doivent être imprimés ou autrement reproduits sans son autorisation.

# Canada

**University of Alberta**

**Library Release Form**

**Name of Author:** Panos Hatsis

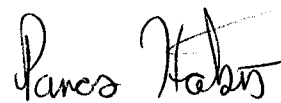
**Title of Thesis:** High-Speed Ion Chromatography

**Degree:** Doctor of Philosophy

**Year this Degree Granted:** 2003

Permission is hereby granted to the University of Alberta Library to reproduce single copies of this thesis and to lend or sell such copies for private, scholarly or scientific research purposes only.

The author reserves all other publication and other rights in association with the copyright in the thesis, and except as herein before provided, neither the thesis nor any substantial portion thereof may be printed or otherwise reproduced in any material form whatever without the author's prior written permission.



30 Vimy Ave.  
Halifax, Nova Scotia  
Canada B3M 1G6

03/12/2003  
Date

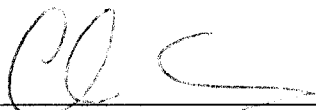
“Ἐν οἶδα ὅτι οὐδέν οἶδα”

Σωκράτης

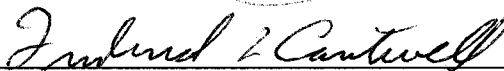
University of Alberta

Faculty of Graduate Studies and Research

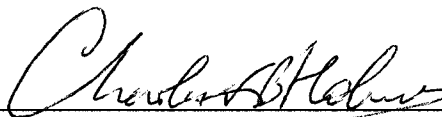
The undersigned certify that they have read, and recommend to the Faculty of Graduate Studies and Research for acceptance, a thesis entitled "High Speed Ion Chromatography" submitted by Panos Hatsis in partial fulfillment of the requirements for the degree of Doctor of Philosophy.



Supervisor, Dr. Charles Lucy, Dept. of Chemistry



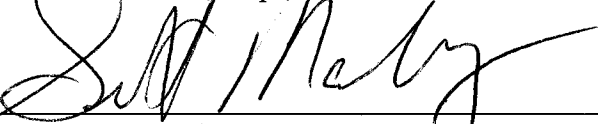
Dr. Frederick Cantwell, Dept. of Chemistry



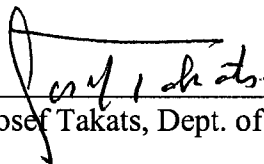
Dr. Charles Holmes, Dept. of Biochemistry



Dr. X. Chris Le, Dept. of Public Health Sciences



External Examiner, Dr. Scott Mabury,  
Dept. of Chemistry, University of Toronto



Dr. Josef Takats, Dept. of Chemistry

Mar 11/03

Date

This thesis is dedicated to my parents: John and Ipioni Hatsis.

## **ABSTRACT**

Ion chromatography (IC) is a method that has gained acceptance in industry for the separation and quantification of ions. Currently, analytical labs are faced with the challenge of increasing sample throughput. For this reason, high-speed separations are extremely sought after. This thesis investigates methods for reducing analysis time in IC. In particular, two approaches were examined: elevated temperature and monolithic columns.

IC separations are usually performed at room temperature, however, an increase in column temperature decreases eluent viscosity which in turn decreases the pressure necessary to achieve a given flow rate. Therefore, the flow rate can be further increased at elevated temperatures before the pressure maximum of the IC column is reached. However, elevated temperatures also affect the retention of ions. The first part of the thesis deals with the characterization and modeling of the effect of temperature on IC separations. It was found that increasing the column temperature results in significant changes in retention, and in particular, the retention of ions could decrease, increase or not be affected at all, depending on the type of stationary phase and eluent. These studies facilitated the implementation of elevated temperatures for high-speed cation separations. A 35% improvement in separation speed was obtained by operating at 60 °C for a mixture of lithium, sodium, ammonium, potassium, rubidium, cesium, magnesium, calcium and strontium.

Alternatively, high-speed IC can be performed with monolithic columns. Monolithic columns result in a much lower resistance to flow than columns packed with particles since they contain large channels for eluent flow. Therefore, high flow rates can

be used with modest pressure drops. Separations were performed on a reversed-phase monolith using either ion-interaction chromatography, or permanent coating of the monolith with a hydrophobic surfactant (didodecyldimethylammonium bromide, DDAB) to convert it into an ion exchanger. Both approaches resulted in the separation of anions in less than one minute, which represents about a ten-fold improvement in separation speed. Finally, this thesis shows that monoliths are better suited for high-speed IC than elevated temperature.



## **ACKNOWLEDGEMENTS**

I would like to thank Dr. Charles Lucy for his continual support and guidance throughout my graduate degree program. Past and present group members are also gratefully acknowledged for their help over the years, but especially Jeremy Melanson, Nicole Baryla, Mary Woodland and Chris Harrison who made my transition into a new research group as smooth as possible. I am grateful to Robert Bujalski and Dr. Frederick Cantwell for their many helpful discussions and equipment loans. I would like to express thanks to Jenny Chong for her patience and commitment in the lab that made my role as a supervisor enjoyable and rewarding. I am also indebted to the machine and electronics shops here at the University of Alberta for their technical support of my research. Finally, I would like to acknowledge Andy Szigety whose dream of high-speed ion analysis provided the impetus for this thesis.

This thesis research was supported by the Natural Sciences and Engineering Research Council of Canada, the University of Alberta, Dow Chemicals, Metrohm Ion Analysis and Dionex Corporation. Also, special thanks are in order for Ole Hindsgaul for loan of an HPLC system.

## TABLE OF CONTENTS

### CHAPTER ONE. Introduction

1.1	Motivation.....	1
1.2	Introduction to Chromatography.....	3
1.2.1	The Process of Separation.....	3
1.2.2	Basic Chromatographic Terms.....	5
1.2.3	Optimization of Separations.....	7
1.2.4	Band Broadening.....	8
1.2.4.1	van Deemter Equation.....	8
1.2.4.2	A-Term.....	9
1.2.4.3	B-Term.....	9
1.2.4.4	C-Term.....	11
1.2.4.5	The van Deemter Equation and Maximizing Efficiency.....	15
1.2.4.6	Extra-Column Band Broadening.....	17
1.3	Ion Chromatography.....	19
1.3.1	The Process of Ion-Exchange.....	19
1.3.2	General Instrumentation.....	20
1.3.2.1	Suppression.....	20
1.3.2.2	Conductivity Detection.....	23
1.3.2.3	Ultraviolet Absorbance Detection.....	27
1.3.3	Selectivity in IC.....	29
1.3.3.1	Importance of Selectivity.....	29
1.3.3.2	Properties of Analyte and Eluent Ion Affecting Selectivity.....	30
1.3.3.3	Effect of Mobile Phase on Selectivity.....	31
1.3.3.4	Effect of Stationary Phase of Selectivity.....	33
1.3.3.4.1	General Support Construct.....	33
1.3.3.4.2	Role of Column Material in Selectivity.....	35
1.3.3.4.3	Role of the Type of Ion Exchange Site in Selectivity.....	35
1.3.3.4.4	Role of the Structure of the Ion Exchange Site in Selectivity.....	36
1.3.4	Ion-Interaction Chromatography.....	37
1.4	Summary and Overview of Thesis.....	39
1.5	References.....	40

### CHAPTER TWO. Effect of Temperature on Retention and Selectivity in Ion Chromatography of Anions.

2.1	Introduction.....	43
2.2	Experimental.....	44

2.2.1	Apparatus.....	44
2.2.2	Reagents.....	45
2.2.3	Procedure.....	46
2.2.4	Calculations.....	47
2.3	Results and Discussion.....	48
2.3.1	Van't Hoff Plots.....	48
2.3.2	Effect of Eluent on Temperature Dependence of Retention.....	56
2.3.3	Effect of Stationary Phase on Temperature Dependence of Retention.....	58
2.3.4	Effect of Temperature on Selectivity.....	61
2.3.5	Changes in Efficiency and Peak Asymmetry as a Function of Temperature.....	66
2.3.6	Thermal Stability of Anion Exchangers.....	68
2.4	Conclusions.....	68
2.5	References.....	70

**CHAPTER THREE. Evaluation of Column Temperature as a Means to Alter the Selectivity Between Cations in Ion Chromatography**

3.1	Introduction.....	73
3.2	Experimental.....	74
3.2.1	Apparatus.....	74
3.2.2	Reagents.....	75
3.2.3	Procedure.....	75
3.2.4	Calculations.....	76
3.3	Results and Discussion.....	77
3.3.1	Van't Hoff Plots of Metals and Amines.....	77
3.3.2	Eluent Effects of Temperature Behaviour.....	84
3.3.3	Effect of Temperature on Selectivity.....	88
3.3.4	Effect of an Organic Modifier on Selectivity.....	92
3.3.5	Efficiency Improvements.....	94
3.4	Conclusions.....	97
3.5	References.....	98

**CHAPTER FOUR. High-Temperature High-Speed Ion Chromatography of Inorganic Cations**

4.1	Introduction.....	101
4.2	Experimental.....	103

4.2.1	Apparatus.....	103
4.2.2	Reagents.....	105
4.2.3	Procedure.....	106
4.3	Results and Discussion.....	107
4.3.1	Effect of Temperature on Retention.....	107
4.3.2	Eluent of Temperature on Viscosity and Column Backpressure.....	112
4.3.3	Band Broadening.....	113
4.3.4	Effect of Eluent Strength.....	120
4.4	Conclusions.....	126
4.5	References.....	127
<b>CHAPTER FIVE. Ultra-Fast Separation of Common Anions Using a Monolithic Stationary Phase</b>		
5.1	Introduction.....	130
5.2	Experimental.....	137
5.2.1	Apparatus.....	137
5.2.2	Reagents.....	137
5.2.3	Procedure.....	138
5.3	Results and Discussion.....	140
5.3.1	Stationary Phase Concerns.....	140
5.3.2	Eluent Conditions.....	140
5.3.3	Fast Anion Separations.....	143
5.3.4	Analysis of an Industrial Water Sample.....	147
5.3.5	Ultra-Fast Separations.....	149
5.4	Conclusions.....	152
5.5	References.....	152
<b>CHAPTER SIX. Improved Sensitivity and Characterization of High-Speed Ion Chromatography of Anions</b>		
6.1	Introduction.....	154
6.2	Experimental.....	155
6.2.1	Apparatus.....	155
6.2.2	Reagents.....	155
6.2.3	Coating Procedure.....	156
6.2.4	Band Broadening Studies.....	157
6.2.5	Calculations.....	157

6.3	Results and Discussion.....	159
6.3.1	Preparation of DDAB-Coated Column.....	159
6.3.2	Band Broadening from the Column.....	160
6.3.3	Band Broadening from Extra-Column Effects.....	167
6.3.4	High-Speed Separations.....	170
6.3.5	Stability and Reproducibility of the Coated Column.....	178
6.3.6	Validation of High-Speed IC.....	181
6.3.7	Considerations in High-Speed IC.....	181
6.4	Conclusions.....	183
6.5	References.....	185
 <b>CHAPTER SEVEN. Conclusions and Future Work</b>		
7.1	Conclusions.....	187
7.2	Future Work.....	188
7.2.1	Ultra-Fast Anion Separations with Polymeric Monoliths.....	188
7.2.2	Ultra-Fast Sample Preconcentration.....	190
7.2.3	Improved Implementation of Elevated Temperature for Selectivity Control in Anion Exchange.....	191
7.2.4	High Efficiency and Mass Spectrometric Compatible Separation of Amines.....	192
7.3	Future Directions.....	194
7.4	References.....	196
 <b>APPENDIX ONE.</b>		
	Peak-Fitting Program.....	198

## LIST OF TABLES

1-1.	Ions with useful UV absorbance.....	28
2-1.	Slopes, standard deviations, correlation coefficients and p-values from the van't Hoff plots of various anions.....	52
2-2.	Slopes, standard deviations, correlations coefficients and p-values from the van't Hoff plots of various organic compounds.....	55
2-3.	Slopes of van't Hoff plots for anions separated using different eluents.....	57
2-4.	Changes in the slopes of the van't Hoff plots of anions caused by an increase in eluent concentration.....	59
2-5.	Comparison of the slopes of van't Hoff plots on Dionex AS11 and AS14 columns.....	60
2-6.	Groups of anions showing similar temperature behaviour.....	63
2-7.	The effect of temperature on peak asymmetry and plate number.....	67
3-1.	Slopes, standard deviations, correlation coefficients and p-values from the van't Hoff plots of the alkali and alkaline earth metals.....	80
3-2.	Slopes, standard deviations, correlation coefficients and p-values from the van't Hoff plots of amines.....	82
3-3.	Effect of eluent concentration on the slope of a van't Hoff plot.....	85
3-4.	Effect of sulfuric acid eluent on the slope of a van't Hoff plot.....	86
3-5.	The effect of temperature on peak asymmetry and efficiency of metals and amines.....	96
4-1.	van't Hoff temperature dependencies for cation exchange retention.....	109
4-2.	van Deemter parameters for sodium, potassium and magnesium at 27 and 60 °C.....	117
4-3.	Regression parameters for the effect of eluent strength on retention.....	124
5-1.	Detection limits for common anions using direct conductivity and indirect conductivity detection.....	145
5-2.	Comparison of levels of anions determined by two different methods.....	148
6-1.	Capacity of the DDAB-coated column as a function of the amount of acetonitrile present in the coating solution.....	162
6-2.	van Deemter equation coefficients for iodate, phosphate and sulfate.....	166
6-3.	Detection limits achieved with suppressed and direct (non-suppressed) conductivity detection.....	176
6-4.	Comparison of concentrations of anions determined by conventional and high-speed IC.....	182

## LIST OF FIGURES

1-1.	Diagrammatic representation of the non-uniform flow pattern.....	10
1-2.	Band broadening caused by slow equilibration between mobile and stationary phase.....	12
1-3.	A van Deemter plot.....	16
1-4.	Schematic of IC instrumentation.....	21
1-5.	A membrane suppressor for anion exchange separations.....	24
1-6.	Schematic representation of a pellicular particle for IC.....	34
1-7.	Diagrammatic representation of IIC.....	38
2-1.	van't Hoff plots for anions separated on a Dionex AS11 column.....	50
2-2.	van't Hoff plots for anions separated on a Dionex AS14 column.....	51
2-3.	van't Hoff plots for organic compounds separated on a reversed phase C <sub>18</sub> column.....	53
2-4.	Changes in selectivity caused by increased temperature.....	64
2-5.	Elution order changes caused by increased temperature.....	65
2-6.	Degradation pathways of anion exchangers at elevated temperatures and basic solution.....	69
3-1.	van't Hoff plots for alkali and alkaline earth metals separated on a Dionex CS12A column.....	79
3-2.	van't Hoff plots for amines separated on a Dionex CS12A column.....	81
3-3.	van't Hoff plots of metals and amines showing selectivity changes caused by temperature.....	89
3-4.	Changes in selectivity of cation separations caused by increased temperature.....	91
3-5.	Effect of acetonitrile on the selectivity of a separation of metals and amines..	93
3-6.	Scatter plot showing differences in selectivity caused by acetonitrile and temperature.....	95
4-1.	Modifications to a typical IC system for performing high temperature high-speed IC.....	104
4-2.	van't Hoff plot of cations.....	108
4-3.	Separation of nine cations at 27 and 60 °C.....	110
4-4.	High-speed separation of nine cations.....	114
4-5.	van Deemter plots of sodium potassium and magnesium at 27 and 60 °C.....	115
4-6.	Diagrammatic representation of thermal mismatch band broadening.....	118
4-7.	Effect of split ratio on efficiency of separation.....	121
4-8.	Plots of log k vs. log[MSA].....	123
4-9.	High-speed separation of 6 common cations.....	125
5-1.	The fabrication process of silica monoliths.....	132
5-2.	A silica monolith compared to silica particles.....	133
5-3.	Macroporous and mesoporous structure of a monolith.....	134
5-4.	Pressure vs. linear velocity for various columns.....	136
5-5.	Plot of plate height (H) vs. flow rate for nitrate on a monolithic column.....	141
5-6.	One-minute separation of common anions.....	144
5-7.	Calibration curve and sensitivity plot for sulfate using conductivity detection	146
5-8.	Separation of common anions in 30 and 15 seconds.....	150

6-1.	Breakthrough curve of DDAB on the monolith.....	161
6-2.	Effect of column capacity on the separation of anions.....	163
6-3.	van Deemter curves for iodate, phosphate and sulfate.....	165
6-4.	Effect of splitting on efficiency.....	172
6-5.	High-speed separation of seven anions.....	174
6-6.	Calibration curve and sensitivity plot for chloride using suppressed conductivity detection.....	177
6-7.	Calibration curve and sensitivity plot for chloride using non-suppressed conductivity detection.....	179
6-8.	Long-term stability of DDAB-coated column.....	180
6-9.	Thirty-second separation of seven anions.....	184



## LIST OF SYMBOLS AND ABBREVIATIONS

Symbol	Parameter
$A^-$	Analyte anion
$A^+$	Analyte cation
$A_s$	Asymmetry factor
$b$	Path length
$B_o$	Specific permeability
$C_A$	Concentration of analyte A
$C_{A^-}$	Concentration of analyte $A^-$
Cap	Stationary phase capacity
$C_{DDAB}$	Concentration of DDAB
CE	Capillary electrophoresis
$C_{i,M}$	Concentration of i in the mobile phase
$C_{i,S}$	Concentration of i in the stationary phase
Const	Constant of arbitrary value
D	Diffusion coefficient
DDAB	Didodecyldimethylammonium bromide
De	Dean number
$D_M$	Diffusion coefficient in mobile phase
$d_p$	Particle diameter
$E^-$	Eluent anion
$E^+$	Eluent cation
EMG	Exponentially modified gaussian function

erf()	Error function
ESI-MS	Electrospray ionization mass spectrometry
exp	Exponential function
f	Porosity
F	Flow Rate
H	Plate height
h	Peak height
HPLC	High performance liquid chromatography
i.d.	Internal diameter
IC	Ion chromatography
IIC	Ion interaction chromatography
IIR	Ion interaction reagent
$i_M$	Component i in the mobile phase
$i_S$	Component i in the stationary phase
k	Retention factor
K	Cell constant
$K_{A,B}$	Ion exchange selectivity constant for ion A over ion B
$K_{A,E}$	Ion exchange selectivity constant for ion A over ion E
$k_B$	Boltzmann constant
$k_i$	Retention factor of component i
$k_j$	Retention factor of component j
$K_{sp}$	Solubility product constant
$k_T$	Retention factor in connecting tubing

$L_C$	Length of column
$L_T$	Length of tubing
MSA	Methanesulfonic acid
N	Efficiency
n	Number of data points
$n_{i,M}$	Moles of i in the mobile phase
$n_{i,S}$	Moles of i in the stationary phase
$P^+$	Pairing ion or ion interaction reagent
PEEK	Polyetheretherketone
$pK_a$	Negative logarithm of the acid dissociation constant
Q	Reaction quotient
R	Universal gas constant
$R^-$	Cation exchanger
$R^+$	Anion exchanger
$r^2$	Correlation coefficient
$r_C$	Radius of the column
Re	Reynolds number
$r_h$	Hydrodynamic radius
RPLC	Reversed-phase liquid chromatography
$R_s$	Resolution
RSD	Relative standard deviation
$r_T$	Radius of connecting tubing
Sc	Schmidt number

$t$	Time
$T$	Temperature
$t_b$	Breakthrough time
$t_D$	Desorption time
$t_{ex}$	Extra-column time
$t_g$	Centroid of a Gaussian function
$t_o$	Void time
$t_r$	Retention time
$u$	Linear velocity
UV	Ultraviolet
$V_{Cell}$	Detector cell volume
$V_{inj}$	Injection volume
$V_M$	Volume of mobile phase
$w$	Baseline width of a peak
$W_s$	Weight of stationary phase
$x$	Charge of analyte ion
$y$	Charge of eluent ion
$z_A$	Charge of ion A (arbitrary magnitude)
$z_B$	Charge of ion B (arbitrary magnitude)
$\Delta A$	Change in absorbance
$\Delta G$	Change in conductance
$\Delta H$	Enthalpy of retention/ion exchange
$\Delta P$	Pressure drop

$\Phi$	Phase ratio
$\Pi$	Swelling Pressure
$\alpha_{A,B}$	Selectivity factor between ion A and ion B
$\alpha_{i,j}$	Selectivity factor between i and j
$\chi$	Ratio of tubing inner radius to coil radius
$\varepsilon_b$	External porosity of a packed bed
$\varepsilon_{EY^-}$	Molar absorptivity of eluent ion
$\gamma_o$	Obstruction factor
$\gamma_t$	Tortuosity factor
$\eta$	Viscosity
$\kappa_i$	Distribution coefficient of component i
$\lambda_A^-$	Ionic equivalent conductivity of analyte anion
$\lambda_E^+$	Ionic equivalent conductivity of eluent cation
$\lambda_E^-$	Ionic equivalent conductivity of eluent anion
$v_A^*$	Molar solvated volume of ion A
$v_B^*$	Molar solvated volume of ion B
$\theta_A$	Degree of dissociation of analyte
$\theta_E$	Degree of dissociation of eluent
$\rho$	Density
$\sigma$	Standard deviation
$\sigma^2_{V,cell}$	Variance due to detector cell volume
$\sigma^2_{V,inj}$	Variance due to injection volume

$\sigma^2_{V,R}$	Variance due to detector response time
$\sigma^2_{V,T}$	Variance due to connecting tubing
$\sigma^2_{X,i}$	Variance of component i in distance units
$\tau$	Exponential time constant
$\omega_A$	Packing factor (A-term)
$\omega_C$	Packing factor (C-term)

## CHAPTER ONE. Introduction\*

### 1.1 Motivation

Ion chromatography (IC) refers to the separation and determination of trace ions using highly efficient methods based upon ion exchange resins. The beginnings of IC can be traced back to the seminal work of Hamish Small and co-workers in 1975.<sup>1</sup> They demonstrated the determination of parts-per-million anions and cations at a rate of 1-3 ions per minute. Since 1975, there have been continuous advances in the technique, with respect to separation speed, detection limits and separation selectivity. Currently, the mainstay of IC is the determination of inorganic anions and is most commonly employed for the parts-per-billion determination of the seven common inorganic anions (fluoride, chloride, nitrite, bromide, nitrate, phosphate and sulfate). IC has also found widespread use for the determination of carboxylic acids, the six common cations (lithium, sodium, ammonium, potassium, magnesium and calcium) and small amines.

The objective of IC, as with any analytical technique, is to provide the user with information on the system of interest. For example, in an industrial setting, chemical analyses are routinely performed for the control and optimization of chemical processes, as well as for monitoring product quality and plant effluents.<sup>2,3</sup> However, most analyses are performed in a laboratory far-removed from the processing site. This means that there is a delay between when a sample is taken for analysis and when the results of the analysis are known. Therefore, it is difficult to ensure that the plant is *constantly* operating under established limits. In light of this, there is an increasing emphasis on

---

\* A version of this chapter has been submitted for publication. Lucy, C.A.; Hatsis, P. "Ion Chromatography", in *Chromatography*, 6th ed., E. Heftmann, Ed., Elsevier. Chapter 4 of Fundamentals, submitted October 1, 2002.

real-time monitoring of chemical processes in industry.<sup>4, 5</sup> Real-time monitoring requires continuous measurements and as such has been restricted to those analytical techniques/instruments that have fast analysis response times, *e.g.*, pH electrodes, infrared absorption spectroscopy and gas chromatography to name a few.<sup>2</sup>

The prospect of performing real-time measurements with IC is a very attractive one. Everyday, a number of industries, *e.g.*, power, environmental, food and beverage, electronics, petrochemical, rely on IC for the separation and analysis of ions in a wide range of matrices.<sup>6-10</sup> Real-time monitoring (or at least higher sample throughput in the lab) would mean increased operating efficiency, lower costs and ultimately larger profits.<sup>3</sup>

The impediment in realizing this goal is that IC separations are usually performed in about 10 minutes. This is too slow for continuous monitoring of many processes, which have time constants on the order of minutes.<sup>11</sup> Therefore for IC to be useful for real-time monitoring, it is necessary to significantly reduce the time it takes to perform separations of ions. Surprisingly, fast inorganic ion separations (< 1 min) received little attention before the pioneering work of Connolly and Paull.<sup>12-14</sup> In this thesis, possibilities for fast IC separations are further explored and expanded upon. In particular, two novel approaches are examined as a means to achieve this goal: the use of above-ambient temperatures during separation and the use of monolithic stationary phases.



## **1.2 Introduction to Chromatography**

### **1.2.1 The Process of Separation<sup>15,16</sup>**

In a broad sense, analytical chemistry is concerned with the development of methods for determining the chemical composition of samples of matter. However, samples are often exceedingly complex in terms of the number and variety of chemical species present. This makes the determination of the analyte a daunting task. It is for this reason that analysis usually involves the separation of a sample into its components to greatly facilitate the determination of the analyte. Chromatography is the name given to a group of techniques that allow the separation of samples into individual components. In all chromatographic techniques, the sample is transported by a mobile phase through an immiscible stationary phase. Separation is achieved based on the distribution of sample components between the mobile and stationary phases. A component that spends most of its time in the stationary phase is said to be strongly retained and will be washed off (or eluted from) the column by the mobile phase (or eluent) at a slower rate than a component that is weakly retained. In other words, components of a sample are separated based on their different speeds of migration through the column. The underlying process behind chromatography is thermodynamic in nature. Unfortunately, there exists a second phenomenon in chromatography that serves to degrade the separation between two components. This is the broadening of zones containing each component during the separation. This process is non-equilibrium in nature and is irreversible. However, the rate of zone broadening is slower than the rate of separation so that chromatography can achieve separations. These phenomena will be discussed in Sections 1.2.2 and 1.2.4.

At this point it should be mentioned that this thesis is entirely concerned with liquid chromatographic techniques, and more specifically, high performance liquid chromatographic (HPLC) techniques. HPLC is characterized by the use of columns packed with small diameter (3 –15  $\mu\text{m}$ ) stationary phase particles. The presence of tightly packed small particles creates a huge resistance to flow, so that a high-pressure pump is needed to drive the mobile phase through the column. However, HPLC offers more efficient separations than conventional column liquid chromatographic techniques.

There are different modes of HPLC, but the one that will be dealt with exclusively in this thesis is IC. IC can be thought of as the adaptation of conventional ion exchange methods to HPLC format, *i.e.*, small particles and high pressure. IC will be discussed in detail in Section 1.3. Another mode of HPLC is reversed-phase liquid chromatography (RPLC). Currently, most of the chromatography performed in the world is RPLC. Consequently, a fair amount of the literature cited in this thesis is in the area of RPLC and frequent comparisons are made between IC and RPLC. A detailed discussion of RPLC is not presented, however there exist numerous textbooks on the subject.<sup>17-19</sup> Suffice it to say that the stationary phase in RPLC is hydrophobic, and the mobile phase is relatively polar. Typically,  $\text{C}_{18}$  (octadecyl) chains bonded to silica are used as the stationary phase in RPLC. The mobile phase is usually water with a certain percentage of an organic modifier (*e.g.*, methanol, acetonitrile, tetrahydrofuran). RPLC is used for the separation of hydrophobic and slightly polar compounds. The higher the hydrophobicity of a compound the more strongly it is retained. Retention in RPLC is moderated through an increase in the percentage of organic modifier in the eluent.

### 1.2.2 Basic Chromatographic Terms<sup>15, 16</sup>

The distribution of a sample component,  $i$ , between the mobile (M) and stationary phase (S) can be depicted as:

$$i_M \rightleftharpoons i_S \quad (1-1)$$

The equilibrium constant for this process is known as the distribution coefficient,  $\kappa_i$ , and is simply:

$$\kappa_i = \frac{C_{i,S}}{C_{i,M}} \quad (1-2)$$

where  $C_{i,S}$  and  $C_{i,M}$  are the concentrations of component  $i$  in the stationary and mobile phases, respectively. However, chromatographers use the retention factor,  $k_i$ , to describe the ratio of the amount of  $i$  in the stationary phase to the amount in the mobile phase.

The relationship between the retention factor and distribution coefficient is:

$$k_i = \frac{n_{i,S}}{n_{i,M}} = \kappa_i \Phi = \kappa_i \frac{W_S}{V_M} \quad (1-3)$$

where  $n$  represents the moles of component  $i$ ,  $W_S$  is the weight of stationary phase and  $V_M$  is the volume of mobile phase. Since the weight of stationary phase is difficult to determine once a column is packed, it is more convenient to express the retention factor as:

$$k_i = \frac{t_r - t_o}{t_o} \quad (1-4)$$

where  $t_r$  is the retention time of a component and is the time between injection onto the column and elution, and  $t_o$  is the time for a completely unretained component to exit the column (*i.e.*,  $\kappa_i = 0$ ). These values are easily determined from the chromatogram after the separation is completed.

Chromatographers are concerned with the extent of separation between two components  $i$  and  $j$ , and this can be quantified by means of the selectivity factor,  $\alpha_{i,j}$ , given by the equation:

$$\alpha_{i,j} = \frac{k_j}{k_i} \quad (1-5)$$

However, the actual extent of disengagement does not only depend on the degree of separation between the zones, but also on their width, *i.e.*, the broadening of zones mentioned above. Chromatographers use the resolution between two components,  $R_s$ , as a measure of the degree of separation. The resolution between components  $i$  and  $j$  can be determined from a chromatogram with the help of the equation:

$$R_s = \frac{2\Delta t_r}{(w_1 + w_2)} \quad (1-6)$$

where  $\Delta t_r$  is the difference in retention time between the two components and  $w$  is the width at baseline of each component zone. In chromatography, component zones are observed to be approximately Gaussian in shape. Gaussian curves are conveniently described in terms of their standard deviation,  $\sigma$ . As a component zone travels down the column it broadens such that its standard deviation gets progressively larger. The extent of band broadening can be expressed with the plate height,  $H$ :

$$H = \frac{\sigma_{X,i}^2}{L_C} \quad (1-7)$$

In other words, the plate height expresses the amount of variance ( $\sigma_{X,i}^2$ ) produced per unit length of the column,  $L_C$ . The tendency of a particular column to produce band broadening is expressed in terms of the efficiency,  $N$ :

$$N = \frac{L_c}{H} \quad (1-8)$$

The larger the efficiency, the less peaks broaden while they are in the column and the easier it is to achieve a separation.

### 1.2.3 Optimization of Separations<sup>15, 16</sup>

In order to optimize the separation of a sample into its components, a chromatographer has to take into account the distribution equilibria (*i.e.*,  $k$  and  $\alpha$ ) as well as the tendency of component zones to broaden as they travel down the column (*i.e.*,  $N$ ). In this way, control of the resolution between component zones is achieved. An expression that gives the dependence of  $N$ ,  $k$  and  $\alpha$  on resolution is:

$$R_s = \frac{\sqrt{N}}{4} \frac{\alpha_{j,i} - 1}{\alpha_{j,i}} \frac{k_j}{k_j + 1} \quad (1-9)$$

Equation 1-9 shows that there are three factors that affect the resolution of component zones in chromatography: the efficiency of the column, the selectivity and the retention. Firstly, the effect of retention will be examined. Equation 1-9 states that no resolution will be obtained if there is no retention. However, the retention term in Equation 1-9 has a limiting value of 1, which is almost reached when  $k = 10$ . Therefore, there is little to be gained by increasing the retention factor past 10. Secondly, the efficiency term in Equation 1-9 has a square root dependence. This means that if the efficiency is quadrupled, the resolution will only improve by a factor of two. Efficiency is a characteristic of a particular column and an improvement of more than a factor of 2 is unrealistic in terms of today's column technology. Finally, selectivity is considered. At a selectivity value of 2, components  $i$  and  $j$  are adequately resolved even though only one half of the maximum value of the selectivity term has been achieved. Therefore,

selectivity is the most rewarding of all variables in terms of improving the resolution between two components after retention and efficiency have been optimized. This is why selectivity is given special emphasis during method development in chromatography. IC separation selectivity is discussed in Section 1.3.3.

#### 1.2.4 Band Broadening

##### 1.2.4.1 *van Deemter Equation*<sup>16, 17, 20</sup>

The broadening of zones in chromatography can be understood in terms of the van Deemter equation:

$$H = A + \frac{B}{u} + Cu \quad (1-10)$$

where  $H$  is the overall plate height (the variance produced per unit length of the column),  $A$ ,  $B$  and  $C$  have to do with the various processes inside the column that result in broadening of the component zone (*i.e.*, contribute to an increase in the overall plate height) and  $u$  is the linear velocity of the mobile phase. Clearly, from Equation 1-10 the broadening of component zones can exhibit a velocity (or flow rate) dependence. As an aside it is worth mentioning that equations other than the van Deemter equation can be used to model band broadening. Examples include the Knox equation and Giddings' coupled equation.<sup>16, 17</sup> However, the van Deemter equation was used in this thesis since it is widely cited in the literature<sup>16, 17, 21</sup> and is straightforward to use.

##### 1.2.4.2 *A-Term*

The A-term is also known as the multipath band broadening term, and has to do with the variety of flow paths that an individual molecule follows before it exits the column. The different flow paths are caused by non-uniformities in the packing structure of a column, which lead to differences in linear velocities at various points across the

column, *i.e.*, a non-uniform flow profile across the column. (Larger spaces between particles result in a higher linear velocity compared to smaller spaces.) This is depicted diagrammatically in Figure 1-1A. Multiple flow paths lead to band broadening because some molecules move faster or slower than others depending on which flow stream they are in. However, the band broadening is partially relaxed by lateral convective mass transfer, which causes molecules to switch flow streams as they move down a column (Figure 1-1B). The A-term is expressed by the equation:

$$H_A = 2\omega_A d_p \quad (1-11)$$

where  $H_A$  is the plate height due to multipath band broadening (*i.e.*, the A-term),  $\omega_A$  is the packing factor (smaller for more regularly packed columns) and  $d_p$  is the particle diameter. The A-term decreases with particle diameter since a molecule will travel a shorter distance in a given flow stream before it moves into another one.

#### 1.2.4.3 B-Term

The B-term is otherwise known as the longitudinal diffusion term and deals with the diffusion of sample from the centre of a zone to the less concentrated regions immediately ahead and behind the zone centre. Longitudinal diffusion is proportional to the sample diffusion coefficient. However, the diffusional length is somewhat restricted by the packed particles present in the column. The band broadening associated with the B-term is expressed with the equation:

$$H_B = \frac{2\gamma_0 D_M}{u} \quad (1-12)$$

where  $H_B$  is the plate height due to the B-term,  $\gamma_0$  is the obstruction factor which takes into account the restricted diffusion and  $D_M$  is the sample diffusion coefficient in the

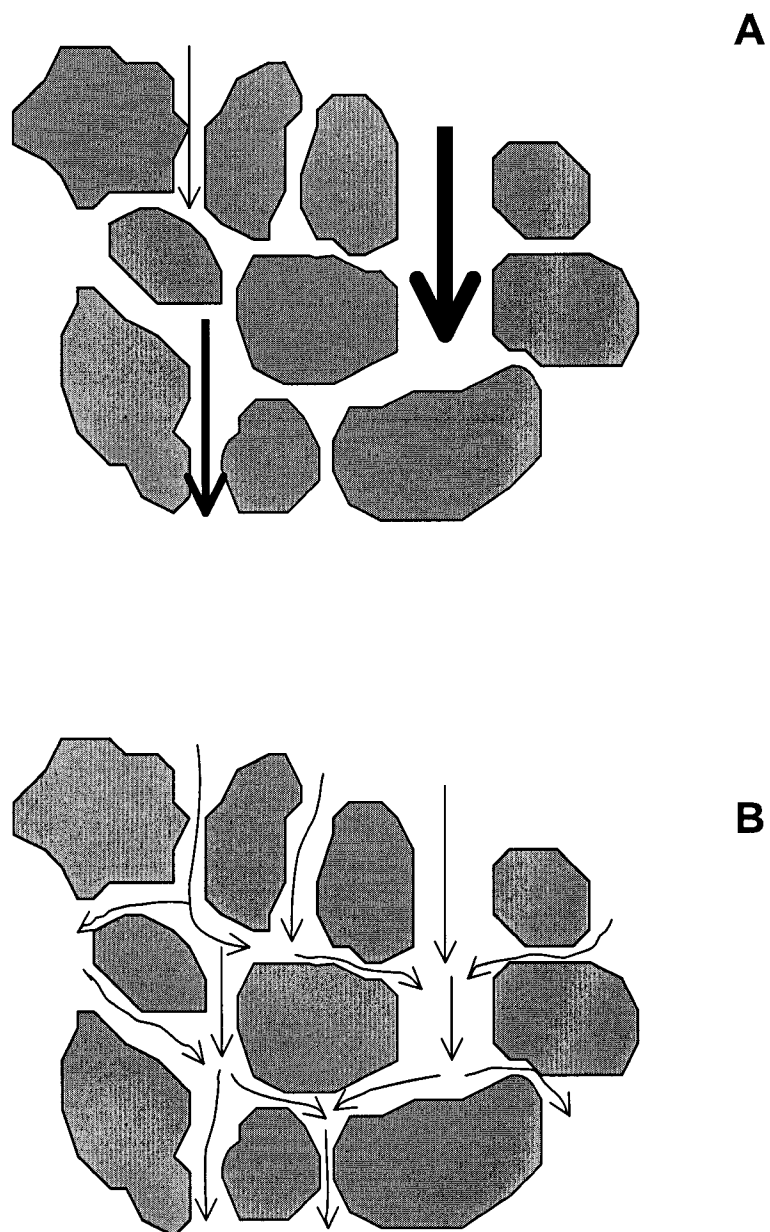


**Figure 1-1.** A) Diagrammatic representation of the non-uniform flow pattern. Thickness of the arrows is proportional to linear velocity. B) Relaxation of band broadening due to lateral convective mixing. Adapted from Ref. 16.



mobile phase.  $H_B$  is inversely proportional to linear velocity since as the linear velocity increases the component zone has less time to broaden by longitudinal diffusion.

#### 1.2.4.4 C-Term

The C-term is composed of a number of time-dependent band broadening processes. The first that will be considered is resistance to mass transfer in the stationary phase ( $H_S$ ). Resistance to mass transfer in the stationary phase is caused by the finite rate of transfer of solute into and out of the stationary phase. Consequently, molecules that are at the front of the sample zone are swept away by the mobile phase before they have the opportunity to equilibrate with the stationary phase and thus do not satisfy the distribution equilibrium shown in Equation 1-2. Consequently, the front half of the sample zone will have a disproportionately high concentration of sample in the mobile phase, as shown in Figure 1-2A. An analogous phenomenon occurs at the end of the sample zone where molecules are left behind in the stationary phase by the mobile phase. This results in the back half of the sample zone having a disproportionately high concentration of sample in the stationary phase. However, the overall zone shape is Gaussian at the centre of which the overall concentration ratio of sample in the two phases satisfies Equation 1-2 (Figure 1-2B). The band broadening associated with resistance to mass transfer in the stationary phase is given by:

$$H_S = 2 \frac{k}{(1+k)^2} t_D u \quad (1-13)$$

where  $H_S$  is the plate height due to resistance to mass transfer in the stationary phase,  $k$  is retention factor,  $t_D$  is the time a sample molecule spends in the stationary phase before re-entering the mobile phase and  $u$  is linear velocity. According to Equation 1-13,  $H_S$  has a dependence on retention. The retention term is zero when the analyte molecules do not

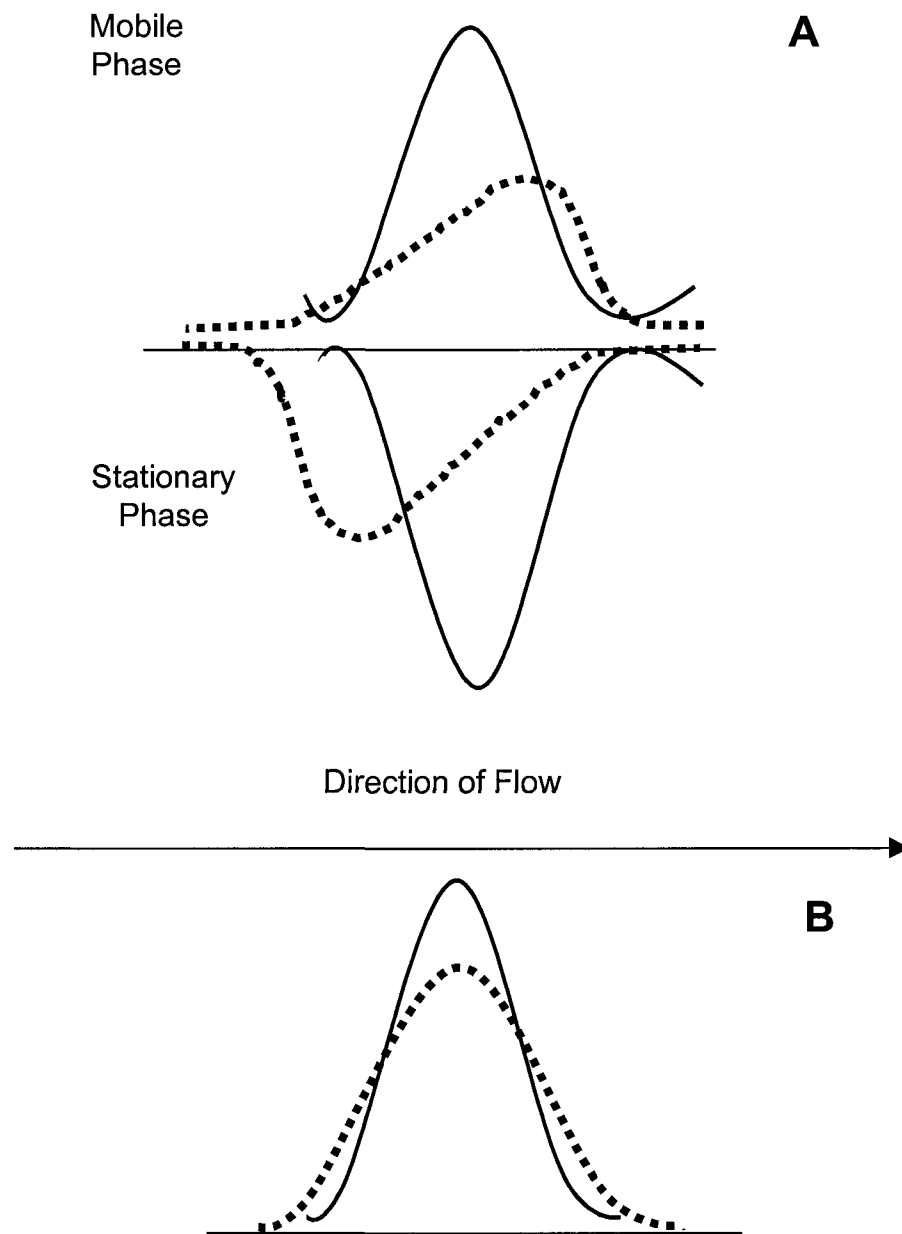


**Figure 1-2.** A) Band broadening caused by slow equilibration between mobile and stationary phase. B) The overall Gaussian band shape. Solid lines represent the case of instantaneous equilibrium whereas dotted lines represent the real case. Adapted from Ref. 16.

interact with the stationary phase (*i.e.*,  $k = 0$ ). The retention term reaches a maximum when  $k = 1$  and gets progressively smaller as retention increases, *i.e.*, as the analyte spends more time in the stationary phase, and is therefore able to approach distribution equilibrium. Similarly, the slower the linear velocity of the mobile phase, the more time there exists for the analyte to reach distribution equilibrium.

A related contribution to the C-term is resistance to mass transfer in the stagnant mobile phase ( $H_{SM}$ ). This comes into play when porous particles are used, as is typical in reversed phase HPLC. The vast majority of surface area in porous particles is inside the particle itself. For example, the external surface area of a 5  $\mu\text{m}$  particle is 0.02  $\text{m}^2$  per mL of packed bed. However, a porous 5  $\mu\text{m}$  particle has a surface area of about 150  $\text{m}^2$  per mL of packed bed.  $H_{SM}$  takes into account the fact that in order to enter the stationary phase, analyte molecules must first diffuse through the stagnant (non-flowing) mobile phase in the pores of the particle before they can reach the surface of the stationary phase. The reverse is true when the analyte leaves the particle. The end result is analogous to resistance to mass transfer in the stationary phase discussed above, with the stationary phase being replaced by the stagnant mobile phase. The equation associated with resistance to mass transfer in the stagnant mobile phase is:

$$H_{SM} = \frac{f(p,k)d_p^2}{\gamma_t D_M} u \quad (1-14)$$

where  $f(p,k)$  is a function of porosity ( $p$ ) and retention ( $k$ ), respectively,  $d_p$  is particle size,  $\gamma_t$  is a tortuosity factor (value between 0 and 1),  $D_M$  is the diffusion coefficient of the analyte in the mobile phase and  $u$  is linear velocity.  $H_{SM}$  decreases with particle size since the distances through which diffusional mass transfer must occur are shorter for

smaller particle sizes. Conversely, the time required for this diffusion will be shorter for sample molecules with large diffusion coefficients. Smaller linear velocities will allow more time for diffusion to occur and will bring the phase distribution closer to equilibrium.  $H_{SM}$  also depends on the fraction of the total mobile phase that is stagnant and on the fraction of time that sample molecules spend in the various phases, *i.e.*, a function of  $p$  and  $k$  respectively. Finally, the tortuosity factor,  $\gamma$ , considers that a molecule diffusing through a porous particle cannot follow a straight line but must follow a tortuous path, which affects the mass transfer.

Most stationary phases in IC employ pellicular packings (Section 1.3.3.4.1). Pellicular particles consist of a non-porous core on the surface of which is deposited a thin layer of stationary phase. This serves to reduce resistance to mass transfer in the stagnant mobile phase due to the smaller distances for diffusion. That is, the particle diameter in Equation 1-14 would be replaced with the thickness of the pellicular layer,  $d_f$ .

The final contribution to the C-term that will be considered is resistance to mass transfer in the mobile phase ( $H_M$ ). As with the A-term, this also deals with the non-uniform flow pattern of the mobile phase in the column. However, in this case lateral diffusion instead of lateral convection is assumed to relax the non-uniform flow profile. If lateral diffusion occurred infinitely fast then there would be no band broadening due to the non-uniform flow pattern effect because differences in the concentration across the bed would be instantly relaxed and hence would not exist. However, lateral diffusion occurs at a finite rate so that there is a net band broadening effect. The plate height associated with resistance to mass transfer in the mobile phase is:

$$H_M = \frac{\omega_c d_p^2}{D_M} u \quad (1-15)$$

where  $\omega_C$  is a packing factor (smaller for more uniformly packed beds),  $d_p$  is the particle size,  $D_M$  is the analyte diffusion coefficient in the mobile phase and  $u$  is linear velocity.  $H_M$  is proportional to particle size since the space between particles is less for smaller particles and diffusional mass transfer does not have to occur over as large a distance. As with the other resistance to mass transfer terms,  $H_M$  decreases at low linear velocities since more time is allowed for equilibration.

#### 1.2.4.5 *The van Deemter Curve and Maximizing Efficiency*

A plot of plate height against linear velocity, *i.e.*, a van Deemter plot is shown in Figure 1-3. The contributions of the individual plate height terms are also shown. The van Deemter curve shows a minimum (optimum) in plate height and therefore a maximum in efficiency. Ideally, the linear velocity (or flow rate) for a particular analysis would be set to the optimum. However, the optimum linear velocity is usually far too slow for practical work. Therefore, liquid chromatographers usually operate at linear velocities well to the right of the optimum in the interest of saving time. Unfortunately, this carries a penalty with it, *i.e.*, an increase in plate height. Provided that the right hand side of the van Deemter curve (*e.g.*, the C-term) is not too steep, then negligible increases in plate height will be seen. This is why there is a trend to smaller particle sizes in HPLC (see Equations 1-14 and 1-15). Smaller particle sizes would also decrease the A-term, provided the column is still packed well, so that  $\omega_A$  does not increase. Further, if diffusion is enhanced (*e.g.*, through an increase in temperature), the C-term will decrease and plate height will improve. Finally, note that the B-term is only significant at linear velocities below the optimum. Since the work in this thesis always uses flow rates well

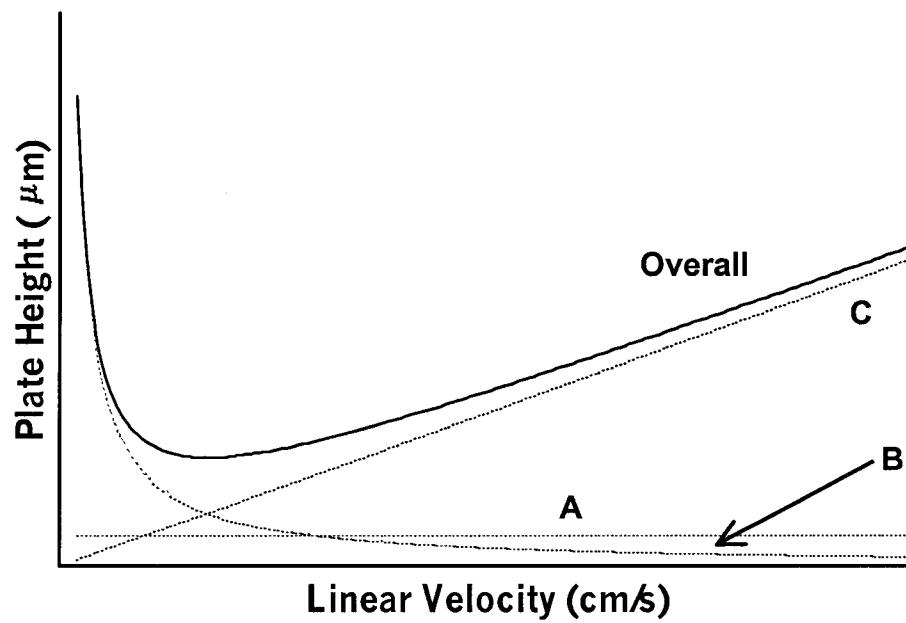


**Figure 1-3.** A van Deemter plot (solid line). The individual contributions to the plot are shown in dashed lines.

above the optimum, longitudinal diffusion is neglected as a significant determinant of overall band broadening.

#### 1.2.4.6 *Extra-Column Band Broadening*

Extra-column band broadening refers to the broadening of analyte zones by devices that do not retain the analyte. Examples include injectors, connecting tubing, and detector cells.

The band broadening produced by injectors is characteristic of the type of injector and its design. Ideally, a sample should be injected as a narrow plug onto a chromatographic column. In this case the band broadening is given by:

$$\sigma_{V,inj}^2 = \frac{V_{inj}^2}{12} \quad (1-16)$$

where  $\sigma_{V,inj}^2$  is the additional variance imparted to a chromatographic peak due to injection and  $V_{inj}$  is the injection volume. An injector that does not behave ideally will introduce an exponential tail to the plug due to a mixing effect, resulting in considerably more band broadening:

$$\sigma_{V,inj}^2 = V_{inj}^2 \quad (1-17)$$

Detector cells also exhibit mixing effects and result in an exponential distortion of the Gaussian chromatographic peak. Detector cell band broadening is given by:

$$\sigma_{V,cell}^2 = V_{cell}^2 \quad (1-18)$$

where  $\sigma_{V,cell}^2$  is the variance due to the detector cell and  $V_{cell}$  is the volume of the detector cell.

However, the most important form of extra-column band broadening with respect to this thesis is from components that exhibit flow rate dependencies on the band

broadening they produce, *e.g.*, connecting tubing and detector response time. The additional variance imparted to a chromatographic peak when it passes through connecting tubing is frequently quantified by means of the equation<sup>22-24</sup>:

$$\sigma_{V,T}^2 = \frac{\pi F L_T r_T^4}{24 D_M} \quad (1-19)$$

where  $\sigma_{V,T}^2$  is the peak variance due to the tubing (volume units),  $F$  is flow rate,  $L_T$  is the length of the tubing,  $r_T$  is the tubing radius and  $D_M$  is the diffusion coefficient of the analyte in the mobile phase. It is important to note that Equation 1-19 only allows a rough estimation of the variance imparted to a chromatographic peak due to connecting tubing. This is due to assumptions in the derivation of Equation 1-19 that are untenable. One assumption of Equation 1-19 is the requirement for a tube that is long enough so that there is enough time for diffusion to relax the non-uniform flow profile that exists in connecting tubing. The second assumption requires that the tubing be remarkably straight, *i.e.*, absolutely no curvature. These assumptions are rarely satisfied in routine HPLC.

Another consideration for high-speed HPLC is the detector response time. The response time is a result of the finite amount of time it takes a detector to respond to a change at its input. Ideally the response of the detector would be instantaneous, however in practice there is always a delay. This can be a significant source of broadening in high-speed HPLC since peaks travel through the detector much faster than in regular separations. The effect of detector response time on peak variance is given by<sup>25</sup>:

$$\sigma_{V,R}^2 = (F \tau)^2 \quad (1-20)$$

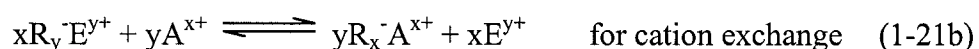


where  $\sigma_{V,R}^2$  is the variance due to detector response time,  $F$  is the flow rate and  $\tau$  is the detector response time.

### 1.3 Ion Chromatography<sup>26</sup>

#### 1.3.1 The Process of Ion Exchange

Separations in IC are achieved through the exchange of ions between the stationary and mobile phase. The stationary phase consists of an insoluble network (usually a polymer) of fixed charge sites. A positively charged stationary phase is used for anion exchange separations and negatively charged stationary phase is used for cation exchange separations. The mobile phase contains oppositely charged counter-ions to maintain electroneutrality. The mobile phase counter-ion has a charge of the same sign as the ions of interest and acts as the eluent. For example, the counter-ion for anion exchange is negatively charged (*e.g.*, hydroxide, bicarbonate or carbonate) and the counter-ion for cation exchange is positively charged (*e.g.*, hydronium). Separation is achieved by the stoichiometric exchange of solute ions with the counter-ions on the fixed charged sites of the stationary phase. This reversible exchange can be described by the following chemical equations:



where  $R$  represents the stationary phase,  $E$  is the mobile phase counter-ion with a charge of  $y$ , and  $A$  is the analyte of interest with a charge of  $x$ .

### 1.3.2 General Instrumentation

Figure 1-4 is a schematic diagram of IC instrumentation. The pump is used to control the flow of eluent through the ion exchange column. This is usually done at flow rates ranging from 0.2 mL/min to 2 mL/min and at pressures from 1500 psi to 4000 psi. Sample is introduced onto the column by means of an injection valve and typical injection volumes range from 2  $\mu$ L to 1 mL. The separation of a sample into its individual components takes place inside a column packed with a suitable stationary phase (Section 1.3.3.4). Detection in IC is usually by conductivity (Section 1.3.2.2), which is most commonly performed in conjunction with a suppressor (Section 1.3.2.1). Data acquisition for the experiments performed in this thesis was entirely by computer.

#### 1.3.2.1 *Suppression*

Suppression is a post column reaction whose primary function is to enhance the sensitivity of conductivity detection by reducing the conductivity of the eluent ion. When performing anion exchange separations the suppressor is a cation exchanger, and when performing cation exchange separations the suppressor is an anion exchanger. A typical eluent anion  $E^-$  is the conjugate base of the weak acid HE. Exchange of the counter ion (*e.g.*,  $Na^+$ ) of the eluent with  $H^+$  from the suppressor results in the formation of the weak acid HE.



The product of this neutralization process is the weak acid HE. HE will partially dissociate and yield background conductivity:



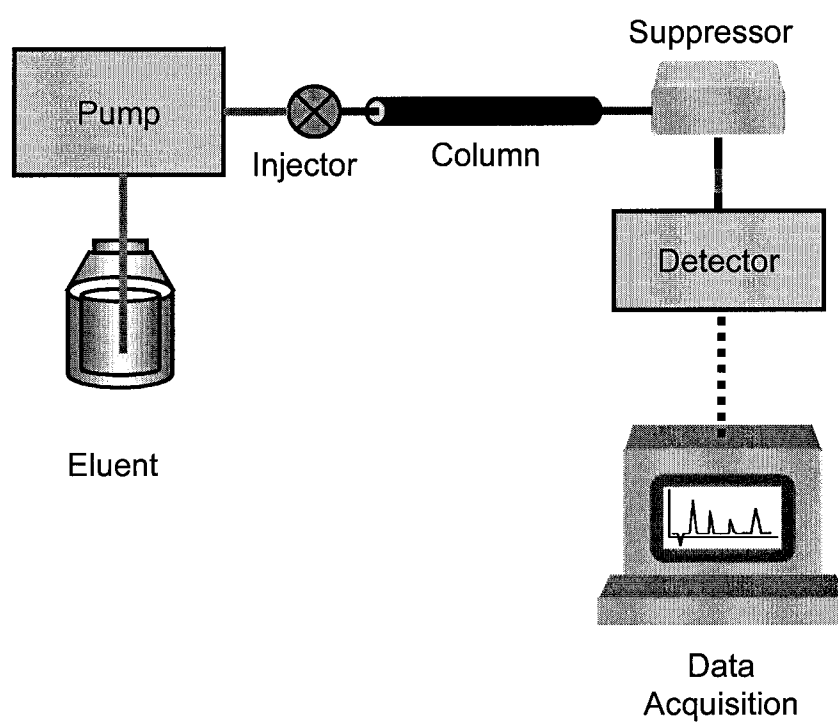
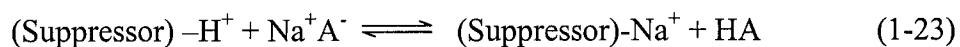


**Figure 1-4.** Schematic of IC instrumentation.

The magnitude of this background correlates with the strength of the acid HE. For instance, typical background conductivities after suppression are 12-15  $\mu\text{S}/\text{cm}$  for bicarbonate/carbonate eluents ( $\text{pK}_{\text{a},1} = 6.35$ ) and ideally 0.06  $\mu\text{S}/\text{cm}$  for hydroxide ( $\text{pK}_{\text{w}} = 14$ ). It is for this reason that eluents in IC should possess a  $\text{pK}_{\text{a}}$  greater than 7.

Simultaneous with the neutralization of the eluent, the counter-ion ( $\text{Na}^+$ ) associated with the analyte anion ( $\text{A}^-$ ) is also exchanged for  $\text{H}^+$ .



If HA is a strong acid it will fully dissociate yielding  $\text{A}^-$  and  $\text{H}^+$ . Since the conductivity of  $\text{H}^+$  ( $350 \text{ S}\cdot\text{cm}^2\cdot\text{eq}^{-1}$ ) is very high relative to  $\text{Na}^+$  ( $50 \text{ S}\cdot\text{cm}^2\cdot\text{eq}^{-1}$ ) and all other cations, there is an overall enhancement in the conductivity signal due to  $\text{A}^-$ .

The principles for the suppression of eluents for cation exchange are analogous to those for anion exchange. Briefly, in cation exchange the eluent ion is usually hydronium ion and the suppressor usually contains hydroxide. Exchange of the counter ion of hydronium (*e.g.*, sulfate) with hydroxide results in the formation of water, and the eluent is effectively neutralized.

In the original work of Small *et al.* the suppressor was a 9 mm x 250 mm column packed with 200-400 Mesh Dowex 50W-X8 in the  $\text{H}^+$  form.<sup>1</sup> However, column suppression has a number of drawbacks. Firstly, the suppressor column has limited capacity, and so had to be regenerated or replaced periodically. Secondly, the large volume of the suppressor added considerably to peak broadening. Thirdly, retention times of weak acid analytes vary due to variation in Donnan exclusion of these analytes as the cation exchange bed of the suppressor becomes exhausted. Consequently, the most popular type of suppressor in use today is a membrane suppressor, which circumvents the

above-mentioned problems. The heart of a membrane suppressor for anion determination is a cation exchange membrane, as shown in Figure 1-5. Effluent ( $\text{Na}^+\text{A}^-$ ,  $\text{Na}^+\text{E}^-$ ) flows on one side of the membrane and sulfuric acid regenerant ( $\text{H}^+\text{HSO}_4^-$ ) flows on the other side. Cations move freely through the cation exchange membrane. Thus,  $\text{H}^+$  transfers from the regenerant into the effluent to generate  $\text{H}^+\text{A}^-$  and  $\text{HE}$ , while the eluent cation ( $\text{Na}^+$ ) passes simultaneously into the regenerant. The effluent is sandwiched between two cation exchange membranes to maximize the cation flux and thereby the suppression capacity. Meanwhile anions experience Donnan exclusion and so do not pass through the membrane.

The experiments presented in Chapters Two, Three and Four employ a membrane suppressor before conductivity detection. However, Chapter Six shows that membrane suppressors are not amenable to high-speed separations. Therefore, a novel column suppressor was used for suppressed conductivity detection in high-speed IC. The suppressor consists of three small packed beds (low dead-volume) housed in a three-position rotary valve. At a given time, one bed is suppressing effluent, the second is being chemically regenerated with sulfuric acid and the third is being rinsed prior to returning to service. Although each bed has sufficient capacity for 20 minutes of operation, the valve was rotated prior to each chromatographic run. This suppressor circumvents the problems associated with the original column suppressors and is amenable to high-speed IC.

### 1.3.2.2 *Conductivity Detection*

Conductivity detection is the most widely used detection scheme for IC due to the universal response of conductivity detection to all ions. Conductivity detection is

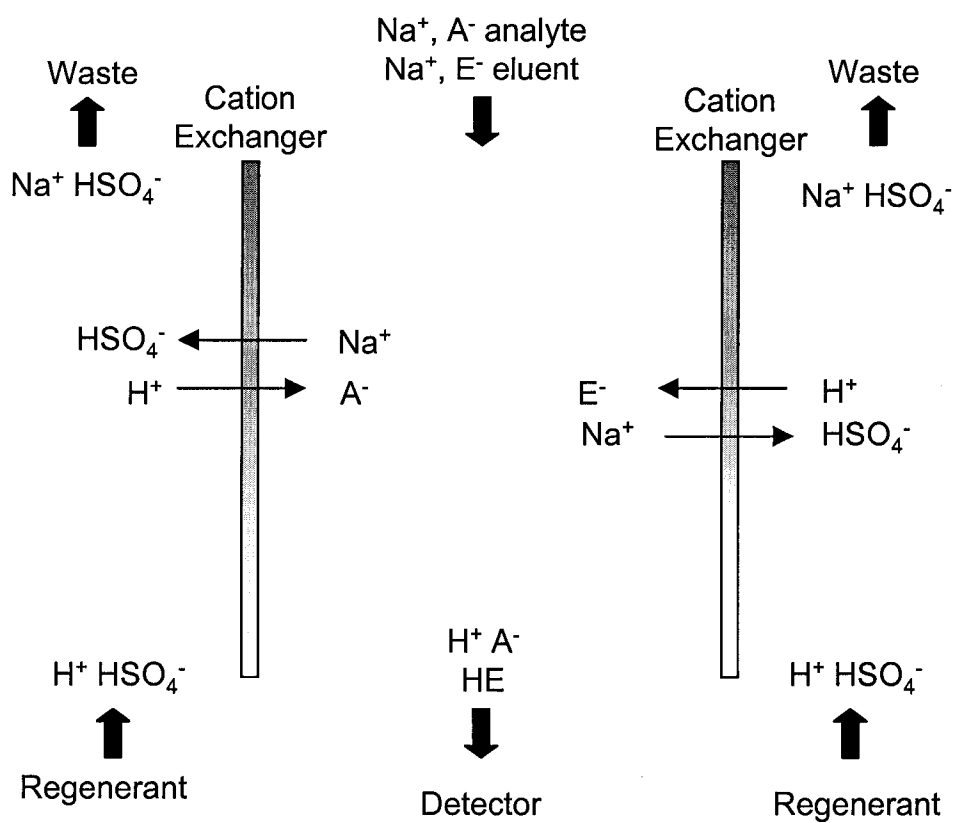


**Figure 1-5.** A membrane suppressor for anion exchange separations. Cation exchange membranes in suppressor are in  $\text{H}^+$  form (*i.e.*, sulfuric acid is regenerant). Adapted from Figure 9.21 of Ref 26.

performed with a detector cell consisting of two electrodes to which an electric potential is applied. The ions passing through the detector cell move in response to the electrical field, *i.e.*, anions move to the anode and cations to the cathode. The moving ions generate a current and it is this current that is the analytical signal. The generated current is dependent on the ionic conductance and concentration of the ion passing through the detector cell. To avoid polarization of the ions, the potential is an alternating current (AC) in the range of 50 to 10000 Hz. The amplitude of this AC potential should be as high as possible to maximize the resultant current but must be low enough to avoid redox reactions at the electrode surfaces.

In the absence of analyte ions, the conductivity signal is due entirely to the eluent ions. During elution, analyte ions displace eluent co-ions, such that when analyte ions pass through the conductivity cell there is an increased concentration of analyte ions and a decreased concentration of eluent ions. The resultant detection signal is then dependent on the difference in ionic conductance between the eluent ions and the analyte ions. The change in conductance,  $\Delta G$ , during elution is given through the equation<sup>27</sup>:

$$\Delta G = \frac{(\lambda_{E^+} + \lambda_{A^-})\theta_A - (\lambda_{E^+} + \lambda_{E^-})\theta_E}{10^{-3} K} C_{A^-} \quad (1-24)$$

where  $E^+$  and  $E^-$  are the cation and anion of the eluent,  $\lambda$  is the ionic equivalent conductivity of an ion,  $\theta_A$  and  $\theta_E$  are the degree of dissociation of the analyte and eluent, and  $K$  is the cell constant of the detector. Therefore, Equation 1-24 predicts that an enhancement in signal can be obtained if the conductivity of the eluent is reduced. In the special case of complete dissociation of the analyte and eluent ions Equation 1-24 becomes<sup>27</sup>:

$$\Delta G = \frac{(\lambda_{A^-} - \lambda_{E^-})}{10^{-3} K} C_{A^-} \quad (1-25)$$

There are a couple of ways to reduce the background conductivity of the eluent and this has been at the source of a lot of controversy, especially in the days when eluent suppression was a patented technique. Firstly, and most obviously, a suppressor can be used to reduce the background conductivity and simultaneously enhance the conductivity of the analyte ion (Section 1.3.2.1.). In this case,  $\theta_E$  in Equation 1-24 becomes 0 and the change in conductivity will arise from the analyte ion and an equivalent amount of  $H^+$ :

$$\Delta G = \frac{(\lambda_{H^+} + \lambda_{A^-}) \theta_A}{10^{-3} K} C_{A^-} \quad (1-26)$$

Alternately, the eluent contribution to the background conductivity can be decreased by employing small concentrations of weakly conducting eluent ions<sup>28</sup>. Suitable eluent ions for non-suppressed anion exchange are organic aromatic acids such as salicylate, phthalate, benzoate etc., whereas for cation exchange organic bases, *e.g.*, aniline, benzylamine, methylpyridine etc., can be used. In this way, detection can be accomplished without a suppressor, thus tremendously simplifying the IC instrumentation.

The primary mode of detection for the experiments presented in this thesis is suppressed conductivity detection. This decision was based on the method's superior detection limits. However, the experiments presented in Chapter Five employ non-suppressed (direct) conductivity detection. The switch to non-suppressed conductivity detection was made since the method under investigation is not compatible with suppression.



### 1.3.2.3 Ultraviolet Absorbance Detection

As in most of HPLC, direct monitoring of ultraviolet (UV) absorbance is the most straightforward mode of detection. Many analytes routinely encountered in IC exhibit useful UV absorbance, as presented in Table 1-1.<sup>26</sup> The sensitivity of UV detection can be enhanced by incorporation of a suppressor when the eluent is UV absorbing in its deprotonated state (*e.g.*, hydroxide or acetate).

For non-UV absorbing ions, indirect UV detection can be used.<sup>29</sup> In this technique, the wavelength of detection is chosen such that the absorbance of analyte ions is zero whereas the absorbance of the eluent ion is very high. Therefore, when an analyte ion passes through the detector cell, it displaces an equimolar amount of eluent co-ions and the absorbance of the eluent decreases. This results in negative peaks for all analytes. Typical eluents employed with indirect UV detection are aromatic carboxylic acids (as was used for non-suppressed conductivity) for anion separations and copper, cobalt, cerium salts or aromatic amines for cation separations.

The sensitivity of indirect UV detection can be described with the equation<sup>26</sup>:

$$\Delta A = (-x/y) (\epsilon_{E_{y^-}}) (C_{A^-}) b \quad (1-27)$$

where  $\Delta A$  is the change in absorbance upon elution of an analyte,  $x$  is the charge on the analyte ion,  $y$  is the charge on the eluent ion,  $\epsilon_{E_{y^-}}$  is the molar absorptivity of the eluent ion,  $C_{A^-}$  is the concentration of analyte and  $b$  is the path length of the UV detector. Equation 1-27 assumes that the analyte ion does not absorb light at the wavelength of analysis, which is an assumption that is satisfied in this thesis (Chapter Five). Equation 1-27 leads to the conclusion that sensitivity in indirect UV detection is higher when the

**Table 1.1.** Typical operating conditions for the detection of anions by UV. Taken from Ref. 26.

Ion	Wavelength (nm)
$\text{Br}^-$	215
$\text{BrO}_3^-$	210
$\text{C}_2\text{O}_4^{2-}$	205
$\text{CrO}_4^{2-}$	365
$\text{HCOO}^-$	190
$\text{IO}_3^-$	210
$\text{NO}_2^-$	210
$\text{NO}_3^-$	215
$\text{S}_2\text{O}_3^{2-}$	205
$\text{SCN}^-$	195

molar absorptivity of the eluent is large and the charge on the eluent ion is small (*i.e.*, a singly charged eluent ion is preferred over a doubly charged eluent ion).

Indirect UV detection is used as an additional mode of detection (along with conductivity) in Chapter Five. Direct monitoring of UV absorbance was used for one experiment in Chapter One as well.

### 1.3.3 Selectivity in IC

#### 1.3.3.1 Importance of Selectivity

As was mentioned in Section 1.2.3, the selectivity of a separation is of utmost importance during method development. Common ways of altering selectivity are through changes in the mobile phase (*e.g.*, eluent type, eluent strength, pH, additives) and in the stationary phase (*e.g.*, support, ion exchange site). In IC, selectivity is most often altered through changes in the stationary phase chemistry. The reasons for this are firstly, that IC separations performed with suppressed conductivity detection are restricted to eluents that can be suppressed (Section 1.3.2.1. and 1.3.2.2.). Secondly, as will be shown in Section 1.3.3.3, the selectivity between ions of similar charge cannot be influenced through changes in the eluent concentration.

Selectivity in IC (or more specifically, ion exchange) can be qualitatively described as the likelihood of exchange occurring between two ions, one being the analyte of interest and the other being the eluent ion in the stationary phase as was shown in Equation 1-21.<sup>30</sup> The selectivity coefficient,  $K_{A,E}$ , is the equilibrium constant for Equation 1-21a (assuming that activity coefficients are approximately equal to one):

$$K_{A,E} = \frac{[R_x^+ A^{x-}]^y [E^{y-}]^x}{[A^{x-}]^y [R_y^+ E^{y-}]^x} \quad (1-28)$$

The selectivity coefficient can be moderated in number of ways, since it is a function of the analyte, the eluent ion and the stationary phase.

### 1.3.3.2 *Properties of Analyte and Eluent Ion Affecting Selectivity*

Perhaps the most intuitively obvious factor that affects retention of ions in ion exchange is the charge of the ion. As might be expected, highly charged ions (*e.g.*, sulfate) are much more strongly retained than singly charged ions (*e.g.*, chloride). Alternatively, if an ion is the conjugate base of a weak acid, the pH of the eluent may be used to control the degree of ionization of the ion and therefore its retention. However, in most cases this is only possible when employing non-suppressed detection modes. Suppression necessitates that the eluent be acidic for cation separations and basic for anion separations (Section 1.3.2.1.).

Apart from the charge of an ion, the solvation of ions also plays a significant role in retention. Since ion exchange is a process that occurs in aqueous solution, ions are surrounded by solvation spheres.<sup>31</sup> If an ion is to leave the solution phase (*i.e.*, the mobile phase) and enter the ion exchanger, it must rearrange and eventually partially shed its solvation sphere. This is so the ion can get close to the ion exchange site. The more an ion sheds its solvation sphere, the closer it gets to the ion exchange site and the more strongly it is bound to the site (*i.e.*, retained). The eluent ion undergoes similar processes. Generally speaking, the ion exchanger prefers the ion with the smallest hydration sphere. It is for this reason that elution in anion exchange follows the order fluoride, chloride, bromide and cation exchange is lithium, sodium, potassium etc.

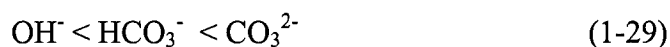
A class of ions that display unique selectivity in ion exchange is the *polarizable* ions. These ions are very strongly retained on anion exchangers due to the secondary

interactions they undergo. This interaction stems from these ions (*e.g.*, iodide, thiocyanate and especially perchlorate) being relatively large and poorly hydrated ions. This makes them unable to form a proper solvation sphere in the solution phase. The end result of this is that polarizable ions disturb the structure of water in the mobile phase and therefore enter the stationary phase where the structure of water is less ordered.<sup>32</sup> Further, according to Diamond, polarizable ions may participate in water structure-enforced ion pairing with the anion exchange site, which further increases their retention.<sup>33</sup> This type of interaction is stronger between two large, poorly hydrated ions (*e.g.*, tetra-alkylammonium and perchlorate). Therefore, polarizable ions are very strongly retained on most anion exchangers.

As an aside it is worth mentioning that associating the above-mentioned phenomenon with the polarizability of ions (as is always done in IC literature) is misleading. For example, perchlorate is much more strongly retained on anion exchangers than iodide, even though it is considered a “hard anion” by inorganic chemists, *i.e.*, not at all polarizable. Since the strong interaction of these ions with anion exchangers stems from the disruption of water structure in the mobile phase, a better term would be *chaotropic*. This will be used in the remainder of this thesis.

### 1.3.3.3 *Effect of mobile phase on selectivity*

As can be seen in Equation 1-21, the eluent ion is necessary to the process of ion exchange and impacts on retention through its nature and concentration. The general order of eluent strength (considering the most commonly used eluents for suppressed conductivity detection (Section 1.3.2.1 and 1.3.2.2)) in anion exchange is:



Monovalent anions tend to be weak eluents due to their small charge. Conversely, carbonate is a powerful eluting ion due to its double charge. Commonly, bicarbonate and carbonate are used together, as this provides a well-buffered eluent over the pH range 8-11 whose eluent strength is easily varied by altering the ratio of the two anions. Aromatic organic acids can also be used as eluents in IC. Typically, these are used when performing non-suppressed conductivity detection (Section 1.3.2.2). Examples include, salicylic acid, benzoic acid and phthalic acid.

The usual eluent ion for cation exchange is hydronium although the exact acid used can vary considerably (*e.g.*, sulfuric acid, nitric acid, citric acid, tartaric acid). Typical eluents for suppressed conductivity detection are sulfuric acid or methanesulfonic acid.

Based on the equilibrium shown in Equation 1-21 and basic chromatographic principles, ion retention is governed by:<sup>34-36</sup>

$$\log k = \frac{1}{y} \log K_{A,E} + \frac{x}{y} \log \left( \frac{Cap}{y} \right) + \log \left( \frac{W_s}{V_m} \right) - \frac{x}{y} \log [E^{y-}] \quad (1-30)$$

where  $k$  is the retention factor of the analyte,  $K_{A,E}$  is the ion exchange selectivity constant between the analyte and the eluent competing ion ( $E^{y-}$ ) (Equation 1-28),  $Cap$  is the effective ion-exchange capacity of the stationary phase,  $W_s$  is the mass of the stationary phase and  $V_m$  is the volume of the mobile phase.

For a given column and given eluent ion, equation 1-30 reduces to:<sup>34-36</sup>

$$\log k = \text{const} - \frac{x}{y} \log [E^{y-}] \quad (1-31)$$

Thus increasing the eluent concentration results in a dramatic decrease in retention. For instance doubling the concentration of sodium hydroxide will halve the retention of

chloride and nitrate and quarter the retention of sulfate and oxalate. Thus, the use of high concentrations of hydroxide compensates for its weak eluent strength.

While eluent concentration strongly affects retention, it has little effect on the selectivity of ions of the same charge. However, eluent concentration can have dramatic effects on selectivity between ions of differing charge. In other words, if the eluent concentration is high enough, it is possible to have multiply charged analytes (*e.g.*, sulfate and phosphate) elute before singly charged analytes (*e.g.*, bromide and nitrate). Therefore, eluent concentration is extremely important in bridging the gap between analytes of differing charge in chromatograms.

#### *1.3.3.4 Effect of Stationary Phase on Selectivity*

##### *1.3.3.4.1 General support construct*

In contrast to traditional porous silica particles, IC stationary phase<sup>30</sup> particles tend to be polymeric and are 5-15  $\mu\text{m}$  in diameter. These particles are usually pellicular, *i.e.*, the stationary phase particle is composed of a solid inner core (essentially non-porous) on the surface of which is deposited a thin layer of stationary phase in the form of small latex beads. This is shown in Figure 1-6. Typically, stationary phases are constructed from a functional (or base) monomer to create the ion exchange site and a cross-linking monomer to control water content.

Common base materials are ethylvinylbenzene, methacrylate, polyvinyl alcohol and polystyrene. These base monomers need to be crosslinked to control water content and mechanical strength. The choice of crosslinker depends on the base material used. Divinylbenzene is the most popular crosslinking material for aromatic base materials

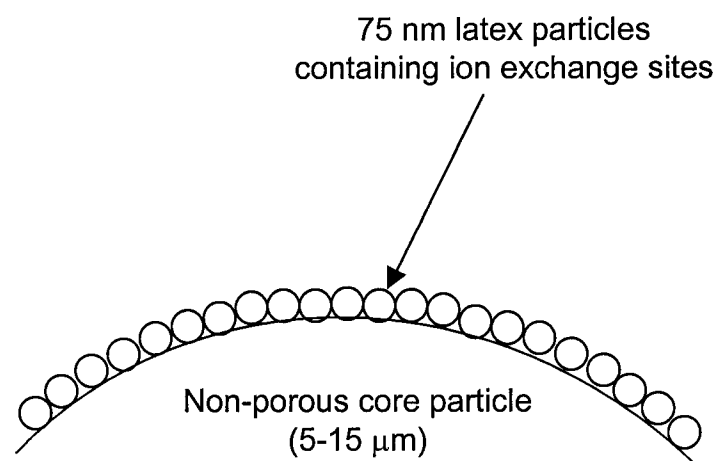


**Figure 1-6.** Schematic representation of a pellicular particle for IC.



(*e.g.*, ethylvinylbenzene or polystyrene) whereas ethyleneglycol dimethacrylate (among others) can be used for methacrylate-based resins.

#### 1.3.3.4.2 *Role of column material in selectivity*

The materials used in the synthesis of a stationary phase can have a pronounced effect on the selectivity of a separation. For example, methacrylate based stationary phases tend to have higher water contents and as such are amenable to the separation of chaotropic species (Section 1.3.3.2). Conversely, aromatic base materials, which tend to have lower water contents, are more suitable for the separation of the seven common anions, particularly bromide and nitrate. The water content of stationary phases is controlled with the degree of cross-linking, with higher percentages of cross-linking resulting in low water contents. This means that methacrylate base materials need a higher percentage of cross-linking than aromatic base materials to achieve the same water content.

#### 1.3.3.4.3 *Role of the type of ion exchange site in selectivity*

Different types of ion exchange sites can be produced through the functionalization of the base monomers. By convention, ion exchangers are classified according to their type of functionality (*i.e.*, ion exchange site). Cation exchangers are broadly classified into strong acid (*e.g.*, sulfonate) and weak acid (*e.g.*, carboxylate) whereas anion exchangers can be classified into strong base (*e.g.*, quaternary ammonium) or weak base (*e.g.*, tertiary ammonium) types. Strong acid/base ion exchangers retain their capacity over a wide pH range since the ion exchange site remains fully charged as the pH is varied. Conversely, weak acid/base ion exchangers undergo changes in capacity with pH. The ability to vary the capacity of the stationary phase imparts an

additional method of modifying retention in addition to the eluent. Anion exchange separations are usually performed on quaternary ammonium stationary phases and as such, selectivity variations in these materials are introduced through changes in the structure of the ion exchange site rather than through the type of ion exchange site. This will be discussed in Section 1.3.3.4.4. However, cation exchange selectivity is usually altered through the use of different types of functional groups (*e.g.*, sulfonate, carboxylate, phosphonate).

#### 1.3.3.4.4 *Role of the structure of the ion exchange site in selectivity*

Changes in the structure of quaternary ammonium functional groups ( $-\text{NR}_3^+$ ) are introduced through their alkyl chains. For example, a quaternary ammonium group can be made bulkier and more hydrophobic by lengthening some or all of the alkyl chains (*e.g.*, methyl to ethyl). Alternatively, an ion exchange site can be made hydrophilic through the incorporation of alcohol functionality (*e.g.*, an alkanolamine). Generally speaking, the retention of hydrophilic, polyvalent anions (*e.g.*, sulfate and phosphate) decreases as the size of the functional group increases (*e.g.*, on going from a methyl to an ethyl substituent). This is due to the charge density of the ion exchange site decreasing as its size becomes larger. Therefore coulombic attraction between the solute and ion exchange site is not as strong. For the separation of chaotropic anions (*e.g.*, iodide, thiocyanate and perchlorate), the hydration of the ion exchange site is of utmost importance. Usually there is an increase in the retention of these ions as the ion exchange site becomes more hydrophobic (less hydrated) and vice versa.

### 1.3.4 Ion-Interaction Chromatography<sup>16, 26</sup>

Ion-interaction chromatography (IIC) is a technique employed for the separation of ions using RPLC stationary phases. Most ions show little or no retention on RPLC stationary phases, with the exception of large hydrophobic ions. IIC greatly enhances the retention of all ions so that separations with RPLC stationary phases are obtained. IIC can be considered as an alternative to the ion exchange separations discussed in Section 1.3.1. At the heart of this technique is an ion-interaction reagent, IIR (otherwise known as a pairing ion,  $P^+$ ), which is hydrophobic, but possesses a charge opposite to that of the analytes of interest. Electroneutrality is maintained by the counter-ion of the IIR. Examples of IIR include quaternary ammonium salts for the separation of anions and alkane sulfonates for the separation of cations.

IIC is depicted diagrammatically in Figure 1-7. It begins with the formation of a dynamic equilibrium between the stationary phase and the mobile phase, which contains the IIR. This results in the formation of an electrical double-layer at the surface of the stationary phase. The retained IIR forms a primary layer of charge to which is attracted a diffuse secondary layer of oppositely charged ions, consisting mainly of the IIR counter-ions. The amount of charge in the primary and secondary layers is dependent on the amount of IIR that is retained by the stationary phase. This in turn depends on the concentration of the IIR, the hydrophobicity of the IIR and the percentage of an organic modifier (*e.g.*, acetonitrile or methanol) in the eluent. The retention of analyte ions in IIC depends on electrostatic effects, *i.e.*, exchange with a counter-ion in the secondary layer, and on reversed-phase (*i.e.*, hydrophobic) interactions with the bare RPLC stationary phase.

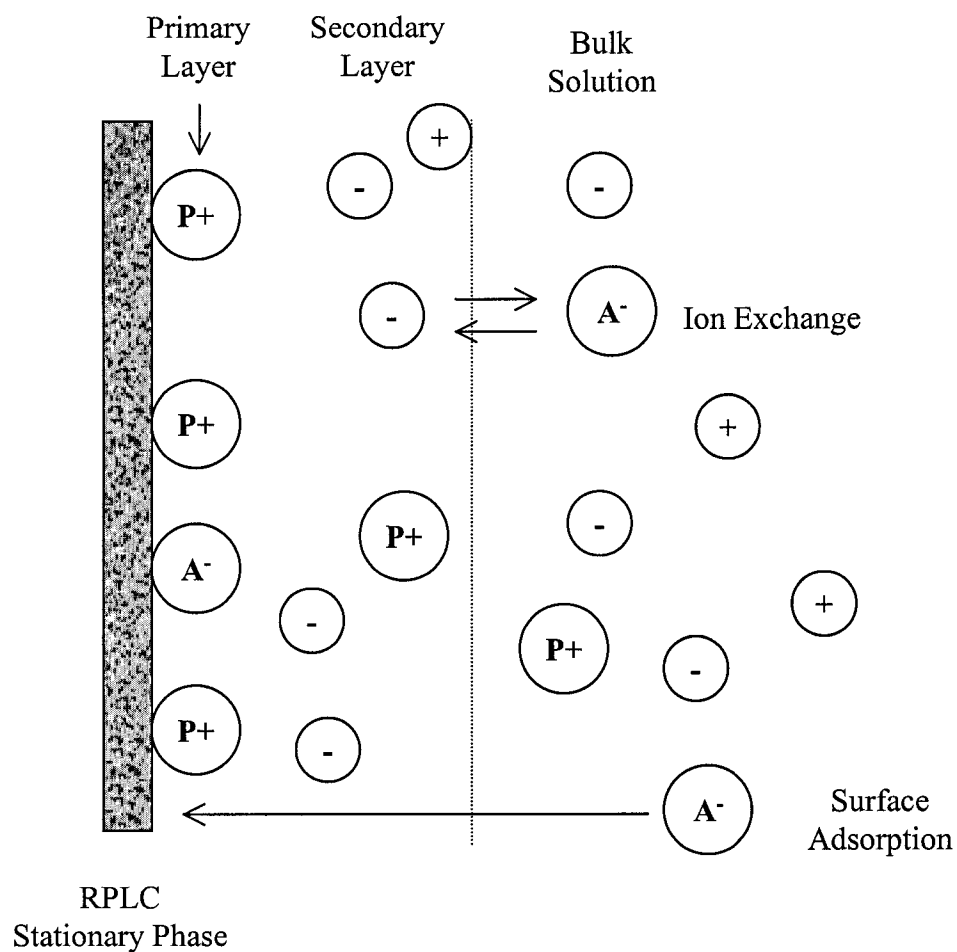


**Figure 1-7.** Diagrammatic depiction of IIC.  $P+$  is the pairing ion,  $A^-$  is the sample ion,  $+$  is a positive counter ion (e.g., sodium) and  $-$  is a negative counter ion (e.g., chloride). Adapted from Ref. 16.

#### 1.4 Summary and Overview of Thesis

Clearly, IC separation selectivity is overwhelmingly governed by the stationary phase with the mobile phase playing only a limited role. Consequently, selectivity is something that an IC user buys into at the time of purchase of the column. This also means that typically, an IC column is suitable for only one type of analysis. Therefore, it would be most desirable if the user could tailor the selectivity themselves without having to purchase a new column (\$1500) for different analyses. This is why as a tangent, temperature will be explored in this thesis as a means to alter selectivity in IC. The research performed in this area will be presented in Chapters Two and Three.

The other area where the abilities of IC are limited is with respect to separation speed. High-speed separations in RPLC employ particles of 3  $\mu\text{m}$  diameter or less, which results in rather high efficiencies ( $N = 100\,000$  plates per metre).<sup>17</sup> This allows the length of columns to be shortened considerably resulting in tremendous savings in analysis time.<sup>37-39</sup> Furthermore, small diameter particles allow the use of flow rates much higher than the optimum with negligible losses in efficiency (Section 1.2.4.5). However, IC stationary phase particles are around 10  $\mu\text{m}$  in diameter, with a recent trend toward 5  $\mu\text{m}$ . Therefore, column technology in IC is not on par with RPLC. A further consideration in IC is the use of polymeric supports, which are inherently not as efficient as the silica supports widely used in RPLC.<sup>40-42</sup> Therefore, reducing analysis time in IC is a challenging problem, and is the main focus of this thesis. The theory and application of above ambient temperatures for reducing analysis time in IC will be presented in Chapter Four. Chapters Five and Six move away from the use of above ambient temperatures and explore the application and benefits of monolithic materials for

reducing analysis time. Ultimately, this thesis will show that the use of monolithic materials is a superior approach for the reduction of analysis time in IC compared to the application of elevated temperatures.

## 1.5 References

- (1) Small, H.; Stevens, T. S.; Bauman, W. C. *Anal. Chem.* **1975**, *47*, 1801-1809.
- (2) Hirschfeld, T.; Callis, J. B.; Kowalski, B. R. *Science* **1984**, *226*, 312-318.
- (3) Illman, D. L.; Callis, J. B.; Kowalski, B. R. *Am. Lab.* **1986**, *18*, 8-10.
- (4) Workman, J., Jr.; Creasy, K. E.; Doherty, S.; Bond, L.; Koch, M.; Ullman, A.; Veltkamp, D. J. *Anal. Chem.* **2001**, *73*, 2705-2718.
- (5) Doyle, M. J.; Newton, B. J. *CAST* **2002**, *Jan/Feb*, 9-12.
- (6) Toofan, M.; Stillian, J. R.; Pohl, C. A.; Jackson, P. E. *J. Chromatogr. A* **1997**, *761*, 163-168.
- (7) Barkley, D. J.; Bennett, L. A.; Charbonneau, J. R.; Pokrajac, L. A. *J. Chromatogr.* **1992**, *606*, 195-201.
- (8) Cox, D.; Harrison, G.; Jandik, P.; Jones, W. *Food Technol. (Chicago)* **1985**, *39*, 41-44.
- (9) Vanatta, L. E. *Trends Anal. Chem.* **2001**, *20*, 336-345.
- (10) Kadnar, R. *J. Chromatogr. A* **1999**, *850*, 289-295.
- (11) Honigs, D. E. *Am. Lab.* **1987**, *19*, 48-51.
- (12) Connolly, D.; Paull, B. *J. Chromatogr. A* **2001**, *917*, 353-359.
- (13) Connolly, D.; Paull, B. *Anal. Chim. Acta* **2001**, *441*, 53-62.
- (14) Connolly, D.; Paull, B. *J. Chromatogr. A* **2002**, *953*, 299-303.

- (15) Schoenmakers, P. J. *Optimization of Chromatographic Selectivity*; New York, 1986.
- (16) Cantwell, F. F. *Analytical Separations Class Notes*; University of Alberta: Edmonton, 1998.
- (17) Neue, U. D. *HPLC Columns: Theory, Technology and Practice*; Wiley-VCH: New York, 1997.
- (18) Snyder, L. R.; Kirkland, J. J. *Introduction to Modern Liquid Chromatography*, 2 ed.; John-Wiley & Sons, Inc.: New York, 1979.
- (19) Snyder, L. R.; Glajch, J. L.; Kirkland, J. J. *Practical HPLC Method Development*.: New York, 1996.
- (20) van Deemter, J. J.; Zuiderweg, F. J.; Klinkenberg, A. *Chem. Eng. Sci.* **1956**, *5*, 271.
- (21) Yan, B.; Zhao, J.; Brown, J. S.; Blackwell, J.; Carr, P. W. *Anal. Chem.* **2000**, *72*, 1253-1262.
- (22) Taylor, G. I. *Proc. Roy. Soc. (London)* **1953**, *A219*, 186-203.
- (23) Aris, R. *Proc. Roy. Soc. (London)* **1965**, *A235*, 67-77.
- (24) Atwood, J. G.; Golay, M. J. E. *J. Chromatogr.* **1981**, *218*, 97-122.
- (25) Kirkland, J. J.; Yau, W. W.; Stoklosa, H. J.; Dilks Jr., C. H. *J. Chromatogr. Sci.* **1977**, *15*, 303-316.
- (26) Haddad, P. R.; Jackson, P. E. *Ion Chromatography: Principles and Applications*; Elsevier: New York, 1990.
- (27) Buchberger, W. W. *Trends Anal. Chem.* **2001**, *20*, 296-303.
- (28) Gjerde, D. T.; Fritz, J. S.; Schmuckler, G. *J. Chromatogr.* **1979**, *186*, 509-515.

- (29) Small, H.; Miller, T. E., Jr. *Anal. Chem.* **1982**, *54*, 462-469.
- (30) Pohl, C. A.; Stillian, J. R.; Jackson, P. E. *J. Chromatogr. A* **1997**, *789*, 29.
- (31) Rabin, S.; Stillian, J. *J. Chromatogr. A* **1994**, *671*, 63-71.
- (32) Chu, B.; Whitney, D. C.; Diamond, R. M. *J. Inorg. Nucl. Chem.* **1962**, *24*, 1405-1415.
- (33) Diamond, R. M. *J. Phys. Chem.* **1963**, *67*, 2513-2517.
- (34) Madden, J. E.; Haddad, P. R. *J. Chromatogr. A* **1998**, *829*, 65-80.
- (35) Madden, J. E.; Avdalovic, N.; Jackson, P. E.; Haddad, P. R. *J. Chromatogr. A* **1999**, *837*, 65-74.
- (36) Madden, J. E.; Haddad, P. R. *J. Chromatogr. A* **1999**, *850*, 29-41.
- (37) Martin, M.; Eon, C.; Guiochon, G. *J. Chromatogr.* **1974**, *99*, 357.
- (38) Martin, M.; Eon, C.; Guiochon, G. *J. Chromatogr.* **1975**, *108*, 229.
- (39) Martin, M.; Eon, C.; Guiochon, G. *J. Chromatogr.* **1975**, *110*, 213.
- (40) Ells, B.; Wang, Y.; Cantwell, F. F. *J. Chromatogr. A* **1999**, *835*, 3-18.
- (41) Li, J. Y.; Litwinson, L. M.; Cantwell, F. F. *J. Chromatogr. A* **1996**, *726*, 25-36.
- (42) Li, J. Y.; Cantwell, F. F. *J. Chromatogr. A* **1996**, *726*, 37-44.



## CHAPTER TWO. Effect of Temperature on Retention and Selectivity in Ion Chromatography of Anions \*

One of the approaches outlined in the introduction for high-speed IC is the use of elevated temperatures. However, temperature also affects retention in IC, which could potentially impact on high-speed analysis. Thus, as background to the later work on high temperature high-speed separations, Chapters Two and Three explore the use of temperature as a variable for selectivity control in IC.

### 2.1 Introduction

Selectivity is of critical importance in developing a chromatographic method.<sup>1</sup> Significant changes in selectivity are obtained with modifications in the stationary phase type and mobile phase.<sup>2, 3</sup> Therefore, ion exchange selectivity is usually adjusted by changing the stationary phase<sup>4</sup>, as was discussed in detail in Section 1.3.3. Unfortunately, this approach is expensive. Although modification of the eluent is a cheaper and much simpler method, it has its disadvantages. Firstly, as discussed in Section 1.3.3.3, eluent concentration does not alter the selectivity between analytes that have the same charge.<sup>5</sup> Secondly, optimization becomes increasingly difficult as the number of components in the eluent increases (*e.g.*, carbonate/bicarbonate eluents).<sup>6</sup> Finally, in suppressed IC the choice of eluents is limited to those that can be suppressed (*i.e.*, hydroxide, carbonate).

---

\* A version of this chapter has been published. Hatsis, P.; Lucy, C.A. *Journal of Chromatography A* **2001**, *921*, 3-11.

In recent years temperature has become an increasingly popular parameter in HPLC method development, particularly for reversed-phase liquid chromatography (RPLC).<sup>3</sup> The attractive features of using temperature for optimizing a chromatographic method are: it is experimentally easy to implement; it is applicable to both neutral and charged analytes; and it is easy to model. Despite the growing use of temperature in RPLC, temperature has been a relatively unexploited variable in IC. However, Rey and Pohl did demonstrate that column temperature was an effective means of increasing the separation between monovalent and divalent cations on a Dionex CS12A stationary phase.<sup>7</sup> Similarly, Pirogov *et al.* were able to alter the selectivity in a separation of halides by increasing the temperature from 25 °C to 60 °C.<sup>8</sup> Further, a number of workers have noted changes in elution order upon altering the temperature of a separation.<sup>9, 10</sup>

This chapter focuses on the effect of temperature on the retention factors of inorganic anions on two commercially available IC columns (Dionex AS11 and AS14). The merits of using temperature to alter the selectivity of a separation are then discussed.

## **2.2 Experimental**

### **2.2.1 Apparatus**

A Beckman System Gold Model 125 dual piston pump (Beckman, Fullerton, CA) was used to pump eluent at a flow rate of 0.3 mL/min. Injections were performed manually with a Rheodyne 9125 (Rheodyne, Cotati, CA) six-port injection valve fit with a 2  $\mu$ L loop. All anion exchange separations were performed with a Dionex AS11 strong base anion exchanger (2 mm i.d. x 250 mm) or a Dionex AS14 strong base anion exchanger (2 mm i.d. x 250 mm) (Dionex, Sunnyvale, CA). The AS11 is a more

hydrophilic ion exchanger than the AS14 and is therefore more amenable to the separation of chaotropic species (Section 1.3.3.4.4). Separations of organic analytes were performed with a Waters Delta Pak C18 column (2 mm i.d. x 150 mm) (Waters, Milford, MA, USA). Connecting tubing was 0.005 " i.d. polyetheretherketone (PEEK, Upchurch Scientific, Oak Harbor, WA).

All anion exchange experiments were performed using suppressed conductivity detection with a Dionex AMMS-II suppressor and CDM-3 conductivity detector. A constant pressure pump ( $\cong$  15 psi) was used to pump regenerant (50 mM sulfuric acid) at a flow rate of 5 mL/min through the suppressor. Organic analytes were detected with a Beckman 166 ultraviolet absorbance detector set to 214 nm. Data was collected using a Dionex AI-450 data acquisition system interfaced to a 486 microcomputer.

The column temperature was controlled to within 0.1 °C using an Eppendorf CH-30 (Alltech, Deerfield, IL) column heater equipped with a mobile phase preheater and controlled by an Eppendorf TC-50. Connections to/from the column heater tripled the amount of connecting tubing compared to what would have normally been used. However, the efficiencies achieved with the oven in place were equivalent at the 95 % confidence level to those observed at room temperature (23 °C) without the column oven or extra connecting tubing.

### **2.2.2 Reagents**

All reagent solutions were prepared using distilled deionized water (Nanopure Water System, Barnsted, Chicago, IL, USA). All chemicals were reagent grade or better. Stock solutions of inorganic anions were prepared ( $\cong 10^{-2}$  M) and diluted to the desired concentration ( $\cong 10^{-5}$  M) before use. Bromate (Fisher, Nepean, Canada), nitrite (BDH

Inc., Toronto, Canada), thiosulfate (Anachemia, Toronto, Canada), perchlorate (Anachemia), iodide (BDH), sulfate (BDH) and phosphate (Fisher) were used as their sodium salts. Iodate (ACP Inc., Montreal, Canada), bromide (Fisher), nitrate (BDH), oxalate (Matheson, Coleman & Bell, Norwood, Ohio, USA) and thiocyanate (Fisher) were used as their potassium salts. Sodium carbonate, sodium bicarbonate and sodium hydroxide were obtained from BDH.

Benzonitrile, methyl benzoate, ethyl benzoate, anisole and *p*-xylene were obtained from Aldrich (Milwaukee, WI, USA). Stock solutions ( $\cong 10^{-2}$  M) were prepared in acetonitrile and diluted to the desired concentration ( $\cong 10^{-5}$  M) with water before use. Acetonitrile was obtained from Fisher (HPLC grade).

### 2.2.3 Procedure

Two eluents were used for all of the anion exchange separations in this study: bicarbonate/carbonate and hydroxide. Carbonate eluents were filtered through a 0.45  $\mu\text{m}$  filter before use and were degassed by continually sparging with helium. Hydroxide eluents were prepared fresh each day by adding the appropriate amount of a 50 % (w/w) sodium hydroxide solution to one litre of degassed, filtered (0.45  $\mu\text{m}$  filter) 18 M $\Omega$  water (Barnstead Nanopure, Chicago, IL). Eluents were stored in plastic bottles. Carbonate contamination was minimized by continually sparging with helium.

Temperature studies were conducted from 27 °C to 60 °C. Temperatures higher than 60 °C were not examined so as to avoid potential damage to the columns. The maximum temperature was chosen based on the work of others who also used Dionex columns.<sup>7, 11</sup> Also, according to Poppe and Kraak,<sup>12</sup> the existence of temperature gradients in a column adversely affects the efficiency of a separation. Therefore, the

column was allowed to equilibrate for approximately 30 minutes at the desired temperature. Also, narrow diameter columns were used to reduce the equilibration time of the system and minimize any temperature gradients in the column. The column void time was measured at each temperature using the water dip.

#### 2.2.4 Calculations

Data analysis was performed using Microsoft Excel 97 software. The *Regression* function in the *Data Analysis Tool Pak* was used to obtain linear regression coefficients for the effect of temperature on retention.

Retention times for severely tailing peaks were determined by calculating the peak's first statistical moment using the formula:

$$\text{First Moment} = \frac{1}{\text{Area}} \int_0^{\infty} tCdt \quad (2-1)$$

where *Area* is the area of the peak (zeroth moment), *t* is time and *C* is the concentration at any time *t*.<sup>13, 14</sup> In using Equation 2-1, it was assumed that the detector response at time *t* is equivalent to *C*.

Retention factors, *k*, were calculated according to the formula:

$$k = \frac{t_r - t_o}{t_o - t_{ex}} \quad (2-2)$$

where *t<sub>r</sub>* is the retention time, *t<sub>o</sub>* is the apparent column void time (measured at the water dip) and *t<sub>ex</sub>* is the time spent by an analyte in the injector, connecting tubing and detector.

Peak efficiencies were calculated with the Foley-Dorsey equation:

$$N \approx \frac{41.7 \left( \frac{t_r}{w_{0.1}} \right)^2}{A_s + 1.25} \quad (2-3)$$

where  $N$  is the efficiency,  $t_r$  is retention time,  $w_{0.1}$  is the width at 10% height and  $A_S$  is the asymmetry factor for the peak calculated at 10% of the peak height. Use of this equation takes into account asymmetry in the peak.<sup>15, 16</sup>

## 2.3 Results and Discussion

### 2.3.1 Van't Hoff Plots

The effect of temperature on chromatographic retention is described by the general thermodynamic relationship governing equilibria:<sup>17</sup>

$$\frac{d \ln k}{dT} = \frac{\Delta H^\circ}{RT^2} \quad (2-4)$$

where  $k$  is the retention factor,  $T$  is the temperature in Kelvin,  $R$  is the universal gas constant and  $\Delta H^\circ$  is the enthalpy of exchange. If  $\Delta H^\circ$  is independent of temperature (which is usually true over a small temperature range), and the separation is performed under isocratic conditions, Equation 2-4 can be integrated to:

$$\ln k = \text{const}_1 - \text{const}_2/T \quad (2-5)$$

where  $\text{const}_1$  and  $\text{const}_2$  are constants for a particular analyte. According to Equation 2-5, a plot of  $\ln k$  against the reciprocal of temperature (*i.e.*, a van't Hoff plot) will be linear. As Equation 2-5 has a similar form to the Linear Solvent Strength model, computer-modelling programs such as Drylab can readily be used to model the effect of temperature.<sup>3</sup> This simplicity of modelling coupled with the instrumental ease of controlling column temperature has led to the increased use of temperature in optimizing RPLC separations.<sup>3, 18-21</sup>

Previous studies have observed that retention in ion exchange chromatography obeys the simple thermodynamic relationships given in equations 2-4 and 2-5.<sup>11, 22</sup> For instance, van't Hoff plots were linear over 25 to 56 °C for metal ions retained on a Wescan cation exchange column.<sup>22</sup> Similarly, Smith *et al.* observed linear van't Hoff plots for common anions on a Dionex AS-4A column over the range 10 to 75 °C.<sup>11</sup> However, over more extended temperature ranges (0 °C – 150 °C) some nonlinearity in van't Hoff plots has been observed.<sup>9</sup> This minor nonlinearity in temperature dependence is similar to that observed by Mao and Carr in their studies of RPLC over a temperature range of 30 to 130 °C.<sup>23</sup>

Figures 2-1 and 2-2 show typical van't Hoff plots for anions separated on the Dionex AS11 and AS14 anion exchange columns studied herein. Regression parameters for the anions separated on both columns are presented in Table 2-1. While correlation coefficients are quoted in Table 2-1, they are poor measures of linearity. A better measure of the significance of a linear regression is the *p*-value.<sup>24</sup> A *p*-value is the smallest level of significance at which a linear relationship describes a particular data set. For example, a *p*-value of less than 0.05 indicates a significant linear relationship at the 95% confidence level. Significant linear relationships were observed over the 27-60°C range for all anions studied, except for iodate and bromate on the AS14. For these anions the *p*-value of the van't Hoff plots corresponded to the 90% confidence level. Thus, over the temperature range studied, van't Hoff plots on these IC columns can be considered linear.

Figure 2-3 shows van't Hoff plots for a wide range of organic analytes (*i.e.*, different functional groups) separated on a RPLC column. The corresponding regression

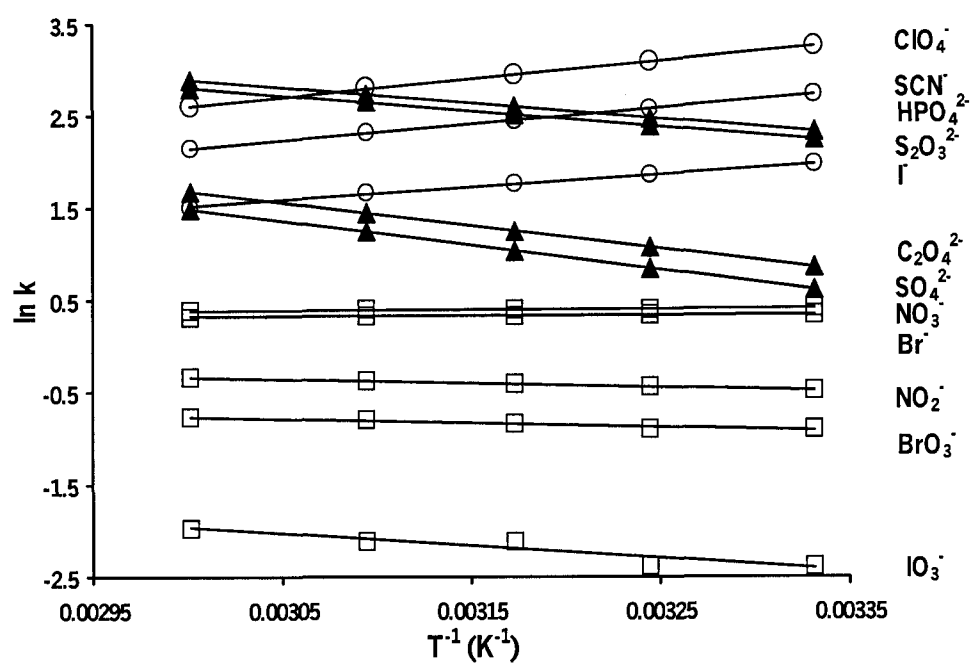


**Figure 2-1.** van't Hoff plots for anions separated on a Dionex AS11 column.

**Experimental Conditions:** 12 mM hydroxide eluent at 0.3 mL/min, 27 °C to 60 °C.



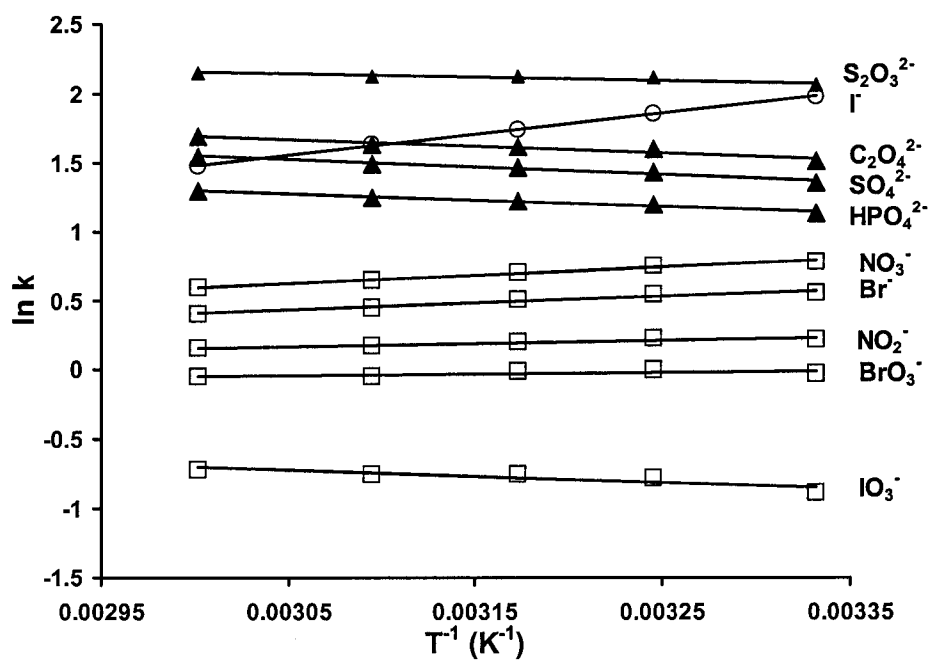


**Figure 2-2.** van't Hoff plots for anions separated on a Dionex AS14 column. **Experimental Conditions:** 3.5 mM carbonate/ 1 mM bicarbonate eluent at 0.3 mL/min, 27 °C to 60 °C.

**Table 2-1.** Slopes, standard deviations, correlation coefficients and *p*-values from the van't Hoff plots of various anions.

	AS11			AS14		
	Slope	$r^2$	<i>p</i> -value	Slope	$r^2$	<i>p</i> -value
IO <sub>3</sub> <sup>-</sup>	-1300 ± 300	0.879	0.018	-200 ± 200	0.901	0.050
BrO <sub>3</sub> <sup>-</sup>	-500 ± 100	0.942	0.006	190 ± 20	0.863	0.071
NO <sub>2</sub> <sup>-</sup>	-400 ± 100	0.995	0.000	310 ± 20	0.987	0.007
Br <sup>-</sup>	100 ± 40	0.898	0.014	590 ± 20	0.993	0.004
NO <sub>3</sub> <sup>-</sup>	100 ± 40	0.898	0.014	670 ± 10	0.992	0.004
SO <sub>4</sub> <sup>2-</sup>	-2600 ± 400	0.999	0.000	-460 ± 20	0.988	0.006
C <sub>2</sub> O <sub>4</sub> <sup>2-</sup>	-2500 ± 300	0.999	0.000	-400 ± 90	0.941	0.030
I <sup>-</sup>	1400 ± 100	0.997	0.000	1530 ± 50	0.998	0.001
S <sub>2</sub> O <sub>3</sub> <sup>2-</sup>	-1700 ± 200	0.999	0.000	-170 ± 30	0.928	0.037
PO <sub>4</sub> <sup>3-</sup>	-1700 ± 200	0.998	0.001	-440 ± 10	0.987	0.007
SCN <sup>-</sup>	1800 ± 200	0.999	0.000	-	-	-
ClO <sub>4</sub> <sup>-</sup>	2000 ± 200	0.999	0.000	-	-	-

**Experimental conditions:** Dionex AS11 column, 12 mM hydroxide eluent at 0.3 mL/min and a Dionex AS14 column, 3.5 mM carbonate/1 mM bicarbonate eluent at 0.3 mL/min. 2 µL injection. Temperature range of 27 °C to 60 °C. The standard deviations are those for the slopes obtained from three replicate runs and are not those for the regression.

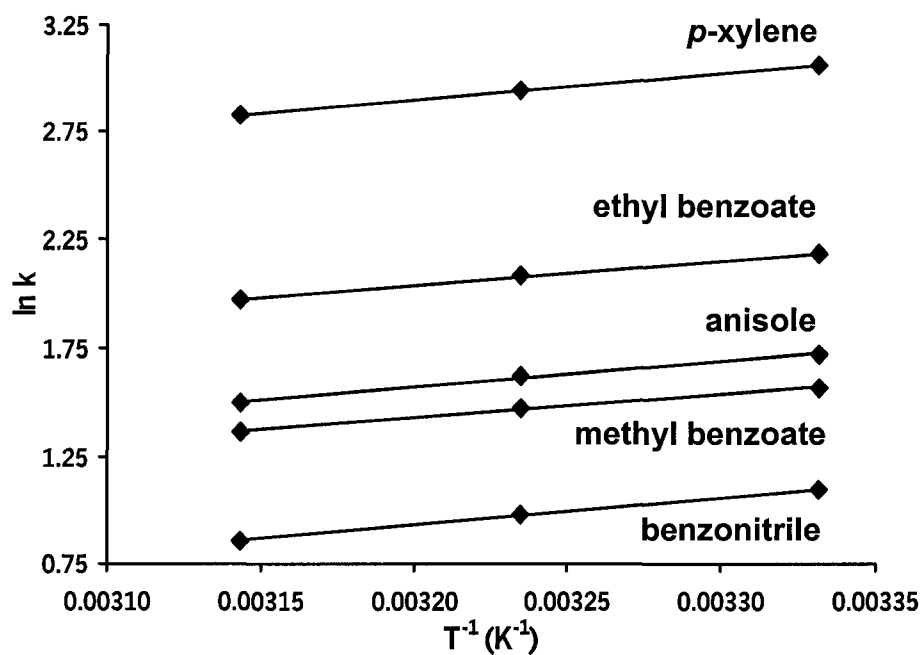


**Figure 2-3.** van't Hoff plots for organic compounds separated on a reversed-phase C<sub>18</sub> column. **Experimental Conditions:** 40/60 acetonitrile/water eluent at 0.2 mL/min, 27 °C to 45 °C.

parameters are shown in Table 2-2. The dominant feature of Figure 2-3 is that the slope of the van't Hoff plot for each analyte is positive, such that retention always decreases with increasing temperature. This is in direct contrast to Figures 2-1 and 2-2 where the slopes of the van't Hoff plots are both negative and positive. Figure 2-3 is consistent with other investigations on the effect of temperature on retention in RPLC, *i.e.*, only exothermic behaviour is observed.<sup>21, 23, 25, 26</sup> That is, retention in RPLC always decreases with increasing temperature. However, in Figures 2-1 and 2-2, both exothermic (decreasing retention with increasing temperature) and endothermic (increasing retention with increasing temperature) behaviour is seen. Similar behaviour has been observed for cation exchange<sup>22</sup> and anion exchange on a Dionex AS-4A column.<sup>11</sup>

It has been stated that the standard enthalpy changes for ion exchange are small (<2 kcal/mol).<sup>27</sup> However, the slopes of the van't Hoff plots in Table 2-1 range from -2600 to +2000 K<sup>-1</sup>. In contrast the slopes of van't Hoff plots for organic non-electrolytes in RPLC on carbon-coated zirconia are around +1900 K<sup>-1</sup> (calculated from van't Hoff plots in Ref. <sup>23</sup>) and about +1200 K<sup>-1</sup> for the analytes shown in Figure 2-3. Thus, the temperature dependence can be as pronounced or more pronounced in IC than in RPLC. However, it is the range of the enthalpies of retention that are important in achieving selectivity changes. In RPLC the enthalpies of retention vary only 10-15% (calculated from van't Hoff plots in Ref. <sup>23</sup> and Table 2-2). Much greater variation in enthalpy is evident in Table 2-1. Thus, as has been stated previously by Mao and Carr,<sup>23</sup> temperature can have a much larger effect on the selectivity of electrolytes than nonelectrolytes. In the following sections, the experimental variables that affect the enthalpy of retention

**Table 2-2.** Slopes, standard deviations, correlation coefficients and *p*-values from the van't Hoff plots of various organic compounds.

	<b>Slope</b>	<b>r<sup>2</sup></b>	<b><i>p</i>-value</b>
Benzonitrile	1250 ± 40	0.999	0.019
Methyl benzoate	1080 ± 50	0.998	0.027
Anisole	1180 ± 70	0.996	0.040
Ethyl benzoate	1120 ± 60	0.997	0.034
<i>p</i> -Xylene	1260 ± 20	0.999	0.001

**Experimental conditions:** Waters Delta Pak C<sub>18</sub> column using a 40/60 acetonitrile/water eluent at 0.2 mL/min. A 2 μL injection was used. Detection wavelength was 214 nm. The van't Hoff plots covered a temperature range of 27 °C to 45 °C. The standard deviations are those for the slopes obtained from three replicate runs and are not those for the regression.

will be investigated, and some general trends in the temperature dependence of anion retention will be identified.

### 2.3.2 Effect of Eluent on Temperature Dependence of Retention

Fortier *et al.* noted that the temperature behaviour of cations changed with the eluent type.<sup>22</sup> In this work the effect of temperature on retention was studied on an AS11 column using 12 mM hydroxide and 7 mM carbonate/1mM bicarbonate. These eluents yielded comparable retention at 27°C. Table 2-3 shows the temperature dependence in terms of the slopes of the van't Hoff plots for various anions using these two eluents. Significant differences in the temperature dependence of retention are evident upon changing the eluent. In Table 2-3, shifting from a hydroxide to a carbonate eluent caused all of the slopes to become larger (more positive). That is, the exchange enthalpies became more exothermic. For anions such as perchlorate and thiocyanate that displayed exothermic behaviour with hydroxide, their retention decreased more dramatically with increasing temperature when a carbonate eluent was used. In contrast, anions such as phosphate and thiosulfate which displayed endothermic behaviour with hydroxide (increasing retention with increasing temperature) became weakly exothermic with carbonate. In other words, their retention now decreases with an increase in temperature.

The temperature dependence of anion retention on an AS14 column was also studied with a 32 mM hydroxide eluent instead of a 1 mM bicarbonate/3.5 mM carbonate eluent (Table 2-3). These eluents also yielded comparable retention at 27°C. Changes in the temperature dependence of anion retention were also seen on the AS14 column when the eluent was changed. In this case, the temperature behaviour of the weakly retained singly charged anions did not change significantly. However, the temperature behaviour

**Table 2-3.** Slopes of van't Hoff plots for anions separated using different eluents.

	AS11 Column			AS14 Column		
	Slope (OH <sup>-</sup> )	Slope (CO <sub>3</sub> <sup>2-</sup> )	Δ (Slope)	Slope (CO <sub>3</sub> <sup>2-</sup> )	Slope (OH <sup>-</sup> )	Δ (Slope)
IO <sub>3</sub> <sup>-</sup>	-1300 ± 500	500 ± 100	1800	-200 ± 400	-230 ± 50	-30
BrO <sub>3</sub> <sup>-</sup>	-500 ± 200	800 ± 50	1300	190 ± 40	180 ± 20	-10
NO <sub>2</sub> <sup>-</sup>	-400 ± 200	700 ± 20	1100	310 ± 40	300 ± 200	-30
Br <sup>-</sup>	100 ± 70	1200 ± 50	1100	590 ± 40	600 ± 400	0
NO <sub>3</sub> <sup>-</sup>	100 ± 70	1300 ± 50	1200	670 ± 20	700 ± 400	0
SO <sub>4</sub> <sup>2-</sup>	-2600 ± 700	-200 ± 100	2400	-460 ± 40	-400 ± 200	60
C <sub>2</sub> O <sub>4</sub> <sup>2-</sup>	-2500 ± 500	-100 ± 40	2400	-400 ± 200	-300 ± 200	100
I <sup>-</sup>	1400 ± 200	2200 ± 40	800	1530 ± 90	1600 ± 600	70
S <sub>2</sub> O <sub>3</sub> <sup>2-</sup>	-1700 ± 400	700 ± 100	2400	-170 ± 60	760 ± 400	930
PO <sub>4</sub> <sup>3-</sup>	-1700 ± 400	300 ± 100	2000	-440 ± 20	-30 ± 200	410
SCN <sup>-</sup>	1800 ± 400	2600 ± 40	800	-	-	-
ClO <sub>4</sub> <sup>-</sup>	2000 ± 400	2800 ± 40	800	-	-	-

**Experimental conditions:** Dionex AS11 column using a 12 mM hydroxide eluent and a 7 mM carbonate/1 mM bicarbonate eluent or a Dionex AS14 column using a 3.5 mM carbonate/1 mM bicarbonate and a 32 mM hydroxide eluent. A flow rate of 0.3 mL/min was used. Injection volume was 2 μL. The slopes were determined over a temperature range of 27 °C to 60 °C. The standard deviations are the 95 % confidence intervals based on three replicate runs and are not those for the regression.

of phosphate became less endothermic and thiosulfate became completely exothermic.

The temperature dependence of retention for anions separated on the AS11 column with a 12 mM hydroxide and a 32 mM hydroxide eluent is given in Table 2-4. The 32 mM hydroxide eluent produced smaller (more negative) slopes for the van't Hoff plots of all anions than the 12 mM hydroxide eluent. However, these differences are not statistically significant at the 95% confidence level. Therefore, the effect of eluent type is more significant than the effect of eluent concentration.

### **2.3.3 Effect of Stationary Phase on Temperature Dependence of Retention**

To investigate the effect of the stationary phase on the temperature behaviour of retention, a 32 mM hydroxide eluent was used with both the AS11 and the AS14 column. The AS11 is a hydrophilic anion exchanger with alkanol quaternary ammonium groups, whereas the AS14 is hydrophobic and contains alkyl quaternary ammonium groups. Therefore, these stationary phases have different selectivity (Section 1.3.3.4.4). Table 2-5 gives the temperature dependences observed for each column. In general, retention on the AS14 column is more exothermic than that on the AS11 column. That is, anions such as nitrate whose temperature behaviour is weakly exothermic on the AS11 column, becomes more exothermic on the AS14 column. Phosphate shows strongly endothermic behaviour on the AS11 column, but almost no temperature dependence on its retention on the AS14 column.

In comparing Tables 2-3 and 2-5, changing the column type has less effect on the temperature dependence of singly charged anions than does changing the eluent type. However, for multiply charged anions the effect of column type on temperature



**Table 2-4.** Changes in the slopes of the van't Hoff plots of anions caused by an increase in eluent concentration.

Anion	Slope (12 mM OH <sup>-</sup> )	Slope (32 mM OH <sup>-</sup> )	Δ (Slope)
NO <sub>3</sub> <sup>-</sup>	100 ± 70	100 ± 200	0
SO <sub>4</sub> <sup>2-</sup>	-2600 ± 800	-3100 ± 400	-500
C <sub>2</sub> O <sub>4</sub> <sup>2-</sup>	-2500 ± 500	-3000 ± 700	-500
I <sup>-</sup>	1400 ± 200	1200 ± 400	-200
S <sub>2</sub> O <sub>3</sub> <sup>2-</sup>	-1700 ± 400	-1900 ± 400	-200
PO <sub>4</sub> <sup>3-</sup>	-1700 ± 400	-2800 ± 700	-1100
SCN <sup>-</sup>	1800 ± 400	1500 ± 400	-300
ClO <sub>4</sub> <sup>-</sup>	2000 ± 400	1800 ± 500	-200

**Experimental conditions:** Dionex AS11 column with 12 mM and 32 mM hydroxide as eluent at 0.3 mL/min. A 2 μL injection was used. Slopes were determined over a temperature range of 27 °C to 60 °C. The standard deviations are the 95 % confidence intervals based on three replicate runs and are not those for the regression.

**Table 2-5.** Comparison of the slopes of van't Hoff plots on Dionex AS11 and AS14 columns.

Anion	Slope (AS11)	Slope (AS14)	$\Delta$ (Slope)
NO <sub>3</sub> <sup>-</sup>	100 ± 200	700 ± 200	600
I <sup>-</sup>	1200 ± 400	1600 ± 500	400
SO <sub>4</sub> <sup>2-</sup>	-3100 ± 400	-400 ± 400	2700
C <sub>2</sub> O <sub>4</sub> <sup>2-</sup>	-3000 ± 700	-300 ± 200	2700
PO <sub>4</sub> <sup>3-</sup>	-2800 ± 700	0 ± 400	2800
S <sub>2</sub> O <sub>3</sub> <sup>2-</sup>	-1900 ± 400	800 ± 200	2700

**Experimental conditions:** Separations were performed on each column with 32 mM hydroxide as eluent at 0.3 mL/min. A 2  $\mu$ L injection was used. Slopes were determined over a temperature range of 27 °C to 60 °C. The standard deviations are the 95 % confidence intervals based on three replicate runs and are not those for the regression.

dependence is greater than that of eluent type. Therefore, the stationary phase has a significant effect on the temperature behaviour of anions, and one that is different from that of eluent type.

### 2.3.4 Effect of Temperature on Selectivity

The van't Hoff plots in Figures 2-1 and 2-2 reveal that temperature significantly affects the selectivity of an ion exchange separation. Therefore, temperature can be used as an aid in method development. Moreover, if a model were available that can explain (or predict) the effect of temperature on selectivity, it would greatly facilitate method development. A previously cited model for ion exchange is that by H.P. Gregor.<sup>27, 28</sup> Gregor proposed the following equation:<sup>27, 28</sup>

$$\ln K_{A,B} = \frac{\Pi}{RT} (|z_A|v_B^* - |z_B|v_A^*) \quad (2-6)$$

where  $K_{A,B}$  is the selectivity constant of  $A$  over  $B$ ,  $\Pi$  is the swelling pressure,  $z_A$  is the charge on ion  $A$ ,  $z_B$  is the charge on ion  $B$ , and  $v_A^*$  and  $v_B^*$  are the molar solvated volumes for ions  $A$  and  $B$ , respectively. According to Equation 2-6, the retention of ion  $A$  increases directly with swelling pressure or charge, whereas it decreases with an increase in molar solvated volume. Gregor went further and proposed that changes in the selectivity coefficient as a function of temperature can be accounted for through the  $(|z_A|v_B^* - |z_B|v_A^*)$  term.<sup>28</sup> In other words, selectivity changes are caused by differences in the relative hydration of ions  $A$  and  $B$  as the temperature is varied. Unfortunately this approach requires values of molar solvated volume at different temperatures. Such values are not readily available. Consequently, this approach is useful only on a qualitative basis (as was used by Gregor<sup>28</sup>) for understanding the effect of temperature on selectivity, and reliable predictions cannot be made.

Although the effect of temperature on the retention of a particular anion cannot be predicted, a number of features can be extracted from the van't Hoff plots. Based on these features, conclusions can be made as to what effect temperature may have on the selectivity between specific anions. In Figures 2-1 and 2-2, three groups of behaviour are evident. These groupings are summarized in Table 2-6. Within a group the temperature behaviour is approximately the same, as evidenced by the more or less parallel lines in Figures 2-1 and 2-2. Since the effect of temperature within a group is approximately the same, temperature has little effect on the selectivity between those anions. However, temperature can cause selectivity changes between anions from different groups. For example as shown in Figure 2-4A, thiosulfate and phosphate (Group 2) elute before thiocyanate (Group 3) at 27 °C. Increasing the column temperature (Figure 2-4B) causes thiocyanate to be eluted before thiosulfate and phosphate, without affecting the selectivity between thiosulfate and phosphate. This illustrates that temperature can be used to tailor the selectivity of a separation.

Similar group behaviour is evident in the temperature dependence of anions on the AS11 column with a 32 mM hydroxide eluent. Figure 2-5 shows chromatograms obtained at 27 °C and 60 °C. Although the retention of the Group 3 anions (iodide, thiocyanate, perchlorate) decreased dramatically with temperature, there is no change in selectivity between these anions. Further, the selectivity between anions in Group 2 stayed the same. However, the selectivity of the Group 2 anions (sulfate, oxalate, phosphate, thiosulfate) changed with respect to nitrate (Group 1). It is apparent that group-wise changes in elution order can be obtained by raising the column temperature.

**Table 2-6.** Groups of anions showing similar temperature behaviour.

	<b>Group Name</b>	<b>Examples</b>	<b>Characteristics</b>
1	Weakly Retained Anions	Iodate, Bromate, Nitrite, Bromide, Nitrate	Retention increases or decreases with increasing temperature
2	Multiply Charged Anions	Sulfate, Oxalate, Phosphate, Thiosulfate	Retention significantly increases with increasing temperature
3	Strongly Retained Singly Charged Anions	Iodide, Thiocyanate, Perchlorate	Retention significantly decreases with increasing temperature

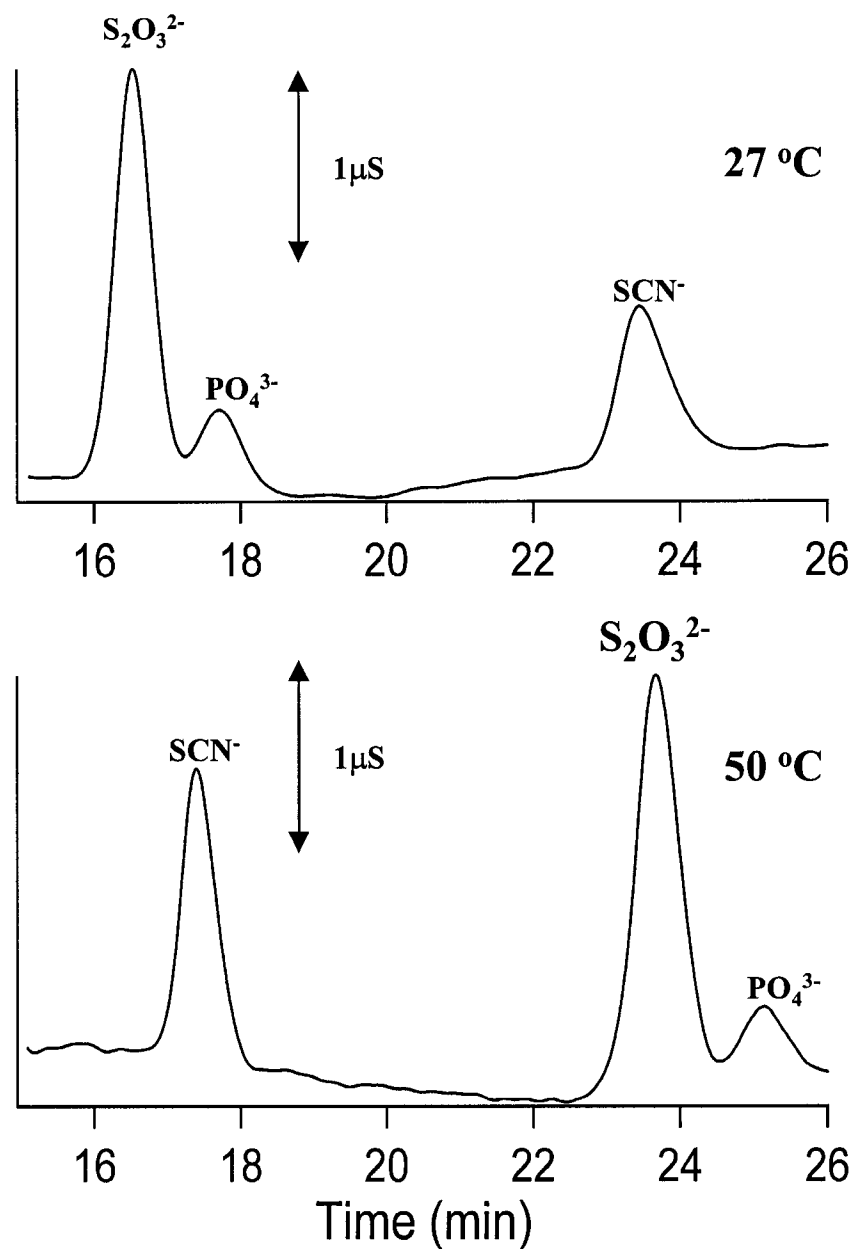


**Figure 2-4.** Changes in selectivity caused by increased temperature.

**Experimental Conditions:** Dionex AS11 column, 12 mM hydroxide at 0.3 mL/min, 2  $\mu\text{L}$  injection.

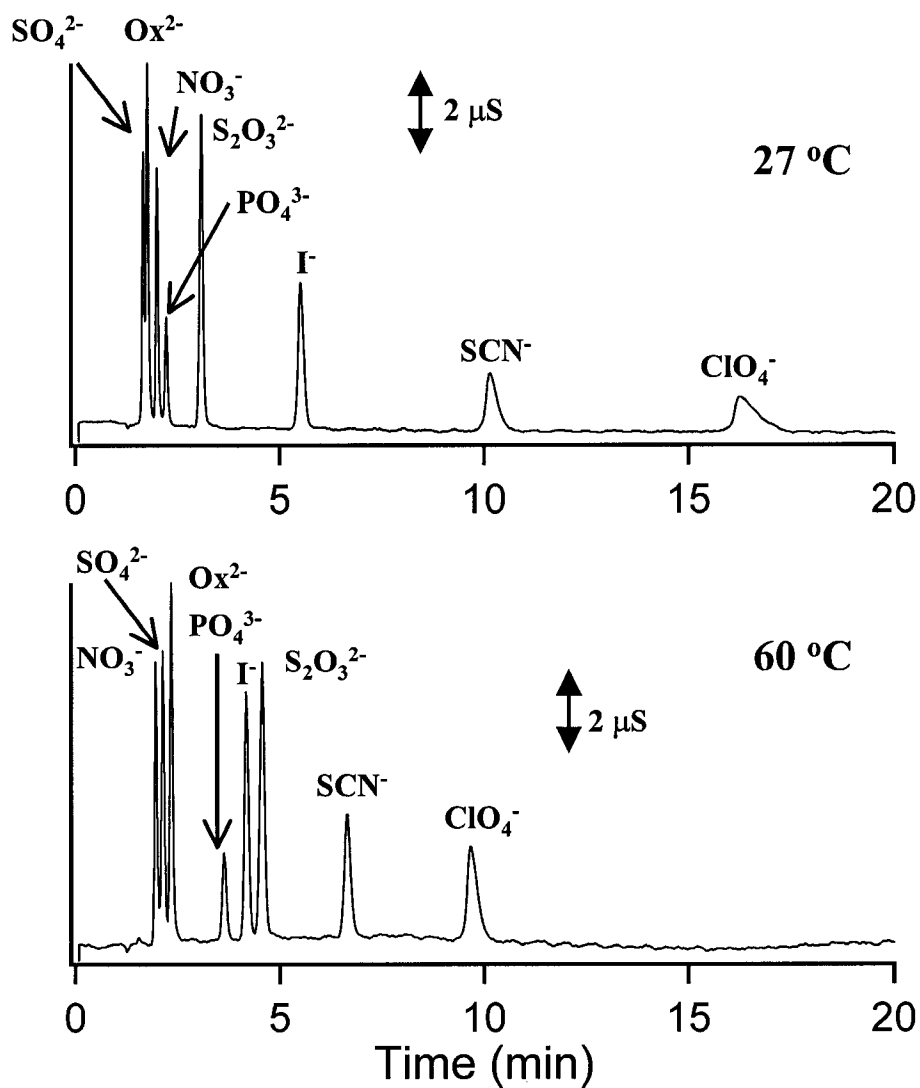


**Figure 2-5.** Elution order changes caused by increased temperature.

**Experimental Conditions:** Dionex AS11 column using a 32 mM hydroxide eluent, 0.3 mL/min, 2 μL injection. Ox<sup>2-</sup> = oxalate

### 2.3.5 Changes in Efficiency and Peak Asymmetry as a Function of Temperature

There are a number of reports in the literature showing improvements in efficiency upon an increase in column temperature. This is true for RPLC<sup>29-33</sup> and ion exchange.<sup>4, 7, 34</sup> The improvement noted in efficiency upon an increase in column temperature is attributed to a reduction in solvent viscosity (Section 1.2.4.4). As a result of the decrease in solvent viscosity, diffusion inside the stagnant mobile phase will be enhanced. Further, the non-uniform flow profile (*i.e.*, resistance to mass transfer in the mobile phase) will be more effectively relaxed due to the improvement in diffusion. In addition, the desorption kinetics of stationary phases improve at elevated temperatures. These effects manifest themselves in a lowered *C*-term in the van Deemter equation and therefore a decrease in plate height and an increase in efficiency (Section 1.2.4). Apart from improvements in efficiency, elevated temperatures can result in improvements in peak shape.<sup>31, 35</sup>

In the case of the Dionex columns used in this work, it was not clear if significant improvements in column efficiency would be obtained. This is due to the pellicular nature of Dionex stationary phases that causes them to already have excellent mass-transfer characteristics (Section 1.3.3.4.1).<sup>36, 37</sup> Table 2-7 shows the efficiency for various analytes at different temperatures. The efficiency improved for all anions upon increasing the column temperature. These improvements ranged from 18 % for thiosulfate to 100 % for perchlorate. Further, the symmetry of all anion peaks improved, particularly that of the thiocyanate and perchlorate peaks.



**Table 2-7.** The effect of temperature on peak asymmetry and plate number.

Anion	Efficiency (± 200)		Peak Asymmetry (± 0.3)	
	(27 °C)	(60 °C)	(27 °C)	(60 °C)
SO <sub>4</sub> <sup>2-</sup>	5800	7400	0.8	0.9
I <sup>-</sup>	5000	7400	1.4	1.1
S <sub>2</sub> O <sub>3</sub> <sup>2-</sup>	5500	6500	1.1	1.1
SCN <sup>-</sup>	3900	6600	1.6	1.2
ClO <sub>4</sub> <sup>-</sup>	2200	4400	3.3	1.8

**Experimental conditions:** Dionex AS11 column with 32 mM hydroxide as eluent at a flow rate of 0.3 mL/min. A 2 µL injection was used. Standard deviations are based on three replicate measurements.

### 2.3.5 Thermal Stability of Anion Exchangers

The maximum temperature of 60 °C used in this work was chosen based on the work of others who have used Dionex columns. It would be extremely beneficial for high-speed separations if higher temperatures were examined. Unfortunately, literature on classical anion exchangers (*e.g.*, Dowex type resins) has shown that quaternary ammonium anion exchangers are unstable at temperatures much higher than 60 °C due to nucleophilic attack by hydroxide on the benzylic and methyl carbon atoms on the anion exchange site.<sup>38-40</sup> This is shown in Figure 2-6 where the reactivity of the benzylic carbon is depicted in Pathway I and the reactivity of the methyl carbon is depicted in Pathway II. Unfortunately, the reactivity of the benzylic carbon atom is four times as high as the methyl carbon atom.<sup>39, 40</sup> This is rather unfortunate as the anion exchange capacity is completely lost in Pathway I. In Pathway II, the weak base anion exchange capacity is preserved, *i.e.*, a more acidic eluent could be used to protonate the tertiary amine. However, acidic eluents are not compatible with suppressed conductivity detection (Section 1.3.2.2). In this work, retention factors decreased on average 30 % after 4 months of using the columns at above ambient temperatures. Although this is not a catastrophic loss in retention, it does preclude the use of elevated temperatures for achieving high-speed anion separations.

## 2.4 Conclusions

This chapter explored the effect of temperature on the retention of various inorganic anions on two commercially available IC columns. Retention in IC can be an endothermic or exothermic process. Thus significant selectivity changes can be achieved

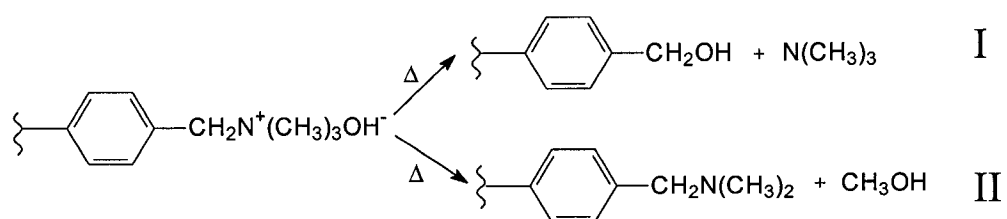


**Figure 2-6.** Degradation pathways of anion exchangers at elevated temperatures and basic solution.

by varying the column temperature. However, the anions studied were found to cluster in groups of behaviour. Namely, weakly retained singly charged anions behaved as one group, multiply charged anions behaved as another group, and the strongly retained singly charged anions behaved as yet another group. Altering the column temperature failed to change the selectivity of anions within a group. However, selectivity changes were seen for anions in different groups, reversing the elution order in some cases. Thus, column temperature can be an effective variable to alter IC selectivity in selected cases.

However, temperature is not a variable that is well suited to the high-speed separation of anions. Firstly, the endothermic retention behaviour of some anions (*e.g.*, sulfate) causes an increase in retention at elevated temperatures. This would mitigate some of the improvements in analysis time from the increase in flow rate at elevated temperatures. Secondly, the limited thermal stability of quaternary ammonium anion exchangers precludes the use of temperatures significantly above ambient. It is for these reasons that an alternative approach for the high-speed separation of anions will be presented in Chapters Five and Six.

## 2.5 References

- (1) Snyder, L. R.; Glajch, J. L.; Kirkland, J. J. *Practical HPLC Method Development*, 2nd ed.; Wiley-Interscience: New York, 1996.
- (2) Zhao, J.; Carr, P. W. *Anal. Chem.* **1999**, *71*, 2623-2632.
- (3) Snyder, L. R. *J. Chromatogr. B* **1997**, *689*, 105-115.
- (4) Pohl, C. A.; Stillian, J. R.; Jackson, P. E. *J. Chromatogr. A* **1997**, *789*, 29.

- (5) Haddad, P. R.; Jackson, P. E. *Ion Chromatography: Principles and Applications*; Elsevier: New York, 1990.
- (6) Madden, J. E.; Avdalovic, N.; Jackson, P. E.; Haddad, P. R. *J. Chromatogr. A* **1999**, *837*, 65-74.
- (7) Rey, M. A.; Pohl, C. A. *J. Chromatogr. A* **1996**, *739*, 87-97.
- (8) Pirogov, A. V.; Obrezkov, O. N.; Shipgun, O. A. *J. Anal. Chem. (Transl. of Zh. Anal. Khim.)* **1997**, *52*, 152-156.
- (9) Kraus, K. A.; Raridon, R. J. *J. Phys. Chem.* **1959**, *63*, 1901-1907.
- (10) Dybczynski, R. *J. Chromatogr.* **1964**, *14*, 79-96.
- (11) Smith, R. G.; Drake, P. A.; Lamb, J. D. *J. Chromatogr.* **1991**, *546*, 139-149.
- (12) Poppe, H.; Kraak, J. C. *J. Chromatogr.* **1983**, *282*, 399-412.
- (13) Yau, W. W. *Anal. Chem.* **1977**, *49*, 395-398.
- (14) Grubner, O. *Anal. Chem.* **1971**, *43*, 1934-1937.
- (15) Bidlingmeyer, B. A.; Warren, F. V. *J. Anal. Chem.* **1984**, *56*, 1583A-1596A.
- (16) Foley, J. P.; Dorsey, J. G. *Anal. Chem.* **1983**, *55*, 730-737.
- (17) Atkins, P. W. *Physical Chemistry*, 6th ed.; Freeman: New York, 1998.
- (18) Zhu, P. L.; Dolan, J. W.; Snyder, L. R. *J. Chromatogr. A* **1996**, *756*, 41-50.
- (19) Zhu, P. L.; Dolan, J. W.; Snyder, L. R.; Djordjevic, N. M.; Hill, D. W.; Lin, J. T.; Sander, L. C.; Van Heukelem, L. *J. Chromatogr. A* **1996**, *756*, 63-72.
- (20) Zhu, P. L.; Snyder, L. R.; Dolan, J. W.; Djordjevic, N. M.; Hill, D. W.; Sander, L. C.; Waeghe, T. J. *J. Chromatogr. A* **1996**, *756*, 21-39.
- (21) Zhu, P. L.; Dolan, J. W.; Snyder, L. R.; Hill, D. W.; Van Heukelem, L.; Waeghe, T. J. *J. Chromatogr. A* **1996**, *756*, 51-62.

- (22) Fortier, N. E.; Fritz, J. S. *Talanta* **1987**, *34*, 415-418.
- (23) Mao, Y.; Carr, P. W. *Anal. Chem.* **2000**, *72*, 110-118.
- (24) Devore, J. L. *Probability and Statistics for Engineering and the Sciences, 4th Ed.*; Duxbury: New York, 1995.
- (25) Wolcott, R. G.; Dolan, J. W.; Snyder, L. R.; Bakalyar, S. R.; Arnold, M. A.; Nichols, J. A. *J. Chromatogr. A* **2000**, *869*, 211-230.
- (26) Djordjevic, N. M.; Houdiere, F.; Fowler, P.; Natt, F. *Anal. Chem.* **1998**, *70*, 1921.
- (27) Helfferich, F. *Ion Exchange*; Dover: Mineola, 1995.
- (28) Gregor, H. P.; Bregman, J. I. *J. Colloid. Sci.* **1951**, *6*, 323.
- (29) Boyes, B. E.; Kirkland, J. J. *Peptide Res.* **1993**, *6*, 249-258.
- (30) Li, J., P.W. Carr *Anal. Chem.* **1997**, *69*, 837-843.
- (31) McCalley, D. V. *J. Chromatogr. A* **2000**, *902*, 311-321.
- (32) Molander, P.; Trones, R.; Haugland, K.; Greibrokk, T. *Analyst* **1999**, *124*, 1137-1141.
- (33) Sheng, G.; Shen, Y.; Lee, M. L. *J. Microcolumn Sep.* **1997**, *9*, 63-72.
- (34) McNeff, C.; Carr, P. W. *Anal. Chem.* **1995**, *67*, 3886-3892.
- (35) Trones, R.; Iveland, A.; Greibrokk, T. *J. Microcolumn. Sep.* **1995**, *7*, 505-512.
- (36) *Dionex Product Selection Guide*; Dionex: Sunnyvale, 1999.
- (37) Antia, F. D.; Horvath, C. *J. Chromatogr.* **1988**, *435*, 1-15.
- (38) Hatch, M. J.; Lloyd, W. D. *J. Appl. Polym. Sci.* **1964**, *8*, 1659-1666.
- (39) Baumann, E. W. *J. Chem. Eng. Data* **1960**, *5*, 376-382.
- (40) Tomoi, M.; Yamaguchi, K.; Ando, R.; Kantake, Y.; Aosaki, Y.; Kubota, H. *J. Appl. Polym. Sci.* **1997**, *64*, 1161-1167.

## **CHAPTER THREE. Evaluation of Column Temperature as a Means to Alter the Selectivity Between Cations in Ion Chromatography\***

### **3.1 Introduction**

Chapter Two examined the use of elevated temperatures for altering the selectivity between anions in IC. The impetus for this work was the recent trend in RPLC to exploit temperature as an additional dimension in optimizing separations. In Chapter Two it was found that retention of anions in IC either increases or decreases with increasing temperature depending on the analyte, stationary phase and eluent. However, retention almost always decreases with increasing temperature in RPLC.<sup>1-5</sup> Consequently, there exists a far greater potential for substantial selectivity changes upon a change in column temperature in IC.<sup>1, 3, 6-8</sup>

In this chapter, the effect of temperature on the selectivity of IC separations is expanded upon. The influence of temperature on the retention of a number of cationic species is modelled, thus providing an understanding of how temperature affects the retention of individual analytes. It was found that the effect of temperature on the retention of inorganic cations is not as pronounced as in the case of inorganic anions. However, temperature shows promise as a separation aid in the determination of small amines in the presence of inorganic cations, which is an important application area in industry.

---

\* A version of this chapter has been published. Hatsis, P.; Lucy, C.A. *Analyst*, **2001**, *126*, 2113-2118.

## 3.2 Experimental

### 3.2.1 Apparatus

A Dionex DX-300 chromatography system (Sunnyvale, CA, USA) was used for all studies in this work. Eluent flow was set at 0.5 mL/min. Two-microlitre injections of sample were performed by means of a Spectra Physics AS3500 autosampler (Thermo Finnigan, Mississauga, Canada) equipped with a Rheodyne 9110 (Rheodyne, Cotati, CA, USA) six-port injection valve. All separations were performed on a Dionex CS12A cation exchanger (3 mm i.d. x 150 mm). Connecting tubing was 0.005" i.d. PEEK (Upchurch Scientific, Oak Harbor, WA, USA).

Detection was suppressed conductivity with a Dionex CDM-3 conductivity detector and a Dionex CSRS-Ultra suppressor. The column was connected to the suppressor with a 15 cm piece of 0.007" i.d. Teflon tubing (Alltech, Deerfield, IL, USA). This tubing was bent into a *U*-shape and immersed in water to lower the temperature of the eluent before it reached the suppressor. Data was collected using a Dionex AI-450 data acquisition system interfaced to a 486 microcomputer running AI-450 Chromatography Automation Software (Version 3.32).

The column temperature was controlled to within 0.1 °C using an Eppendorf CH-30 (Alltech) column heater equipped with a mobile phase preheater and controlled by an Eppendorf TC-50. Connections to/from the column heater tripled the amount of connecting tubing compared to what would have normally been used. However, the efficiencies achieved with the oven in place were comparable at the 95 % confidence level to those observed at room temperature (23 °C) without the column oven or extra connecting tubing.



### 3.2.2 Reagents

All reagent solutions were prepared using distilled deionized water (Nanopure Water System, Barnstead, Chicago, IL, USA). All chemicals were reagent grade or better. Stock solutions of analytes were prepared ( $\cong 10^{-2}$  M) and diluted to the desired concentration ( $\cong 10^{-5}$  M) before use. Lithium (Fisher, Nepean, Canada) and potassium (Fisher) were used as their bromide salts. Sodium (BDH Inc., Toronto, Canada), ammonium (BDH), rubidium (Fisher), cesium (Fisher), magnesium (BDH), calcium (Anachemia, Toronto, Canada) and strontium (Fisher) were used as their chloride salts. Barium nitrate was purchased from Fisher. Ethylamine (hydrochloride salt), propylamine, butylamine, sec-butylamine, tert-butylamine, morpholine, triethanolamine and triethylamine were obtained from Aldrich (Milwaukee, WI, USA) as reagent grade or better. Methanesulfonic acid (99.5%+) was purchased from Aldrich, sulfuric acid was purchased from Anachemia (Reagent ACS) and acetonitrile (HPLC grade) was purchased from Fisher. Caution is needed when working with sulphuric or methanesulfonic acid as they both cause severe burns and are corrosive.

### 3.2.3 Procedure

Methanesulfonic acid eluents were used for most of this work. Sulfuric acid was also used for some studies. Eluents were prepared by weighing out the appropriate amount of acid, transferring it to a volumetric flask and making up to the mark with distilled, deionized water.

The effect of temperature on retention was studied from 27 °C to 60 °C. The maximum temperature was chosen based on the work of others who also used Dionex columns<sup>6, 9</sup>. However, higher temperatures will be examined in Chapter Four. Further,

the column was allowed to equilibrate for approximately 30 minutes at the desired temperature prior to use. This was done to avoid temperature gradients within the column that adversely affect the efficiency of a separation.<sup>10</sup> The elevated temperatures used in this work did not significantly degrade the retention characteristics of the CS12A column. A two-sample  $t$  test<sup>11</sup> was used to compare the retention factors obtained for some alkali and alkaline earth metals when the column was new, to the retention factors obtained after five months of column use. No difference was noted between the two sets of data at the 95% confidence level.

### 3.2.4 Calculations

Data analysis was performed using Microsoft Excel 97 software. The *Regression* function in the *Data Analysis Tool Pak* was used to obtain linear regression coefficients for the effect of temperature on retention.

Retention times for severely tailing peaks were determined by calculating the peak's first statistical moment using the formula:

$$\text{First Moment} = \frac{1}{\text{Area}} \int_0^{\infty} tCdt \quad (2-4)$$

where *Area* is the area of the peak (zeroth moment),  $t$  is time and  $C$  is the concentration at any time  $t$ .<sup>12, 13</sup> In using Equation 2-1, it was assumed that the detector response at time  $t$  is equivalent to  $C$ .

Retention factors,  $k$ , were calculated according to the formula:

$$k = \frac{t_r - t_o}{t_o - t_{ex}} \quad (5-2)$$

where  $t_r$  is the retention time,  $t_o$  is the apparent column void time (measured at the water dip) and  $t_{ex}$  is the time spent by an analyte in the injector, connecting tubing and detector.

Peak efficiencies were calculated with the Foley-Dorsey equation:

$$N \approx \frac{41.7 \left( \frac{t_r}{w_{0.1}} \right)^2}{A_s + 1.25} \quad (2-6)$$

where  $N$  is the efficiency,  $t_r$  is retention time,  $w_{0.1}$  is the width at 10% height and  $A_s$  is the asymmetry factor for the peak calculated at 10% peak height. Use of this equation takes into account asymmetry in the peak.<sup>14, 15</sup>

### 3.3 Results and Discussion

#### 3.3.1 van't Hoff Plots of Metals and Amines

Chapter Two showed that the effect of temperature on retention could be modelled with the general relationship:

$$\ln k = \text{const}_1 - \frac{\text{const}_2}{T} \quad (2-5)$$

where  $k$  is the retention factor and  $\text{const}_1$  and  $\text{const}_2$  are constants for a particular analyte and  $T$  is temperature in Kelvin. Plots of  $\ln k$  vs.  $T^{-1}$  (van't Hoff plot) were linear for all anions studied. Retention of anions was dramatically affected by the column temperature. More specifically, both endothermic (increasing retention with increasing temperature) and exothermic (decreasing retention with increasing temperature) behaviour was seen. Further, the range of temperature dependence of retention (*i.e.*, the

slope of a van't Hoff plot) was found to vary appreciably. Thus, a change in temperature can have a pronounced effect on the selectivity of an anion-exchange separation.

Figure 3-1 shows the van't Hoff plots of alkali and alkaline earth metals separated on the Dionex CS12A stationary phase at various temperatures. The corresponding regression parameters are given in Table 3-1. Significant linear relationships were observed for all cations (except lithium) over the temperature range 27 °C to 60 °C as evidenced by the low  $p$ -values for the regressions. (A  $p$ -value less than 0.05 indicates a significant linear relationship at the 95% confidence interval.)

Examination of Table 3-1 reveals that the slopes of the van't Hoff plots for all metal ions are positive. This means that the retention of cations on the CS12A column is an exothermic process, *i.e.*, decreased retention with increased temperature. It should be mentioned that even though the retention of all ions decreases with increasing temperature, the separation between alkali and alkaline earth metals is enhanced at higher temperatures. This is due to the retention of alkali metals being more sensitive to increasing temperature than that of the alkaline earth metals.

The van't Hoff plots of various amines separated on the CS12A stationary phase are shown in Figure 3-2 and the corresponding regression parameters are given in Table 3-2. All amines showed decreased retention with increased temperature. Some amines, *e.g.*, propylamine and *sec*-butylamine showed very slight curvature in their van't Hoff plots over the temperature range studied. Similar non-linearity has been observed in RPLC<sup>3</sup> and ion exchange<sup>7</sup>. However, significant linear relationships were obtained for the regression of  $\ln k$  vs.  $T^{-1}$  for all amines. Therefore, the data are rectilinear within the small temperature range studied in this work, and so the use of straight lines is justified.

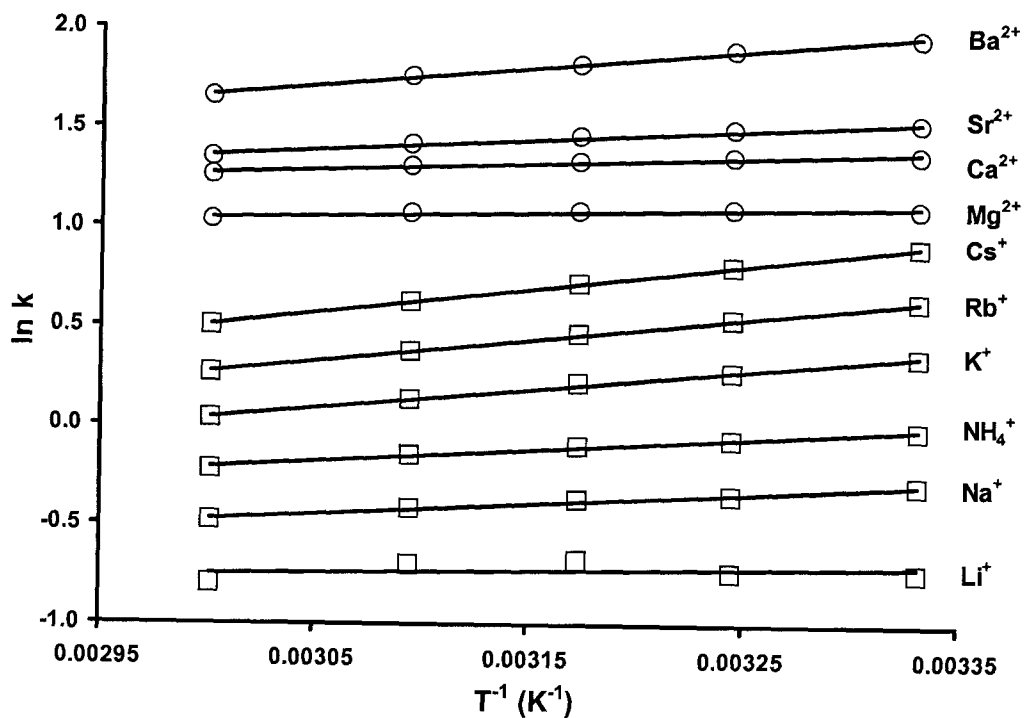


**Figure 3-1.** van't Hoff plots for alkali and alkaline earth metals separated on a Dionex CS12A column. **Experimental Conditions:** 18 mM methanesulfonic acid eluent at 0.5 mL/min. Temperature range: 27 °C to 60 °C.

**Table 3-1.** Slopes, standard deviations, correlation coefficients and *p*-values from the van't Hoff plots of the alkali and alkaline earth metals.

	<b>Slope</b>	<b>r<sup>2</sup></b>	<b><i>p</i>-value</b>
Lithium	120 ± 60	0.120	0.569
Sodium	540 ± 10	0.984	0.000
Ammonium	590 ± 30	0.989	0.001
Potassium	960 ± 40	0.997	0.000
Rubidium	1100 ± 10	0.999	0.000
Cesium	1220 ± 20	0.999	0.000
Magnesium	180 ± 20	0.804	0.039
Calcium	330 ± 30	0.934	0.007
Strontium	520 ± 30	0.978	0.001
Barium	900 ± 40	0.995	0.000

**Experimental conditions:** Dionex CS12A, 18 mM methanesulfonic acid at 0.5 mL/min.

Temperature range: 27 °C to 60 °C. The standard deviations are those for the slopes obtained from three replicate runs and are not those for the regression.

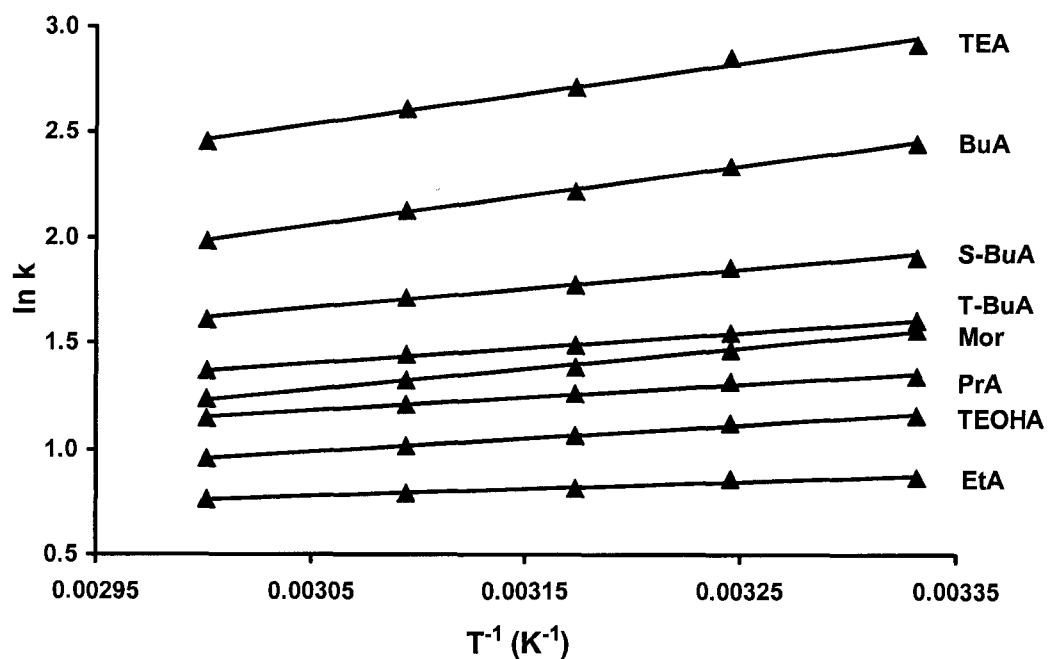


**Figure 3-2.** van't Hoff plots for amines separated on a Dionex CS12A column. **Experimental Conditions:** 13 mM methanesulfonic acid eluent at 0.5 mL/min. Temperature range: 27 °C to 60 °C. EtA = ethylamine, TEOHA = triethanolamine, PrA = propylamine, Mor = morpholine, T-BuA = tert-butylamine, S-BuA = sec-butylamine, BuA = butylamine, TEA = triethylamine.

**Table 3-2.** Slopes, standard deviations, correlation coefficients and *p*-values from the van't Hoff plots of amines.

	<b>Slope</b>	<b>r<sup>2</sup></b>	<b><i>p</i>-value</b>
Ethylamine	380 ± 20	0.940	0.006
Triethanolamine	700 ± 70	0.981	0.001
Propylamine	660 ± 40	0.978	0.002
Morpholine	980 ± 50	0.997	0.000
Tert-butylamine	720 ± 40	0.997	0.002
Sec-butylamine	900 ± 20	0.985	0.001
Butylamine	1450 ± 30	0.998	0.000
Triethylamine	1600 ± 100	0.994	0.000

**Experimental conditions:** Dionex CS12A, 13 mM methanesulfonic acid at 0.5 mL/min.

Temperature range: 27 °C to 60 °C. The standard deviations are those for the slopes obtained from three replicate runs and are not those for the regression.



Examination of Table 3-1 and Table 3-2 reveals that the magnitude of the slopes of the van't Hoff plots for both metals and amines are comparable. Further, within each class of analytes (alkali metals, alkaline earth metals and amines), the slope of a van't Hoff plot generally increases as retention increases, *i.e.*, the effect of temperature on retention becomes more pronounced as retention increases. It is of interest to note that for all analytes examined in this work (except for butylamine and triethylamine), the effect of temperature on retention is less pronounced than that seen in RPLC (+1900 K calculated from van't Hoff plots in Ref. 3, +1500 K averaged from Table I in Ref. 4, +1500 K averaged from Table 2 in Ref. 5 and about +1200 K based on Figure 2-3 and Table 2-3 in Chapter Two). However, it is the range in the slopes of van't Hoff plots that is important in obtaining selectivity changes upon altering the column temperature. In other words, does temperature affect the retention of each analyte similarly (same van't Hoff plot slope for every analyte) or does temperature affect the retention of all analytes differently (different van't Hoff plot slope for each analyte)? There exists a 193 % range in the slopes of van't Hoff plots for the analytes separated on the CS12A cation exchanger used in this work, compared to 65 %<sup>5</sup>, 43 %<sup>4</sup>, and 15 % (Ref. 3 and Table 2-3) for RPLC. (Range in slopes calculated using:  $\text{Range} = [\text{largest slope} - \text{smallest slope}] / \text{average slope}$ .) This means that there is a greater chance for selectivity changes upon an increase in column temperature in IC than in RPLC. It is interesting to note that the 193 % variation in the slope of a van't Hoff plot seen here pales in comparison to the 1040 % variation seen for anions separated on anion-exchangers in Chapter Two. This large variation is a result of positive and negative slopes for the van't Hoff plots of anions.

### 3.3.2 Eluent Effects on Temperature Behaviour

Table 3-3 shows the effect on the slope of a van't Hoff plot when the concentration of methanesulfonic acid was increased from 13 mM to 25 mM. The slopes of the van't Hoff plots of alkali metals and alkaline earth metals were not appreciably affected by an increase in eluent concentration given the variations in slope in going from a low eluent concentration to higher eluent concentration. Therefore, one can conclude that there is not a significant effect on temperature behaviour as a result of changes in eluent concentration. This is in agreement with the results presented in Table 2-4 of Chapter Two.

The use of sulfuric acid instead of methanesulfonic acid as an eluent can dramatically affect the temperature behaviour of alkali and alkaline earth metals. Table 3-4 shows the slopes of the van't Hoff plots for various metals along with some regression parameters when an 11 mM sulfuric acid eluent was used. Significant linear relationships were seen for all metals except for sodium and ammonium. For ammonium the *p*-value corresponded to the 90% confidence level, and the retention of sodium showed no temperature dependence. Note that all metals have smaller (more negative) slopes compared to those obtained when methanesulfonic acid was used as the eluent (Table 3-1). In other words, there was a shift toward endothermic temperature behaviour. This is especially obvious for lithium and the alkaline earth metals that now show completely endothermic temperature behaviour. These observations are in agreement with the results of Rey and Pohl.<sup>9</sup>

The higher hydrogen ion concentration in the sulfuric acid eluent (about 22 mM compared to 18 mM with methanesulfonic acid) is not responsible for the shift toward

**Table 3-3.** Effect of eluent concentration on the slope of a van't Hoff plot.

	Slope (13 mM MSA)	Slope (15 mM MSA)	Slope (18 mM MSA)	Slope (25 mM MSA)
Lithium	200 ± 70	60 ± 50	120 ± 20	0 ± 20
Sodium	490 ± 40	460 ± 70	540 ± 50	440 ± 70
Ammonium	530 ± 50	500 ± 20	590 ± 70	470 ± 20
Potassium	920 ± 70	910 ± 50	960 ± 50	870 ± 20
Magnesium	150 ± 40	160 ± 50	180 ± 40	160 ± 60
Calcium	320 ± 50	340 ± 20	330 ± 70	340 ± 60
Strontium	530 ± 40	550 ± 50	520 ± 40	520 ± 50

**Experimental Conditions:** Dionex CS12A, methanesulfonic acid eluents at 0.5 mL/min  
 Temperature Range: 27 °C to 60 °C. The standard deviations are the 95 % confidence intervals based on three replicate runs and are not those for the regression.

**Table 3-4.** Effect of a sulfuric acid eluent on the slope of a van't Hoff plot.

	<b>Slope</b>	<b>r<sup>2</sup></b>	<b>p-value</b>
Lithium	-280 ± 20	0.970	0.002
Sodium	0 ± 20	0.000	0.966
Ammonium	90 ± 10	0.766	0.052
Potassium	470 ± 30	0.991	0.000
Magnesium	-670 ± 30	0.983	0.001
Calcium	-490 ± 10	0.980	0.001
Strontium	-320 ± 30	0.962	0.003

**Experimental conditions:** Dionex CS12A, 11 mM sulfuric acid eluent at 0.5 mL/min.

Temperature range: 27 °C to 60 °C. The standard deviations are those for the slopes obtained from three replicate runs and are not those for the regression.

endothermic temperature behaviour. The data in Table 3-3 show this is not the case, *i.e.*, there is no dependence of temperature behaviour with eluent concentration. Alternately, in Ref. 9 it was suggested that complexation between analytes and the sulfuric acid eluent might alter the temperature dependence of metal retention relative to that seen with a methanesulfonic acid eluent. However, the authors did not pursue this hypothesis. Unfortunately, the extent of complexation is difficult to calculate since the ionic strength inside the ion exchanger (which would have contributions from the eluent and the fixed charge sites) would have to be accurately known. A simple equilibrium calculation (*i.e.*, not incorporating activity effects) for strontium reveals the following:<sup>16</sup>

$$Q = [Sr^{2+}][SO_4^{2-}] = 10^{-5} M \times 0.011 M = 1 \times 10^{-7} < K_{sp} = 3 \times 10^{-7} \quad (3-1)$$

In other words, complexation may be a possibility for strontium if the ionic strength in the ion exchanger is high enough to “salt out” strontium sulfate. However, the possibility of complexation decreases in going from strontium to calcium to magnesium and is not a possibility for the alkali metals.<sup>17</sup> Thus, complexation is not a reasonable argument for the behaviour seen in Table 3-4.

A possible explanation for the temperature behaviour with sulfuric acid eluents may lie in the change in ionization of sulfuric acid with increasing temperature. The second  $pK_a$  of sulfuric acid is 1.9 and the pH of the eluent is 2.0. Thus the charge of hydrogensulfate ion is extremely sensitive to changes in  $pK_a$  caused by an increase in temperature. In particular, an increase in  $pK_a$  would decrease the charge of hydrogensulfate, thus making it a weaker eluent. This would give the appearance of increasing retention with increasing temperature.

### 3.3.3 Effect of Temperature on Selectivity

Amines are widely used in a number of applications in industry. Morpholine is often used as a corrosion inhibitor in the water cycles of power plants.<sup>18-20</sup> Alkanolamines are used in scrubbers to help remove acid gases (*e.g.*, hydrogen sulfide and carbon dioxide) in oil refineries and natural gas plants.<sup>18, 19, 21, 22</sup> Consequently, the continuous monitoring of these amines is of great importance. However, their determination is often hampered by the presence of other amines, alkali metals and alkaline earth metals.<sup>18-20, 22</sup> Thus, as illustrated in Ref. 18-22, the separation of cations and amines is a problem of great industrial importance. Therefore, methods are needed to adequately resolve the components in a mixture so that proper quantification is possible.

The most powerful way to optimize the resolution of a separation is through proper control of the selectivity.<sup>23, 24</sup> Figure 3-3 shows the van't Hoff plots of various metals and amines separated on the CS12A using a 13 mM methanesulfonic acid eluent. Examination of Figure 3-3 shows that a number of selectivity changes between metals and amines are obtained simply by changing the column temperature. In order to determine when temperature will be most useful in changing the selectivity of a separation, analytes can be categorized into groups with respect to their temperature behaviour, as was done in Chapter Two. Analytes that have van't Hoff plots approximately parallel to one another (*i.e.*, temperature affects their retention in the same way) are considered to behave as a group. Figure 3-3 exhibits three sets of parallel lines, *i.e.*, three different groups of temperature behaviour. These are: the alkali metals, whose retention decreases with increasing temperature; the alkaline earth metals, whose retention slightly decreases with increasing temperature; and the amines, whose retention

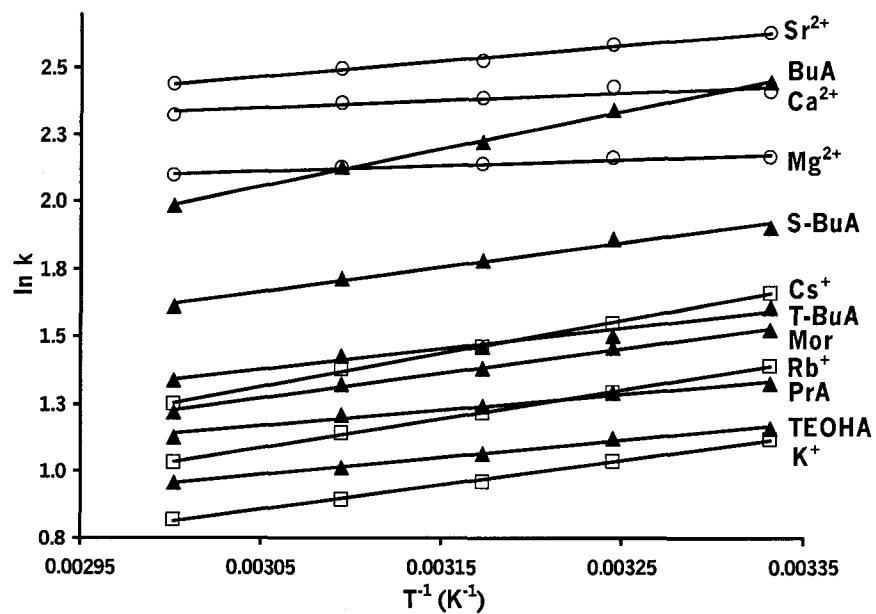


**Figure 3-3.** van't Hoff plots of metals and amines showing selectivity changes caused by temperature. **Experimental Conditions:** Dionex CS12A column, 13 mM methanesulfonic acid eluent at 0.5 mL/min. Temperature range: 27 °C to 60 °C. TEOHA = triethanolamine, PrA = propylamine, Mor = morpholine, T-BuA = tert-butylamine, S-BuA = sec-butylamine, BuA = butylamine

decreases with increasing temperature. A change in column temperature will leave the selectivity between analytes in the same group relatively unchanged, but will change the relative retention for analytes in different groups. For example, the separation between potassium and triethanolamine is enhanced at temperatures above 27 °C, and there is a change in elution order above 37 °C between rubidium and propylamine. Butylamine elutes between calcium and strontium at 27 °C. Increasing the temperature to 46 °C causes butylamine to elute between calcium and magnesium without affecting the selectivity between the alkaline earth metals. This is shown in Figure 3-4. This demonstrates that a number of selectivity changes are possible upon increasing the column temperature. This can be used to make optimization of a separation much easier so that all components of interest are resolved and easily quantified. Further, Figure 3-4 shows improvements in peak shape and efficiency at 46 °C compared to 27 °C. This will be explored in more detail in Section 3.3.5.

The advantage of using temperature as a separation aid lies in the fact that it affects separations in a different manner than eluent concentration. Firstly, consider the equation:

$$\log k = \text{const} - \frac{x}{y} \log[E^{y+}] \quad (1-31)$$

where  $k$  is the retention factor of ion  $A$ ,  $\text{const}$  is a constant,  $x$  is the charge of ion  $A$ ,  $y$  is the charge of the eluent ion and  $[E^{y+}]$  is the concentration of the eluent ion.<sup>25-28</sup> Equation 1-31 predicts that eluent concentration decreases the retention of doubly charged ions more so than singly charged ions (i.e.,  $-x/y = -2$  instead of  $-x/y = -1$ ). However, temperature decreases the retention of doubly charged ions to a lesser extent than that of singly charged ions. Secondly, the selectivity,  $\alpha_{A,B}$ , for two solutes  $A$  and  $B$  having the



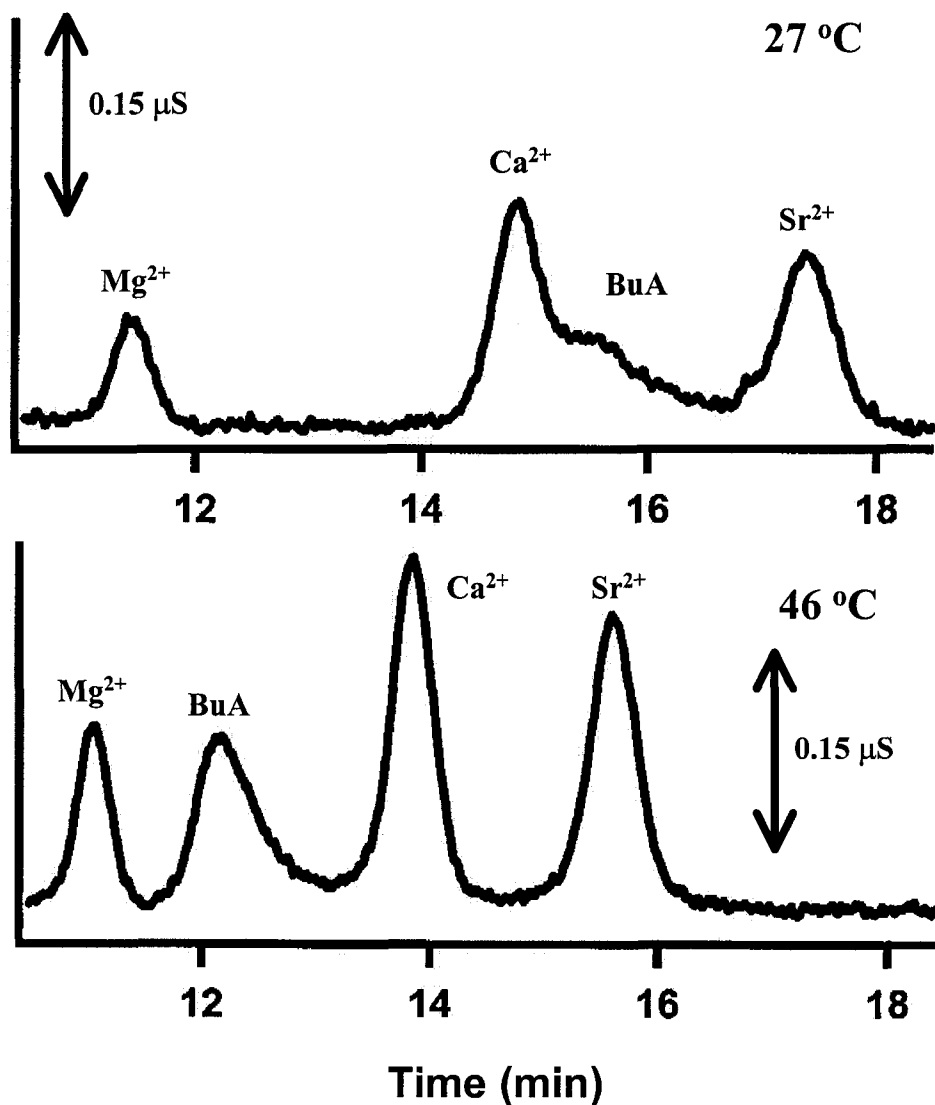


**Figure 3-4.** Changes in selectivity of cation separations caused by increased temperature. **Experimental Conditions:** Dionex CS12A column, 13 mM methanesulfonic acid eluent at 0.5 mL/min. BuA = butylamine.

same charge,  $x$ , depends only on their charge and on the selectivity coefficient,  $K_{A,B}$  according to the equation:

$$\log \alpha_{A,B} = \frac{1}{x} \log K_{A,B} \quad (3-2)$$

In other words, eluent concentration cannot change the selectivity of ions having the same charge.<sup>25, 26</sup> Temperature affects the retention of amines differently than that of the alkali metals, even though they are both singly charged. A possible reason for this is that metals interact with the CS12A exclusively by ion exchange, whereas amines are retained through a combination of ion exchange and reversed-phase interactions<sup>9</sup>. As was mentioned in Chapter Two, ion exchange temperature behaviour is different from RPLC temperature behaviour. Temperature causes retention in RPLC to decrease and no selectivity changes are observed. However, temperature causes retention in ion exchange to increase, decrease or stay the same. Therefore, elevated temperatures will affect the ion exchange component of retention for amines differently than the reversed-phase component, thus causing changes in selectivity between amines and alkali metals.

### 3.3.4 Effect of an Organic Modifier on Selectivity

An alternative means of reducing hydrophobic interactions is to add an organic modifier to the eluent. Figure 3-5 shows the effect of varying amounts of acetonitrile in the eluent on the retention of metals and amines. Addition of acetonitrile reduces the retention of both metals and amines. In general, a 10 °C rise in temperature is approximately equivalent to 2 % acetonitrile added to the eluent.

The retention of the amines relative to the metals was dramatically affected by the acetonitrile in the eluent. There were quite a few elution order reversals between metals and amines, *e.g.*, potassium and propylamine, and even between amines and other

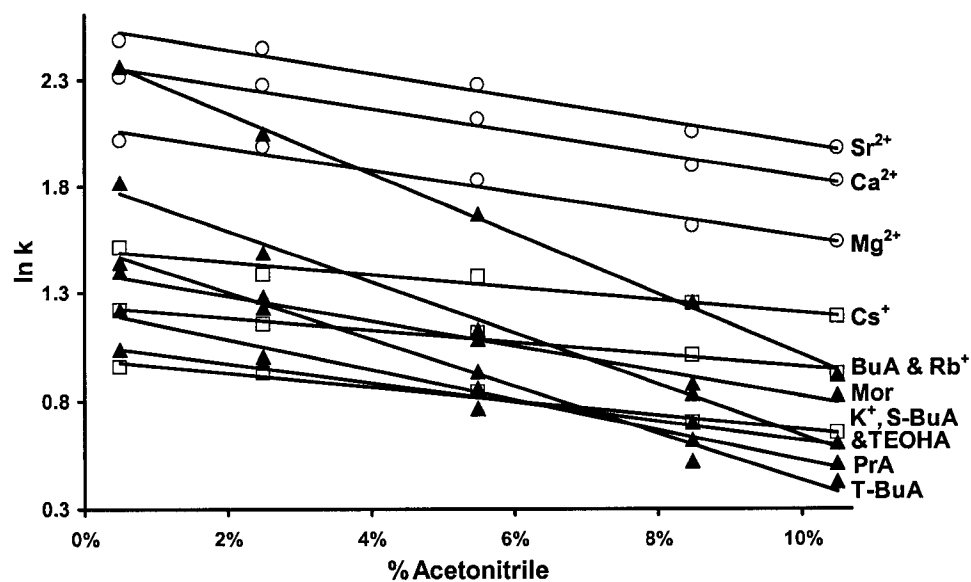


**Figure 3-5.** Effect of acetonitrile on the selectivity of a separation of metals and amines. **Experimental Conditions:** Dionex CS12A column, eluent flow at 0.5 mL/min, 27 °C. Concentration of methanesulfonic acid held constant at 13 mM. TEOHA = triethanolamine, PrA = propylamine, Mor = morpholine, T-BuA = tert-butylamine, S-BuA = sec-butylamine, BuA = butylamine.

amines, *e.g.*, morpholine and tert-butylamine (which was not seen when temperature was varied), but there were no reversals in elution order between metals. It is important to note that the groupings of cations discussed in Section 3.3.3 based on their temperature behaviour are no longer valid when acetonitrile is used to modify selectivity. Although the alkali and alkaline earth metals still behave as independent groups with respect to how acetonitrile changed their retention, the amines have been split up into sub-groups. For example, the butylamines show a very pronounced decrease in retention relative to the other amines when acetonitrile is added to the eluent.

These observations suggest that there may be differences in how acetonitrile affects the selectivity of a separation and how temperature affects it. To assess if acetonitrile affects retention in the same way as temperature does, the slopes from Figure 3-5 (*i.e.*, from the plots of  $\ln k$  vs. % acetonitrile) were plotted against the slopes from Figure 3-3 (*i.e.*, from the van't Hoff plots). The resulting graph is shown in Figure 3-6. If acetonitrile affects retention in a different manner than temperature, then there should be no correlation between the data. This is exactly what is seen in Figure 3-6 and is further corroborated by the low correlation coefficient ( $r^2 = 0.07$ ). Therefore, an organic modifier can be used to change the selectivity of a separation in a totally different way than temperature.

### 3.3.5 Efficiency Improvements

Chapter Two revealed improvements in efficiency and peak asymmetry at 60 °C for the anions that were studied. Table 3-5 presents the efficiencies of some of the metals and amines separated at 27 °C and 60 °C. For the most part, improvements in efficiency can be obtained by operating at elevated temperatures for both metals and amines.

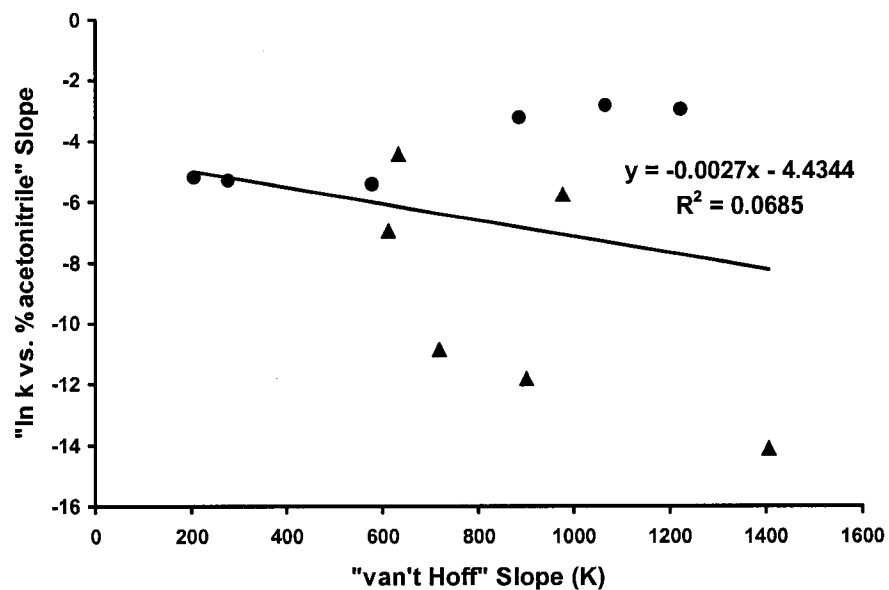


**Figure 3-6.** Scatter plot showing differences in selectivity caused by acetonitrile and temperature. ● refers to metals and ▲ refers to amines.

**Table 3-5.** The effect of temperature on peak asymmetry and efficiency of metals and amines.

	Asymmetry ( $\pm 0.5$ )			Efficiency ( $\pm 300$ )		
	27 °C	60 °C	6% ACN	27 °C	60 °C	6% ACN
Ethylamine	1.3	1.1	1.1	5100	4400	4700
Propylamine	2.1	1.8	1.1	2100	3000	3300
Triethanolamine	3.0	2.6	1.4	1400	1500	2300
Morpholine	2.2	1.8	1.3	1800	2300	2700
Tert-butylamine	1.9	1.8	1.3	1100	2700	2200
Sec-butylamine	2.2	1.6	1.4	1400	2900	3100
Butylamine	2.0	1.7	1.1	800	2600	2500
Triethylamine	4.1	2.6	1.5	100	500	1700
Lithium	1.1	1.1	1.1	3500	4400	3400
Sodium	1.0	1.0	1.0	3900	4300	4000
Ammonium	1.7	1.7	1.8	1600	2200	1300
Potassium	1.0	1.0	1.0	4800	5700	4700
Magnesium	1.1	1.1	1.1	3300	4100	3100
Calcium	1.1	1.1	1.1	3600	4100	3600
Strontium	1.1	1.0	1.0	3200	4300	3000

**Experimental conditions:** Dionex CS12A column, 13 mM methanesulfonic acid (or 94/6 13.8 mM methanesulfonic acid/acetonitrile (ACN)) at 0.5 mL/min. The standard deviations are the 95% confidence intervals based on three replicate measurements.

However, efficiency improvements are more pronounced for the amines than the metals. Note the large improvements in peak asymmetry obtained at elevated temperatures for the amines. They were separated without an organic modifier thus causing them to strongly adsorb to the CS12A through reversed-phase interactions.<sup>9</sup> An increase in temperature helped attenuate some of those interactions, leading to dramatically better peak shape and efficiency.

Addition of small amounts of an organic modifier can also reduce the strong reversed-phase interactions seen with the amines separated on the CS12A. Table 3-5 contains asymmetry factors and efficiencies for analytes separated with an eluent containing 6% acetonitrile. Significant improvements (*i.e.*, in many cases 100% improvement) in the peak asymmetries and efficiencies of the amines were seen upon addition of acetonitrile to the eluent. The peak asymmetries for amines using 6% acetonitrile at 27 °C were better than those achieved using a pure aqueous eluent at 60°C. However, the efficiencies for the amines were comparable at the 95% confidence level (except for triethanolamine and triethylamine) between these conditions. In contrast, the efficiencies of the metals were unaffected by the presence of acetonitrile in the eluent, *i.e.*, they were the same at the 95% confidence level, when comparing an aqueous eluent to an eluent containing 6% acetonitrile at 27 °C. This is expected since the metals do not interact with the stationary phase through hydrophobic interactions.

### 3.4 Conclusions

This chapter explored the application of elevated temperatures to the cation exchange separation of alkali metals, alkaline earth metals and amines. An increase in

column temperature caused the retention of all analytes to decrease. Selectivity changes were seen due to the wide range in temperature dependence of retention. However, selectivity changes were limited to analytes belonging to different groups of temperature behaviour (the alkali metals, alkaline earth metals and amines). Consequently, elevated temperatures were not able to affect the selectivity between analytes in the same group. The addition of small amounts of acetonitrile to the eluent proved to be a useful approach to selectivity modification. It was found that temperature and acetonitrile yield significantly different selectivity changes. Furthermore, elevated temperatures caused improvements in the efficiency of all analytes studied, especially for the amines, which also exhibited reduced peak tailing. Thus column temperature is suited to selectivity modification and efficiency improvement in the cation exchange separation of alkali metals, alkaline earth metals and amines.

This study also showed promise for the application of high temperature high-speed analysis to cation exchange separations. Firstly, the retention characteristics of the column did not degrade over the five months of use at above ambient temperatures. Secondly, the retention of all analytes decreases with an increase in temperature, which would augment the improvement in separation speed achieved from an increase in flow rate. Therefore, Chapter Four will examine the use of elevated temperatures for achieving high-speed separations of cations in IC.

### **3.5 References**

- (1) Ooms, B. *LC-GC* **1996**, *14*, 306-324.
- (2) Pawlowski, T. M.; Poole, C. F. *Anal. Commun.* **1999**, *36*, 71-75.



- (3) Mao, Y.; Carr, P. W. *Anal. Chem.* **2000**, *72*, 110-118.
- (4) Cole, L. A.; Dorsey, J. G. *Anal. Chem.* **1992**, *64*, 1317.
- (5) Li, J.; Carr, P. W. *Anal. Chem.* **1997**, *69*, 837-843.
- (6) Smith, R. G.; Drake, P. A.; Lamb, J. D. *J. Chromatogr.* **1991**, *546*, 139-149.
- (7) Kraus, K. A.; Raridon, R. J. *J. Phys. Chem.* **1959**, *63*, 1901-1907.
- (8) Dybczynski, R. *J. Chromatogr.* **1967**, *31*, 155-170.
- (9) Rey, M. A.; Pohl, C. A. *J. Chromatogr. A* **1996**, *739*, 87-97.
- (10) Poppe, H.; Kraak, J. C. *J. Chromatogr.* **1983**, *282*, 399-412.
- (11) Devore, J. L. *Probability and Statistics for Engineering and the Sciences, 4th Ed.*; Duxbury: New York, 1995.
- (12) Yau, W. W. *Anal. Chem.* **1977**, *49*, 395-398.
- (13) Grubner, O. *Anal. Chem.* **1971**, *43*, 1934.
- (14) Foley, J. P.; Dorsey, J. G. *Anal. Chem.* **1983**, *55*, 730-737.
- (15) Bidlingmeyer, B. A.; Warren, F. V. *J. Anal. Chem.* **1984**, *56*, 1583A-1596A.
- (16) Harris, D. C. *Quantitative Chemical Analysis*; W.H. Freeman: New York, 2003.
- (17) Lide, D. R. *CRC Handbook of Chemistry and Physics, 76th ed.*; CRC Press: New York, 1995-1996.
- (18) Krol, J.; Alden, P. G.; Morawski, J.; Jackson, P. E. *J. Chromatogr.* **1992**, *626*, 165-170.
- (19) Kadnar, R. *J. Chromatogr. A* **1999**, *850*, 289-295.
- (20) *Application Note 86: Determination of Trace Cations in Power Plant Waters Containing Morpholine*; Dionex: Sunnyvale, 1995.

- (21) *Application Update 126: Determination of Diethanolamine and Triethanolamine in Surface Finishing, Waste Water, and Scrubber Solutions*, Dionex, Sunnyvale, CA; Dionex: Sunnyvale, 1991.
- (22) *Application Update 138: Determination of Ethanolamines in Industrial Waters by Cation-Exchange Chromatography*, Dionex, CA, 1998; Dionex: Sunnyvale, 1998.
- (23) Snyder, L. R.; Glajch, J. L.; Kirkland, J. J. *Practical HPLC Method Development*, 2nd ed.; Wiley-Interscience: New York, 1996.
- (24) Schoenmakers, P. J. *Optimization of Chromatographic Selectivity*: New York, 1986.
- (25) Vlacil, F.; Vins, I. *J. Chromatogr.* **1987**, *391*, 133-144.
- (26) Haddad, P. R.; Jackson, P. E. *Ion Chromatography: Principles and Applications*; Elsevier: New York, 1990.
- (27) Haddad, P. R.; Cowie, C. E. *J. Chromatogr.* **1984**, *303*, 321-330.
- (28) Gjerde, D. T.; Schmuckler, G.; Fritz, J. S. *J. Chromatogr.* **1980**, *187*, 35-45.

## **CHAPTER FOUR. High-Temperature High-Speed Ion Chromatography of Inorganic Cations\***

Chapters Two and Three showed that elevated temperature is a powerful tool for the optimization of selectivity in both anion and cation exchange separations, and in doing so, provided some insight into potential issues with the implementation of elevated temperature for high-speed IC. In particular, Chapter Two revealed that elevated temperature cannot be used for high-speed anion separations due to the endothermic retention behaviour of doubly charged anions, as well as the thermal instability of quaternary ammonium anion exchangers. However, elevated temperature can be exploited for high-speed cation separations since cation exchangers are exceptionally thermally stable and the retention of all cations examined decreased with elevated temperature. For these reasons, Chapter Four will demonstrate the theory and implementation of high-temperature high-speed IC with cationic species.

### **4.1. Introduction**

High-speed separations have tremendous practical significance in chemical industry (Section 1.1). Therefore, methods for reducing analysis time are highly sought after. Improvements in separation speed can be realized by decreasing the column length and simultaneously decreasing the particle size, so that analysis time is reduced while maintaining efficiency.<sup>1-3</sup> This approach was used by Connolly and Paull to achieve sub-minute separations of nitrite and nitrate, and a 2.5 minute separation of 9 common anions

---

\* A version of this chapter has been submitted for publication. Chong, J.; Hatsis, P.; Lucy, C.A. *Journal of Chromatography A*, 2002. P. Hatsis co-supervised J. Chong's undergraduate research project.

with a 3  $\mu\text{m}$  particle size, 30 x 4.6 mm RPLC column.<sup>4-6</sup> However, there exists a point where the pressure maximum of the chromatographic system (usually around 4000 psi) is reached and further improvements in separation speed in this manner are no longer possible.

Clearly, significant improvements in separation speed are possible if the pressure necessary for a given linear velocity could be reduced. Recently, Carr and co-workers systematically investigated the effect of elevated temperatures on separation speed in RPLC<sup>7-9</sup>. They found that elevated temperatures (150 °C) substantially decreased the mobile phase viscosity, which in turn, decreased the backpressure across the column. This enabled increases in linear velocity such that separations could be performed 50 times faster than at room temperature. The success of their method for RPLC rests upon the use of zirconia as the chromatographic support, which is extremely thermally stable<sup>10</sup>,<sup>11</sup> and has been used at temperatures as high as 370 °C.<sup>12</sup>

Although zirconia is probably the most thermally stable chromatographic support available today, polymeric materials have also been used successfully at elevated temperatures (up to 210 °C).<sup>13</sup> Specifically, cation exchange resins exhibit exceptional thermal stability. Indeed, the cation exchange sites are formed by reaction of the polystyrene resin with concentrated sulfuric acid at 100°C.<sup>14</sup> In this chapter, the use of temperature for high-speed IC separations of cations is systematically investigated. Previously, Rey studied the use of column temperatures as high as 70 °C for cation separations on a Dionex CS16 column but did not exploit the opportunities that elevated temperatures offered in terms of separation time.<sup>15</sup> The present work demonstrates that

the separation time for common cations can be reduced by 35% through the use of elevated column temperatures.

## **4.2. Experimental**

### **4.2.1. Apparatus**

A schematic of the equipment used for high-temperature high-speed IC is shown in Figure 4-1. A Dionex AGP-1 (Dionex, Sunnyvale, CA, USA) dual-piston pump was used for eluent flow. A Spectra Physics AS3500 (Thermo Finnigan, Mississauga, Canada) autosampler was used to inject 20  $\mu\text{L}$  of sample by means of a Rheodyne 9010 injection valve (Rheodyne, Cotati, CA, USA). Separations were achieved with a Dionex CS-12A cation exchange column (3 mm i.d.  $\times$  150 mm). Detection of the cations was via a Dionex CDM-3 conductivity detector with a Dionex CSRS-Ultra (2 mm) suppressor. The connecting tubing was 0.005" i.d. PEEK (Upchurch Scientific, Oak Harbor, WA, USA). Data was collected at 5 Hz through a Dionex AI-450 data acquisition system linked to a Pentium II microcomputer equipped with Dionex Peak Net 5.0 software. Fifty centimetres of 0.005" i.d. connecting tubing was added after the conductivity cell to provide sufficient backpressure to prevent formation of air bubbles in the cell.

The use of a suppressor at elevated flow rates and temperatures necessitated additional modifications to the chromatographic system. The 2 mm-CSRS suppressors can only tolerate flow rates up to 0.75 ml/min. Thus, the flow was split to maintain a constant flow of 0.5 mL/min through the suppressor. A T-adaptor (1  $\mu\text{L}$  dead volume, Upchurch Scientific) was placed between the column and suppressor. Capillary tubing (Polymicro Technologies, Phoenix AZ, USA) was connected to the third outlet of the T-

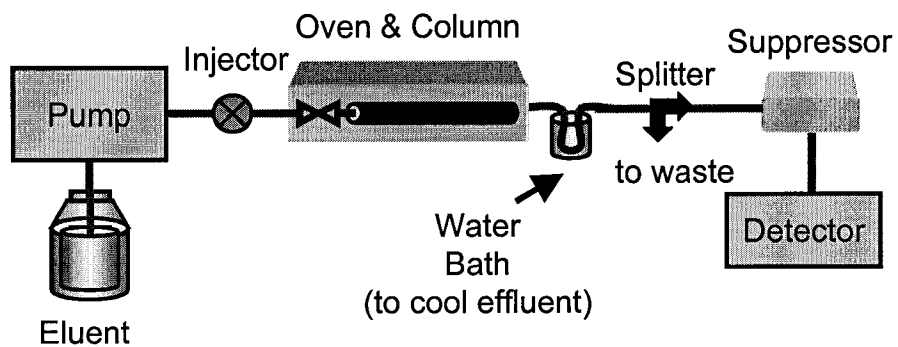


**Figure 4-1.** Modifications to a typical IC system for performing high-temperature high-speed IC.

adapter to act as a flow constrictor, and thus control the flow through the suppressor. Four to twenty centimetres of 75  $\mu\text{m}$  i.d. capillary was used for flow rates of 0.6-1.2 mL/min, and 14 cm of 100  $\mu\text{m}$  i.d. capillary was used for a flow rate of 1.3 ml/min. In addition, the suppressor was unable to withstand temperatures above 30 °C.<sup>16</sup> Thus, the eluent was cooled to room temperature before entering the suppressor, as described below.

An Eppendorf CH-30 column heater and an Eppendorf TC-50 control module (Alltech Associates, Deerfield, IL, USA) were used to pre-heat the eluent and control the column temperature. The eluent was preheated using a 30 cm long piece of connecting tubing (0.005" i.d. PEEK, Upchurch Scientific) wrapped around the mobile phase preheater. The effluent from the column was cooled before entering the suppressor by passage through 10 cm of Teflon tubing (0.007" i.d., Alltech) immersed in a beaker of room temperature water. The efficiencies achieved with the oven in place were the same at the 95% confidence level<sup>17</sup> as those observed at room temperature (23°C) without the column oven and extra connecting tubing.

#### **4.2.2. Reagents**

All sample and eluent solutions were prepared using distilled deionized water (Nanopure Water System, Barnstead, Chicago, IL, USA). Eluents were prepared using 99.5%+ methanesulfonic acid (MSA) purchased from Aldrich (Milwaukee, WI, USA). The eluent was degassed by a continual purge with helium. All chemicals were reagent grade or better. Stock solutions ( $10^{-2}$  M) of the cation samples were prepared and sample solutions ( $10^{-5}$  M) of the desired cations were prepared by dilution. Sodium (BDH Inc., Toronto, Canada), ammonium (BDH), rubidium (Fisher, Nepean, Canada), cesium

(Fisher), calcium (Anachemia, Toronto, Canada), strontium (Fisher), and magnesium (BDH) cations were obtained by dissolving their chloride salts. Lithium (Fisher) and potassium (Fisher) were used in the form of their nitrate salts.

#### 4.2.3. Procedure

Data analysis was performed with Microsoft Excel 97 software (Microsoft Corporation, Seattle, WA, USA). The water dip was used for the void time. Peaks were fit to an exponentially modified Gaussian (EMG) function:<sup>18,19</sup>

$$EMG(t) = \frac{1}{2\tau} \exp\left[\frac{1}{2}\left(\frac{\sigma}{\tau}\right)^2 - \frac{t-t_g}{\tau}\right] \left\{ 1 + \operatorname{erf}\left[\frac{1}{\sqrt{2}}\left(\frac{t-t_g}{\sigma} - \frac{\sigma}{\tau}\right)\right] \right\} \quad (4-1)$$

using an in-house routine for Matlab 6 (Mathworks Inc., Natick, MA, USA) to determine the second statistical moment (*i.e.*, the variance) and subsequently the efficiency and plate height. In Equation 4-1,  $t$  is time,  $t_g$  is the centroid of the Gaussian component,  $\sigma$  is the standard deviation,  $\tau$  is the time constant of the exponential function and  $\operatorname{erf}()$  is the error function. The software routine is included as Appendix One. The variance ( $\sigma_p^2$ ) retention time ( $t_R$ ) and plate height of peaks were calculated as:

$$\sigma_p^2 = \sigma^2 + \tau^2 \quad (4-2a)$$

$$t_R = t_g + \tau \quad (4-2b)$$

$$H = (\sigma_p^2 L_c)/t_R^2 \quad (4-2c)$$

where  $L_c$  is the length of the column. Plate height vs. linear velocity data were fit to the van Deemter equation (Equation 1-10) using GraphPad Prism 3.02 (GraphPad Software Inc., San Diego, CA, USA).



### 4.3. Results and Discussion

#### 4.3.1. Effect of Temperature on Retention

Chapter Three showed that retention in cation exchange separations is predominantly exothermic in nature. That is, retention decreases with increasing column temperature. Fortunately, this phenomenon augments the enhanced separation times that could be achieved through an increase in flow rate at elevated temperature. In Chapter Three, the effect of temperature on the retention of cations was studied between 27 and 60 °C. However, if the benefits of elevated temperature in terms of high-speed IC are to be fully realized, higher temperatures have to be used. Ultimately, the highest temperature that can be examined is 90 °C, since the PEEK casing of the column loses mechanical strength above 100 °C.<sup>20</sup> This necessitates that a van't Hoff plot be reconstructed for each cation to cover the temperature range 27 °C to 90 °C. In this way, an accurate picture of the retention of cations at temperatures up to 90 °C is obtained. The resulting van't Hoff plots are shown in Figure 4-2. The linear regression data associated with these plots are summarized in Table 4-1. The van't Hoff plots of all nine cations studied in this work are linear, as indicated by the small *p*-values (less than 0.05) in Table 4-1. Therefore, the extended temperature range did not introduce any non-linearity in the van't Hoff plots.

Chapter Three showed the selectivity of cation exchange separations can be altered through a change in column temperature. Selectivity changes were most pronounced between cations of differing charge. This is most evident in Figure 4-3 where there is a significant improvement in the separation between cesium and magnesium upon increasing the column temperature from 27 to 60°C. However, for

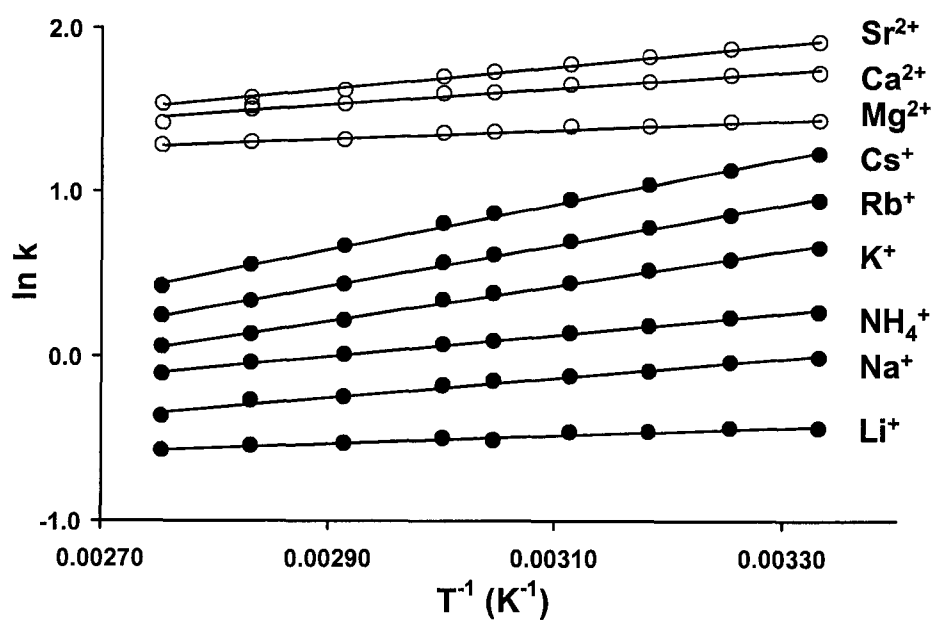


**Figure 4-2.** van't Hoff plots of cations. **Experimental conditions:** Dionex CS-12A, 17 mM MSA at 0.5 mL/min, 20  $\mu$ L injection, temperature range from 27  $^{\circ}$ C to 90  $^{\circ}$ C, 50  $\mu$ M analyte concentration.

**Table 4-1.** van't Hoff temperature dependencies for cation exchange retention.

Cation	Slope	p-value	r <sup>2</sup>
Li <sup>+</sup>	240 ± 30	0.007	0.862
Na <sup>+</sup>	530 ± 20	0.000	0.994
NH <sub>4</sub> <sup>+</sup>	640 ± 10	0.000	0.997
K <sup>+</sup>	1050 ± 20	0.000	0.997
Rb <sup>+</sup>	1230 ± 10	0.000	0.999
Cs <sup>+</sup>	1410 ± 20	0.000	0.995
Mg <sup>2+</sup>	220 ± 10	0.001	0.944
Ca <sup>2+</sup>	520 ± 30	0.000	0.939
Sr <sup>2+</sup>	670 ± 20	0.000	0.994

**Experimental conditions:** Dionex CS-12A column, 17 mM MSA eluent temperature range from 27 to 90°C; flow of 0.5 mL/min, 20 µL injection, 50 µM analyte concentration. Standard deviations are those for three replicate runs.

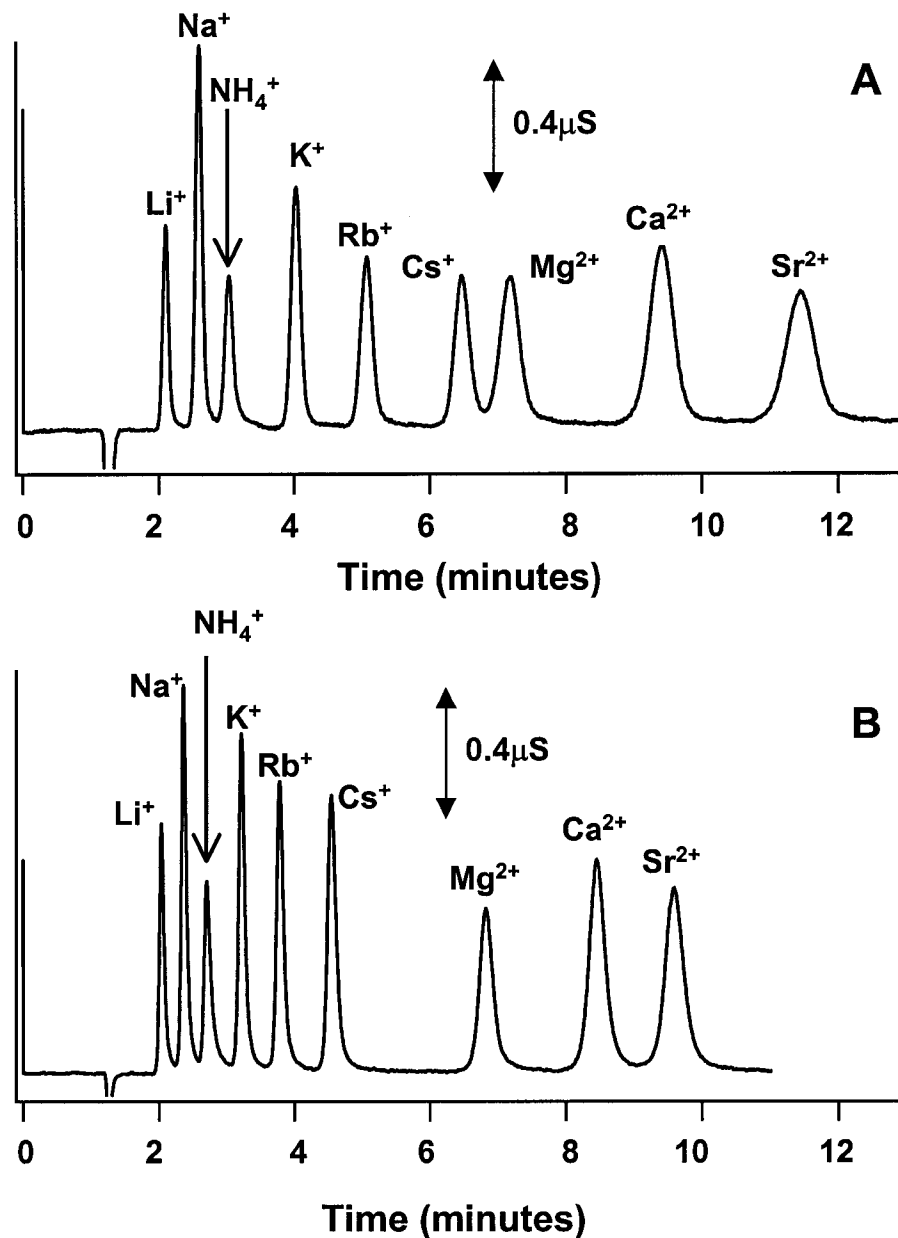


**Figure 4-3.** Separation of nine cations at (A) 27°C, (B) 60 °C. **Experimental Conditions:** Dionex CS-12A column, 17 mM MSA at 0.5 mL/min, 20 μL injection, 50 μM analyte concentration.

cations of the same charge, the more strongly retained cations show a greater van't Hoff plot slope. That is, a greater decrease in retention at elevated temperature is seen for more strongly retained cations. Thus, as the temperature is increased, the more strongly retained cations within a group will elute closer to the more weakly retained species. This differs from the behaviour observed in RPLC, where the van't Hoff plots are *generally* parallel<sup>21,22</sup>, *i.e.*, temperature does not have a significant effect on selectivity in the RPLC of small molecules even over temperature ranges as wide as 30 to 130 °C.<sup>21</sup>

Figure 4-3 compares separations of the nine cations at 27 and 60°C, with the same flow rate and eluent strength. There is a 15% increase in the separation speed due to the decreased retention. However as can be seen in Figure 4-3, the peaks of the monovalent cations begin to converge as the temperature is increased from 27 to 60°C, and similarly for the divalent cations. At temperatures higher than 60°C, baseline resolution is lost (separation not shown). The loss of resolution results from a number of factors. Firstly, retention decreases as the temperature is increased. This results in many of the univalent cations eluting near the dead volume of the column. The eluent strength can be reduced to compensate for the reduced retention at elevated temperatures.<sup>9</sup> However, increasing the retention negates some of the advantages to be gained by using higher column temperatures. Nevertheless, adjustment of the eluent strength is explored in Section 4.3.4. Secondly, extra-column band broadening can severely impact the efficiency of weakly retained analytes.<sup>23</sup> Peak width increases as a compound is more retained. Therefore, unretained compounds have small peak widths, thus extra-column components contribute significantly to the overall peak width, leading to a decrease in efficiency. Finally, the retention factors of the cations converge at high temperature. This is most

evident for the alkaline earth metals in Figure 4-2. For these reasons, 60 °C was chosen as the optimum temperature for further studies.

#### 4.3.2. Effect of Temperature on Viscosity and Column Backpressure

An effective method to increase separation speed is to increase the eluent flow rate. Due to the resistance of the packed particles, the column backpressure increases as the flow rate is increased as shown in Equation 4-3a<sup>24, 25</sup>:

$$\Delta P = \frac{F \eta L_C}{\pi r_C^2 B_o} \quad (4-3a)$$

$$B_o = \frac{1}{185} \frac{\varepsilon_b^3}{(1 - \varepsilon_b)^2} d_p^2 \quad (4-3b)$$

where  $\Delta P$  is the pressure drop,  $F$  is flow rate,  $\eta$  is viscosity of the mobile phase,  $L_C$  is the length of the column,  $r_C$  is the radius of the column,  $B_o$  is the specific permeability,  $\varepsilon_b$  is the external porosity of the packed bed and  $d_p$  is the particle diameter. The pressure limits of the column and chromatographic instruments place a restriction on the maximum flow rate that can be used. At elevated temperatures, there is a decrease in eluent viscosity and consequently the column backpressure. From 27 to 60°C there is a 45% decrease in viscosity, from 0.86 to 0.47 cP.<sup>26</sup> However, the reduction in backpressure is somewhat moderated by the extra column components which remain at near ambient temperatures. For instance, using a flow rate of 0.5 mL/min a 33% decrease in pressure, from 1660 to 1110 psi, was observed in Figure 4-3. Nonetheless, this drop in column backpressure allows an increase in flow rate, and ultimately, will lead to an increase in separation speed.

To compare the separation speed that is achievable at elevated temperatures, the separation of nine cations was performed under flow conditions corresponding to a

constant backpressure of 2400 psi. The column is rated to 4000 psi.<sup>27</sup> However, it was felt that 2400 psi represented a pressure at which the IC could be operated routinely. Figure 4-4A shows the cation separation at 27°C. A flow rate of 0.90 mL/min yielded an analysis time of 8 minutes. In contrast, at 60°C a flow rate of 1.30 mL/min was attained giving an analysis time of 5 minutes (Figure 4-4B). This is a 35% decrease in analysis time. In comparing a run under conventional conditions (Figure 4-4A) to one at 1.30 mL/min and 60°C (Figure 4-4B), there is a 60 % increase in speed due to the combined effects of elevated temperatures on retention time and viscosity.

#### 4.3.3. Band Broadening

Chapters Two and Three showed an improvement in efficiency at elevated temperatures at a constant flow rate. However, increases in flow rate decrease the column efficiency due to the finite rate of mass transfer between the mobile and stationary phases. Therefore, the effect of elevated temperatures on efficiency at varying flow rates was studied.

The effect of flow rate on efficiency can be modeled with the van Deemter equation (Section 1.2.4.1):

$$H = A + \frac{B}{u} + Cu \quad (1-10)$$

where  $H$  is the plate height,  $u$  is the linear velocity of the mobile phase, and  $A$ ,  $B$ , and  $C$  are constants associated with eddy diffusion, longitudinal diffusion, and resistance to mass transfer between the stationary and mobile phase, respectively. These terms were discussed in detail in Section 1.2.4.

The van Deemter plots for sodium, potassium and magnesium at 27 and 60°C are shown in Figure 4-5. For simplicity, plate height is plotted against flow rate instead of

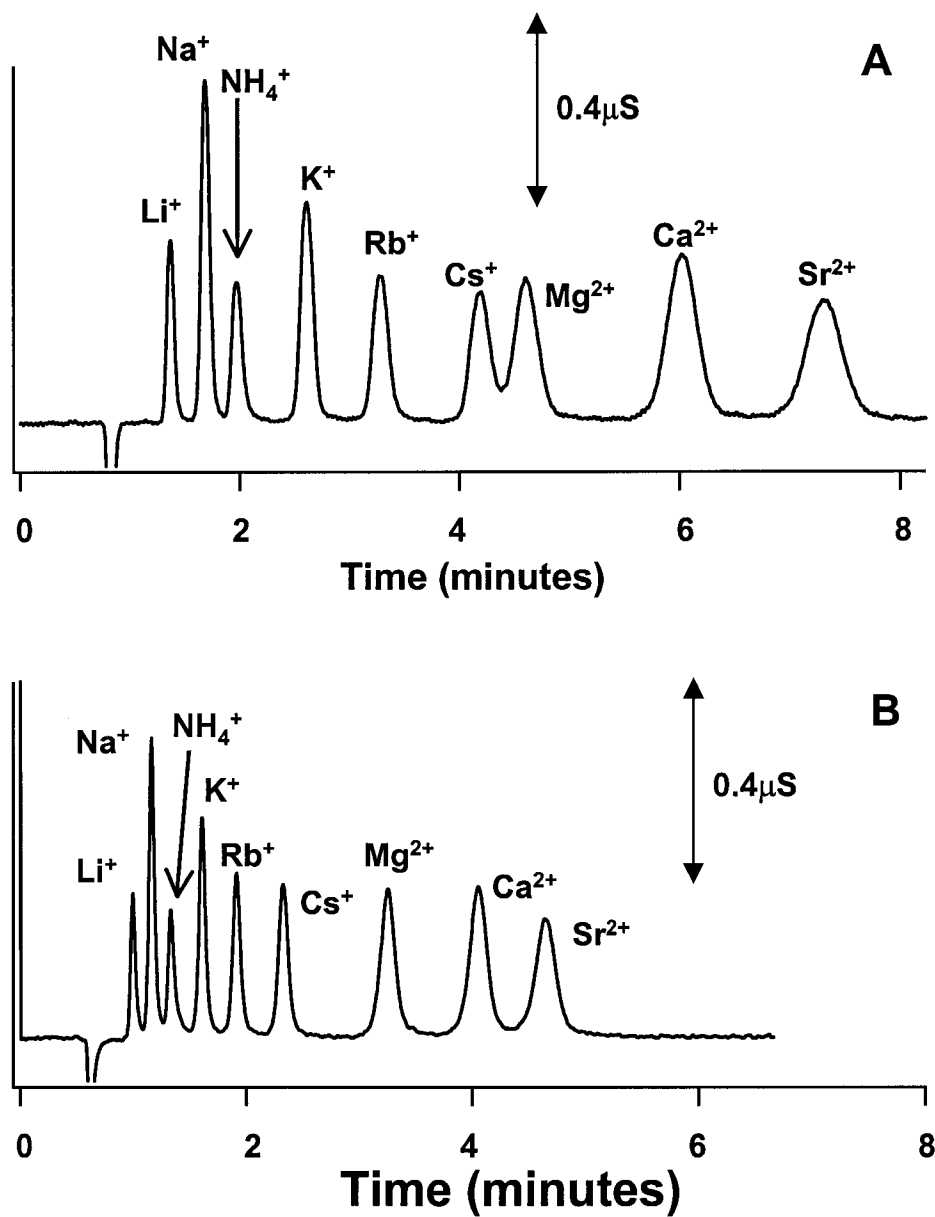


**Figure 4-4.** High-speed separation of nine cations (A) 27 °C and 0.9 mL/min (2410 psi) , (B) 60 °C and 1.3 mL/min (2420 psi). **Experimental Conditions:** Dionex CS-12A column, 17 mM MSA, 20 μL injection, 50 μM analyte concentration.



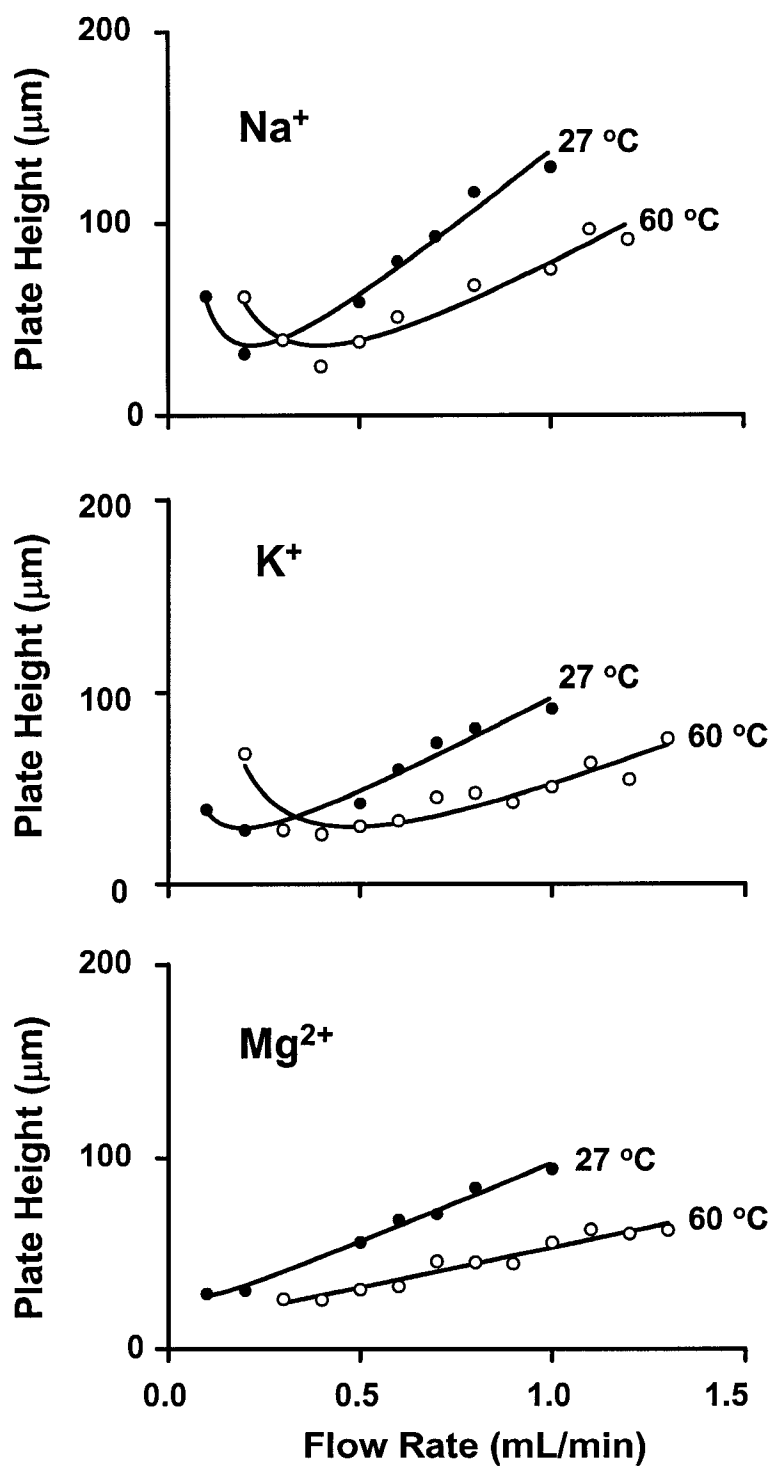


**Figure 4-5.** van Deemter plots of sodium, potassium and magnesium at 27 and 60°C. **Experimental Conditions:** Dionex CS-12A column, 17 mM MSA eluent, 20  $\mu\text{L}$  injection, 50  $\mu\text{M}$  analyte concentration. Flow rate: 0.10 to 1.30 mL/min.

linear velocity. Flow rates below 0.1 mL/min were not studied due to the long analysis times (50 min), poor reproducibility and high background noise. The lines in Figure 4-5 are the fit of the data to the van Deemter equation (Equation 1-10) with the corresponding  $C$ -terms summarized in Table 4-2.

The key conclusion that can be drawn from Figure 4-5 and Table 4-2 is that the  $C$ -term is lower at 60°C compared to 27°C. The decrease in the  $C$ -term is due to a decrease in retention and an increase in mass transfer of the solute in the mobile phase and stationary phase, with the later being of more significance.<sup>7, 28</sup> The increase in mass-transfer is due to the decrease in viscosity of the mobile phase, which in turn improves diffusion according to the Stokes-Einstein relationship<sup>29</sup>:

$$D \cong \frac{k_B T}{6\pi r_h \eta(T)} \quad (4-4)$$

where  $D$  is the diffusion coefficient,  $k_B$  is the Boltzmann constant,  $T$  is temperature,  $r_h$  is the hydrodynamic radius of the molecule, and  $\eta(T)$  is viscosity as a function of temperature. Improvements in mass transfer give lower plate heights, and thus a higher efficiency. Furthermore, the optimum linear velocity is shifted to higher values. In other words, as with RPLC, there is a considerable advantage in performing IC separations at elevated temperatures.<sup>7</sup> In this work, efficiency improved by approximately 30% at 60 °C compared to 27 °C.

However, the van Deemter equation does not explicitly include thermal-mismatch band broadening. Thermal-mismatch band broadening occurs if the eluent entering the column is not at the same temperature as the column.<sup>7, 8</sup> Figure 4-6 depicts thermal mismatch band broadening for the case where the eluent entering the column is cooler than the column itself. This causes longitudinal and radial temperature gradients within

**Table 4-2.** van Deemter parameters for sodium, potassium and magnesium at 27 and 60°C.

Temperature (°C)	Cation	C-term	r <sup>2</sup>
27	Na <sup>+</sup>	0.017 ± 0.002	0.969
	K <sup>+</sup>	0.010 ± 0.001	0.959
	Mg <sup>2+</sup>	0.0083 ± 0.0008	0.988
60	Na <sup>+</sup>	0.012 ± 0.002	0.928
	K <sup>+</sup>	0.006 ± 0.001	0.893
	Mg <sup>2+</sup>	0.0042 ± 0.0009	0.942

**Experimental conditions:** Dionex CS-12A column, 17 mM MSA eluent, 20 µL injection, separated under flow rates from 0.10 mL/min to 1.30 mL/min, 50 µM analyte concentration. Standard deviations represent the uncertainty in the fitting of the C-term.

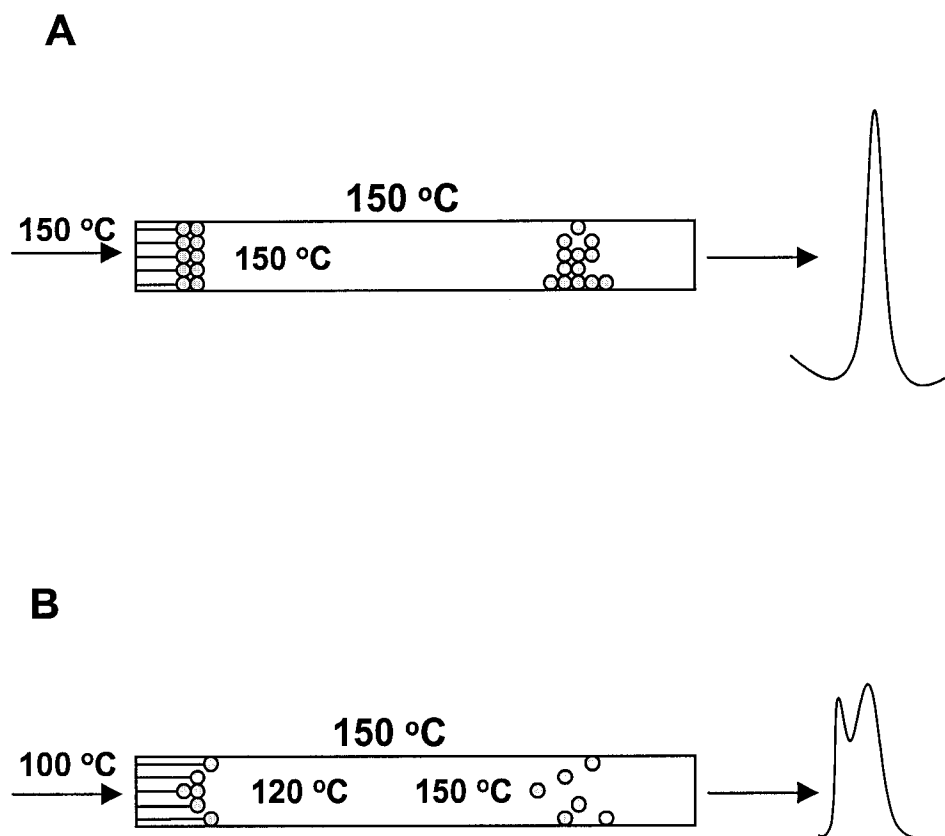


**Figure 4-6.** Diagrammatic representation of thermal mismatch band broadening. A) Eluent entering the column is at the same temperature as the column (150 °C). B) Eluent entering the column is at a lower temperature (100 °C) than the column (150 °C) and eventually equilibrates to an intermediate temperature (120 °C). Length of lines in the column is proportional to linear velocity. Adapted from Ref. <sup>8</sup>.

the column, the most important of which is the radial gradient. Analyte molecules near the column wall (higher temperature) travel faster than molecules in the centre (lower temperature). This is a result of the lower viscosity and lower retention near the wall, which increase the apparent linear velocity of the molecule. The end result is broadening or even splitting of a peak. Thompson *et al.* demonstrated that thermal-mismatch band broadening manifests itself in the *C*-term of the van Deemter equation due to its linear dependence on velocity or flow rate (Section 1.2.4.4)<sup>8</sup>. Therefore, thermal-mismatch band broadening is an extremely important consideration in achieving high temperature, high-speed separations.<sup>7, 8</sup> In particular thermal mismatch band broadening might be important in this work because of the use of an air bath rather than a liquid bath for heating<sup>7, 30</sup> and the low thermal conductivity of PEEK compared to stainless steel (*i.e.*, the thermal conductivity of plastics is at least one order of magnitude lower than stainless steel)<sup>20</sup>.

However, it does not appear that thermal-mismatch band broadening was a significant contribution to the *C*-terms observed in Table 4-2. Traditional mass transfer terms within the *C*-term are inversely dependent upon the diffusion coefficient. The diffusion coefficients of the cations studied in this work roughly double between 27 °C and 60 °C.<sup>26</sup> Thus, the *C*-term at 60 °C should be approximately half what it is at 27 °C. (The effect of retention is ignored, since diffusion and particle size are the major determinants of the *C*-term.<sup>31</sup>) The *C*-terms given in Table 4-2 for potassium and magnesium at 60 °C are indeed half of what they are at 27 °C, while that of sodium about only one third lower. In contrast, thermal mismatch band broadening causes an increase in the *C*-term as the column temperature increases, and can cause the overall *C*-term to be

larger at elevated temperatures than at ambient.<sup>8</sup> This is obviously not the behaviour observed in Figure 4-5. Thus, it does not appear that thermal mismatch is a significant contributor to band broadening under the conditions used in this work.

Another potential determinant of efficiency for the high-temperature, high-speed separations studied in this work is extra column band broadening. It is desirable to keep the flow rate through the suppressor as high as possible to minimize its contribution to the overall band broadening. However, the maximum flow rate of the suppressor is 0.75 mL/min. Figure 4-7 shows two high-speed separations of cations obtained under the same conditions (1.3 mL/min) except for the split ratio (the flow diverted to waste divided by the flow through the suppressor). In Figure 4-7A the split ratio is 1.6 corresponding to a flow of 0.5 mL/min through the suppressor, and in Figure 4-7B the split ratio is 12 corresponding to 0.1 mL/min through the suppressor. Clearly the separation obtained with the higher split ratio shows considerable band broadening. Splitting reduces the volume of peaks, which makes them more susceptible to the effects of extra-column band broadening from the suppressor and detector cell. Therefore, in this work, the flow rate through the suppressor was fixed at 0.5 mL/min, which was comfortably below the suppressor's flow limit, but at the same time, was high enough so that the split ratio was always as low as possible.

#### **4.3.4. Effect of Eluent Strength**

Of the nine cations studied above, only lithium, sodium, ammonium, potassium, magnesium and calcium are commonly present and thus are of greatest interest in industry. The high-speed separation of these six cations at 60°C and 1.30 mL/min

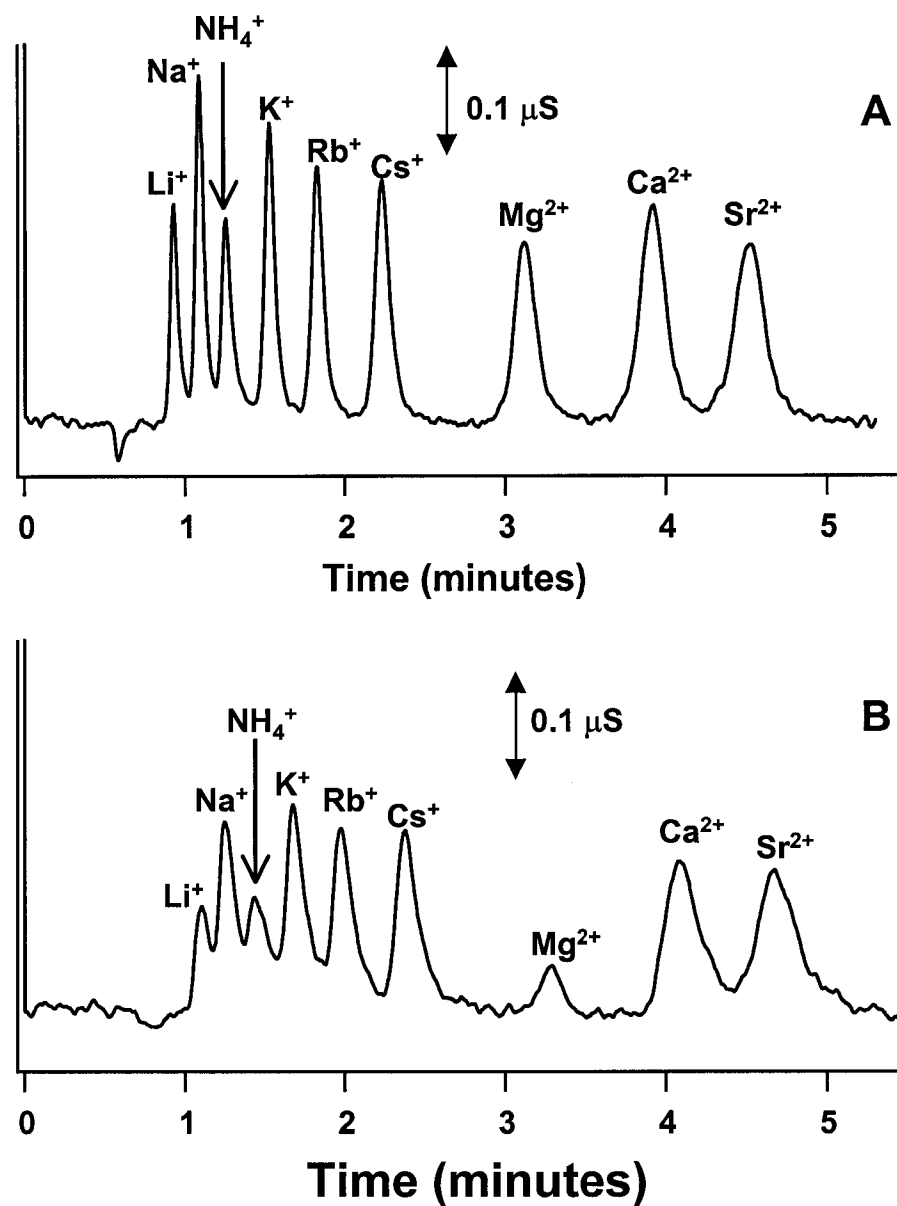


**Figure 4-7.** Effect of split ratio on efficiency of separation (A) Split ratio = 1.6, (B) Split ratio = 12. **Experimental Conditions:** Dionex CS12A column, 17 mM MSA at 1.3 mL/min, 20  $\mu\text{L}$  injection, 50  $\mu\text{M}$  analyte concentration.

(Figure 4-4B) shows a large gap between the potassium and magnesium peaks. If the size of this gap is reduced, the speed of the separation of these six cations could be further increased. Increasing the eluent strength will decrease the retention of all cations. However, the magnitude of the change in retention is a function of the analyte charge (Section 1.3.3.3). Thus when the eluent strength is increased divalent cations should experience twice the decrease in retention compared to univalent cations. This should result in closer elution between the univalent and divalent cations, without sacrificing resolution between cations of the same charge.

Figure 4-8 shows the  $\log k$  vs.  $\log [MSA]$  plot for the six common cations, and Table 4-3 shows a summary of these plots. A linear model adequately describes the data for the six cations at the 95 % confidence level. The slope of these plots is negative with  $\log k$  decreasing with  $\log [MSA]$ ; *i.e.*, retention decreases with increased eluent strength. Further, the slopes for monovalent and divalent cations are close to the theoretical values of  $-1$  and  $-2$ , although some slopes differ from ideality at the 95% confidence interval. Similar deviations from theory have been noted in the past, and apart from experimental error, they have been attributed to activity effects<sup>32</sup>. More importantly herein, Figure 4-8 shows that eluent strength will not significantly affect the separation between cations of equal charge, but will strongly reduce the retention of divalent ions relative to the univalent ions. Figure 4-9 shows a separation for the six cations in less than two minutes using 30 mM MSA. Thus, for the six common cations, the separation speed can be increased a further 50% by raising the eluent strength.

Although theory predicts a negligible loss in resolution, in practice, a small loss in resolution was observed (especially for lithium, sodium, ammonium). This was partly



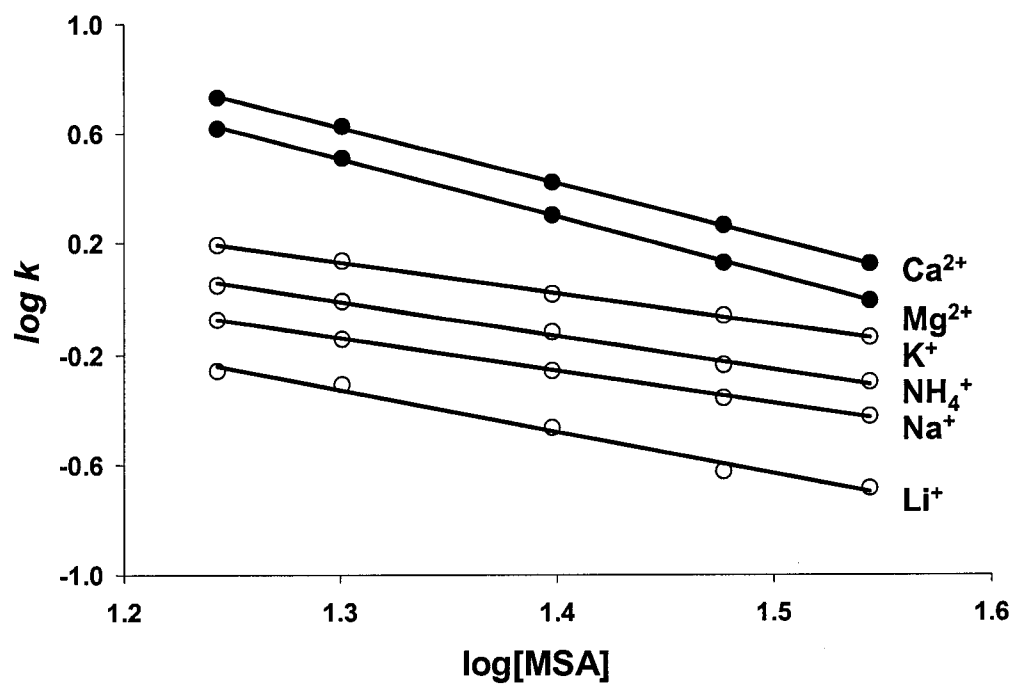


**Figure 4-8.** Plots of  $\log k$  vs.  $\log[MSA]$ . **Experimental Conditions:** Dionex CS12A column, 0.5 mL/min, 60 °C, 20  $\mu$ L injection, 50  $\mu$ M analyte concentration. Eluent range from 17 mM MSA to 35 mM MSA.

**Table 4-3.** Regression parameters for the effect of eluent strength on the retention.

Cation	Slope	p-value	r <sup>2</sup>
Li <sup>+</sup>	-1.5 ± 0.3	0.000	0.987
Na <sup>+</sup>	-1.2 ± 0.1	0.000	0.999
NH <sub>4</sub> <sup>+</sup>	-1.2 ± 0.2	0.000	0.995
K <sup>+</sup>	-1.1 ± 0.1	0.000	0.998
Mg <sup>2+</sup>	-2.0 ± 0.1	0.000	0.999
Ca <sup>2+</sup>	-2.1 ± 0.1	0.000	0.999

**Experimental conditions:** Dionex CS-12A column at 60°C, 1.3 mL/min, 20 µL injection, [MSA] ranging from 17 mM to 35 mM. The uncertainties of the slope represent the 95% confidence intervals calculated from the standard deviation of the regression.

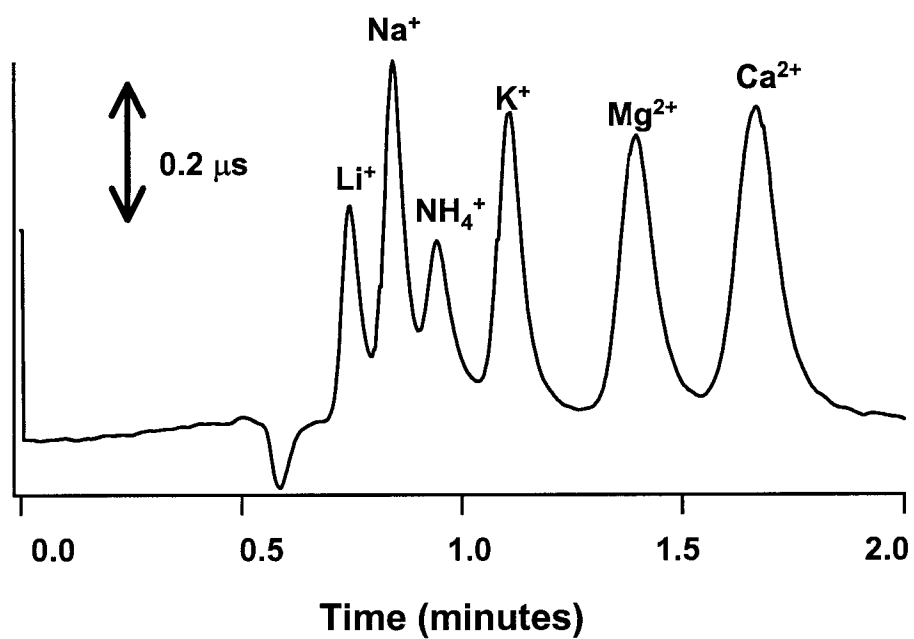


**Figure 4-9.** High-speed separation of 6 common cations.

**Experimental Conditions:** Dionex CS-12A column, 30 mM MSA,

1.3 mL/min, 20 μL injection, 60 °C, 50 μM analyte concentration.

due to the convergence of peaks at 60°C (as shown by Figure 4-3), the decreased retention and the greater impact of extra-column band broadening at low retention. Thompson and Carr showed that efficient high-speed, high temperature separations could be obtained through a decrease in eluent strength, while significant improvements in analysis time could still be realized through the higher flow rates attainable at high temperatures.<sup>9</sup> Since extra-column band broadening is more pronounced for weakly retained species, a decrease in the eluent concentration would counteract the increased band broadening by increasing the retention of weakly retained analytes (*e.g.*, lithium, sodium, ammonium). However, based on Figure 4-8 this approach would result in prohibitively long retention times of the divalent ions. This is not a phenomenon operative in the prior RPLC work.<sup>9</sup> Further, the effect of eluent strength in IC is similar for cations of the same charge. Thus, a decrease in the eluent strength does not compensate for the loss in resolution caused by convergence of the van't Hoff plots at elevated temperatures (Figure 4-3). Therefore, high-speed separations in IC are limited to relatively low temperatures, where selectivity changes are negligible. This again is why 60 °C was chosen as the maximum temperature in this work.

#### **4.4. Conclusions**

The application of elevated temperatures to the separation of cations by IC was demonstrated and resulted in a 35% improvement in analysis time. This was predominantly due to decreased viscosity, and thus lower backpressure at high temperature. Thermal-mismatch broadening did not significantly degrade the separation

efficiencies despite the use of PEEK columns, which provide poor heat transfer relative to traditional stainless steel columns.

Unfortunately, the application of elevated temperature to high-speed IC is restricted to relatively low temperatures resulting in only modest improvements in separation time. Thus, elevated temperature is not as suitable a variable for high-speed separation as it is in RPLC. For this reason, Chapters Five and Six examine the use of monolithic stationary phase materials to obtain unprecedented fast separations of anions.

#### 4.5 References

- (1) Martin, M.; Eon, C.; Guiochon, G. *J. Chromatogr.* **1974**, *99*, 357.
- (2) Martin, M.; Eon, C.; Guiochon, G. *J. Chromatogr.* **1975**, *108*, 229.
- (3) Martin, M.; Eon, C.; Guiochon, G. *J. Chromatogr.* **1975**, *110*, 213.
- (4) Connolly, D.; Paull, B. *J. Chromatogr. A* **2001**, *917*, 353-359.
- (5) Connolly, D.; Paull, B. *Anal. Chim. Acta* **2001**, *441*, 53-62.
- (6) Connolly, D.; Paull, B. *J. Chromatogr. A* **2002**, *953*, 299-303.
- (7) Yan, B. W.; Zhao, J. H.; Brown, J. S.; Blackwell, J.; Carr, P. W. *Anal. Chem.* **2000**, *72*, 1253-1262.
- (8) Thompson, J. D.; Brown, J. S.; Carr, P. W. *Anal. Chem.* **2001**, *73*, 3340 - 3347.
- (9) Thompson, J. D.; Carr, P. W. *Anal. Chem.* **2002**.
- (10) Dunlap, C. J.; McNeff, C. V.; Stoll, D.; Carr, P. W. *Anal. Chem.* **2001**, *73*, 598A-607A.
- (11) McNeff, C.; Zigan, L.; Johnson, K.; Carr, P. W.; Wang, A. S.; Weber-Main, A. *M. LC-GC* **2000**, *18*, 514.

- (12) Kephart, T. S.; Dasgupta, P. K. *Talanta* **2002**, *56*, 977-987.
- (13) Smith, R. M.; Burgess, R. J. *J. Chromatogr. A* **1997**, *785*, 49-55.
- (14) Kraus, K. A.; Raridon, R. J. *J. Phys. Chem.* **1959**, *63*, 1901.
- (15) Rey, M. A. *J. Chromatogr. A* **2001**, *920*, 61-68.
- (16) *Dionex CSRS Ultra User's Manual*; Dionex: Sunnyvale, 2001.
- (17) Devore, J. L. *Probability and Statistics for Engineering and the Sciences, 4th Ed.*; Duxbury: New York, 1995.
- (18) Grushka, E.; Meyers, M. N.; Schettler, P. D.; Giddings, J. C. *Anal. Chem.* **1969**, *41*, 889-892.
- (19) Foley, J. P.; Dorsey, J. G. *Anal. Chem.* **1983**, *55*, 730-737.
- (20) *Upchurch Scientific Product Catalogue*; UpChurch: Oak Harbor, 2002.
- (21) Mao, Y.; Carr, P. W. *Anal. Chem.* **2000**, *72*, 110-118.
- (22) Cole, L. A.; Dorsey, J. G. *Anal. Chem.* **1992**, *64*, 1317.
- (23) Snyder, L. R.; Glajch, J. L.; Kirkland, J. J. *Practical HPLC Method Development*, 2nd ed.; Wiley-Interscience: New York, 1996.
- (24) Cantwell, F. F. *Analytical Separations Class Notes*; University of Alberta: Edmonton, 1998.
- (25) Neue, U. D. *HPLC Columns: Theory, Technology and Practice*; Wiley-VCH: New York, 1997.
- (26) Lide, D. R. *CRC Handbook of Chemistry and Physics*, 76th ed.; CRC Press: New York, 1995-1996.
- (27) *Dionex 1997-1998 Product Selection Guide*; Dionex: Sunnyvale, 1997.
- (28) Lee, S. T.; Olesik, S. V. *Anal. Chem.* **1994**, *66*, 4498-4506.

- (29) Atkins, P. W. *Physical Chemistry*, 6th ed.; Freeman: New York, 1998.
- (30) Poppe, H.; Kraak, J. C. *J. Chromatogr.* **1983**, 282, 399-412.
- (31) Neue, U. D. *HPLC Columns*; Wiley-VCH, Inc.: New York, 1997.
- (32) Haddad, P. R.; Jackson, P. E. *Ion Chromatography: Principles and Applications*; Elsevier: New York, 1990.

## CHAPTER FIVE. Ultra-Fast Separation of Common Anions Using a Monolithic Stationary Phase \*

### 5.1 Introduction

Chapter Four presented research on the use of elevated temperatures to reduce analysis time in IC. However, the gain in separation speed that was observed in Chapter Four was relatively modest (35% improvement). This is due to problems with the implementation of elevated temperatures in IC, *e.g.*, the limited temperature range examined (60 °C) due to the PEEK column and selectivity changes that resulted in a reduction in resolution. For this reason, alternative methods for reducing analysis time in IC continue to be explored.

It was mentioned in Section 1.2.4.5 that a decrease in particle size leads to an improvement in column efficiency. This is the reasoning behind the trend in HPLC to pack columns with smaller particles<sup>1-3</sup>. However, combining Equations 4-3a and 4-3b:

$$\Delta P = F \left( \frac{\text{constan } t}{d_p^2} \right) \quad (5-1)$$

reveals that the pressure drop,  $\Delta P$ , required to achieve a given flow rate,  $F$ , increases inversely with the *square* of the particle diameter,  $d_p$ . Therefore, particle diameter can be reduced to improve efficiency, but there will be a point where the pressure exceeds the limit of the system. Therefore, as was mentioned in Chapter Four, significant improvements in separation speed could be obtained by decreasing the pressure required for a given flow rate, while maintaining the efficiency of the separation. This can be

---

\* A version of this chapter has been published. Hatsis, P.; Lucy, C.A. *Analyst* **2002**, *127*, 451-454.



accomplished through a change in the column geometry. In recent years, monolithic materials have been increasingly used as separation media for HPLC.<sup>4-8</sup> Monolithic columns consist of a single piece of stationary phase material (e.g., silica) with interconnected skeletons to give paths (through-pores) for solvent flow.<sup>7</sup> Monoliths also have small skeleton sizes, which allow for reduced diffusion path lengths. Moreover, large through-pore size to skeleton size ratios are achievable with monoliths, which results in increased column permeability as well as excellent efficiency<sup>7</sup>.

The construction of silica-based monoliths is shown in Figure 5-1. The fabrication process begins with the neutralization of an alkaline solution of tetramethoxysilane or tetraethoxysilane. This is followed by the formation and polymerization of monosilicic acid in the presence of a polymer or surfactant that induces phase separation. The polymer also helps to form the macropores of the monolith. Exchanging the solvent for new/different solvent forms the mesoporous structure. Drying and heat treatment result in a single piece of silica that is ready for cladding, *i.e.*, enclosure into an HPLC column blank. A picture of monolithic silica compared to particulate silica is shown in Figure 5-2.

Monoliths used in HPLC have 1-3  $\mu\text{m}$  macropores for solvent flow and 10-25 nm mesopores to provide the surface area necessary for retention. The porous structure of a monolith is shown in Figure 5-3. The surface area of monolithic structures is comparable to that of silica particles (approximately  $300 \text{ m}^2/\text{g}$ )<sup>7</sup>. For the most part however, the unique structure of monolithic materials makes a direct comparison with particle packed columns nontrivial. Recently, Leinweber *et al.* determined that diffusion limited mass transfer exists in the mesoporous skeleton of silica-based monoliths.<sup>9</sup> This allowed them

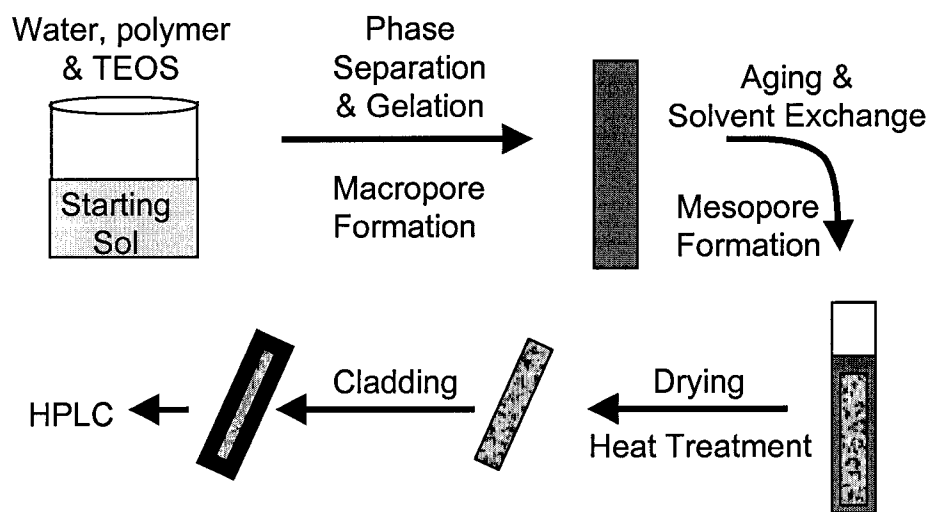


**Figure 5-1.** The fabrication process of silica monoliths. Adapted from Ref. 7.

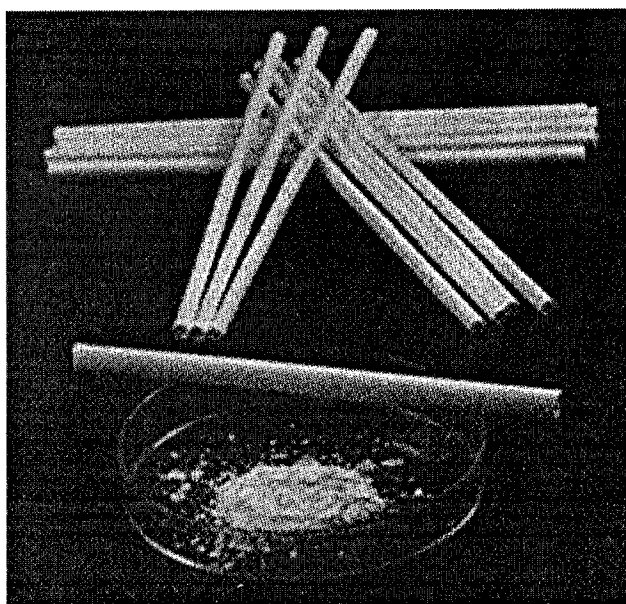


**Figure 5-2.** A silica monolith compared to silica particles. Adapted from Ref. 8.

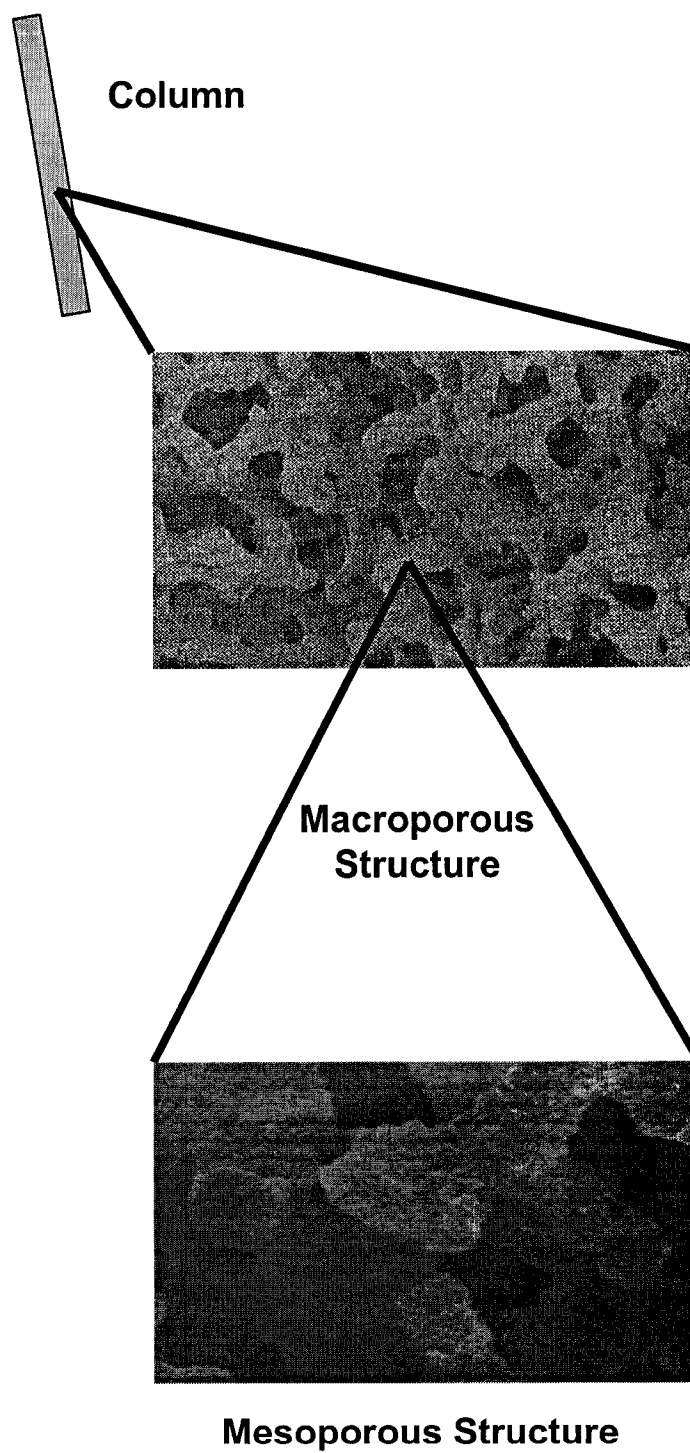


**Figure 5-3.** Macroporous and mesoporous structure of a monolith. Adapted from Ref. 7.

to calculate an equivalent particle diameter for the monolith based on the  $C$ -term of the van Deemter equation. They concluded that in terms of band broadening, their monolithic stationary phases behave equivalent to 3  $\mu\text{m}$  particles, which is the smallest particle size routinely used in HPLC.

However, monoliths also have a high permeability. This is shown in Figure 5-4. Obviously the pressure drop needed for a given linear velocity (or flow rate) is considerably lower with monoliths compared to particle packed columns. For example, a column packed with 5  $\mu\text{m}$  particles has a permeability of approximately  $4 \times 10^{-14} \text{ m}^2$ , whereas a monolith has a permeability of  $1 \times 10^{-12} \text{ m}^2$ .<sup>7</sup> Alternatively, based on the Kozeny-Carman equation (Equation 4-3b), Leinweber *et al.* calculated that silica based monoliths have a permeability equivalent to a bed packed with 15  $\mu\text{m}$  diameter particles<sup>9</sup>. Thus, it can be concluded that monoliths are well suited to high-speed separations.

In this chapter, the suitability of monolithic stationary phase materials for high-speed IC is evaluated. Separations are performed using ion-interaction chromatography with tetrabutylammonium-phthalate as the ion-interaction reagent. Direct conductivity and indirect ultraviolet absorbance detection is used, rendering the method universal to all anions. The viability of the proposed method in real-world ion analysis is demonstrated with an industrial water sample.

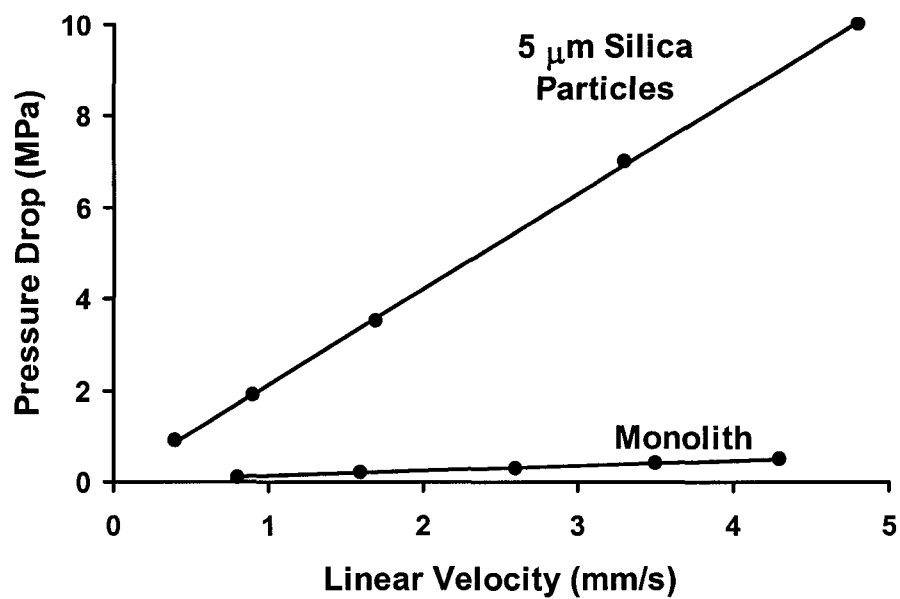


**Figure 5-4.** Pressure vs. linear velocity for various columns. Adapted from Ref. 7.

## 5.2 Experimental

### 5.2.1 Apparatus

Separations were performed with a Dionex DX-300 chromatography system (Sunnyvale, CA, USA). A Waters 590 pump (Waters, Milford, MA, USA) was used for separations requiring flow rates in excess of 10 mL/min. Injection of 20  $\mu$ L of sample was performed with a Spectra Physics AS3500 autosampler (Thermo Finnigan, Mississauga, Canada) equipped with a Rheodyne 9110 (Rheodyne, Cotati, CA, USA) six-port injection valve. All separations were performed on a Chromolith<sup>®</sup> Speed ROD RP-18e column (4.6 mm i.d. x 50 mm) (Merck KGaA, Darmstadt, Germany). Connecting tubing was 0.005" i.d. PEEK (Upchurch Scientific, Oak Harbor, WA, USA).

The primary detection scheme used in this work was direct (*i.e.*, non-suppressed) conductivity detection. This was accomplished with a Dionex ED-50A electrochemical detector. The rise time was set to 0.05 s and data collection was at 20 Hz. Alternatively, a Dionex VDM-II variable wavelength ultraviolet absorbance detector was used for indirect absorbance detection at 255 nm. The rise time was set to 0 s and data collection was also at 20 Hz. Data was collected using a Dionex AI-450 data acquisition system interfaced to a Pentium II computer running Peak Net 5.0 software (Dionex).

### 5.2.2 Reagents

All reagent solutions were prepared using distilled deionized water (Nanopure Water System, Barnstead, Chicago, IL, USA). All chemicals were reagent grade or better. Stock solutions of analytes were prepared ( $\cong 10^{-2}$  M) and diluted to the desired concentration before use. Chloride (BDH Inc., Toronto, Canada), nitrite (BDH), iodide

(BDH), sulfate (BDH), phosphate (Fisher, Nepean, Canada) and chlorate (Fisher) were used as their sodium salts. Bromide (Fisher) and nitrate (BDH) were used as their potassium salts.

Tetrabutylammonium-phthalate was used as the ion-interaction reagent in this work. It was prepared by titrating tetrabutylammonium hydroxide (TBA-OH) (40% (w/w) solution from Aldrich (Milwaukee, WI, USA)) with *o*-phthalic acid (99.5%+, ACS Reagent, Aldrich) as is described in Section 5.2.3. Acetonitrile was obtained from Fisher (HPLC grade).

A water sample from an industrial source was used in a blind test of the method described in this work. The sample was diluted 20-fold and filtered through a 0.45  $\mu\text{m}$  filter before injection. The results are compared with those obtained using a standard suppressed ion chromatography procedure that uses a Dionex AS4A-SC anion-exchange column with a Dionex Atlas suppressor, 1.7 mM sodium bicarbonate/1.8 mM sodium carbonate eluent, 1.75 ml/min eluent flow rate and a 25  $\mu\text{L}$  injection volume.

### 5.2.3 Procedure

Eluents were prepared by titrating the desired amount of TBA-OH with *o*-phthalic acid ( $\text{pK}_{\text{a}2} = 5.5$ ) to pH 5.5. Acetonitrile was added to the solution at 5% (v/v). The eluent was then filtered through a 0.45  $\mu\text{m}$  filter. The eluent was continually degassed by means of helium sparging. Premixed eluents were used rather than machine-mixed eluents so as to minimize pump noise.

Prior to performing any separations, the column was equilibrated for at least one hour with a 95/5-water/acetonitrile eluent. The column was then flushed with the TBA-



phthalate eluent. Separations were performed after the conductivity response became stable.

Data analysis and integration was performed with Peak Net 5.0 software. Detection limits were calculated as the minimum concentration of an anion that can be reported with 99% confidence to greater than the blank.<sup>10</sup> The area of  $n$  (usually  $n = 10$ ) samples with a concentration 1 – 5 times the detection limit were measured and the standard deviation was calculated. The detection limit is the product of the standard deviation and the value of Student's  $t$  for 98% confidence (two-sided) and  $n-1$  degrees of freedom. The efficiency of peaks was calculated using the equation<sup>11</sup>:

$$N = 2\pi \left( \frac{t_r h}{Area} \right)^2 \quad (5-2)$$

where  $N$  is efficiency,  $t_r$  is retention time,  $h$  is the height of the peak and  $Area$  is the area of the peak. Equation 5-2 was used due to its simplicity, however it does assume perfectly Gaussian peaks (*i.e.*, absolutely no tailing). Plate heights were then calculated from efficiencies. Plate height vs. linear velocity data were fit to the van Deemter equation (Equation 1-10) using GraphPad Prism 3.02 (GraphPad Software Inc., San Diego, CA, USA). Linear velocity was calculated with the equation:

$$u = \frac{F}{\pi \varepsilon_b r_c^2} \quad (5-3)$$

where  $u$  is linear velocity (cm/s),  $F$  is flow rate (cm<sup>3</sup>/s),  $\varepsilon_b$  is the external porosity of the monolithic bed and  $r_c$  is the radius of the column (cm). The external porosity of the bed was taken as 0.597 based on the work of Leinweber *et al.*<sup>9</sup>

### 5.3 Results & Discussion

#### 5.3.1 Stationary Phase Concerns

Monolithic columns have been used to perform very fast and highly efficient separations in reversed-phase HPLC.<sup>6, 8</sup> However, it was not clear if the efficiency (and therefore resolution) would be preserved at high flow rates when performing ion-interaction chromatography of inorganic anions. To investigate this further, a van Deemter plot was constructed for nitrate using TBA-phthalate as the ion-interaction reagent. This is shown as Figure 5-5. Clearly, there is a small increase in plate height in going from the optimum linear velocity (0.4 cm/s or 2.5 mL/min) to higher linear velocities (2.7 cm/s or 16 mL/min) for nitrate. For example, the plate height is 13  $\mu\text{m}$  at the optimum flow rate whereas at 2.7 cm/s it increases slightly to 23  $\mu\text{m}$ . This represents a loss in resolution of less than 2% in going between two extremes of flow rate. A more detailed study of the band broadening behaviour of monoliths will be undertaken in Chapter Six. Suffice it to say that the monolith is well suited to the separation of ions at linear velocities higher than the optimum.

#### 5.3.2 Eluent Conditions

Conventional membrane-based suppressors for suppressed conductivity IC are not compatible with the high flow rates that are needed for rapid separations. Furthermore, the limited pH stability of silica (pH 2 to 8) excludes eluents (*e.g.*, carbonate and hydroxide) that are typically used for suppressed conductivity detection. Therefore, direct conductivity and indirect absorbance detection were used herein. As such, an eluent anion was sought which was a weak acid (for buffering action) and possessed a strong chromophore (for indirect absorbance detection). An additional concern was that

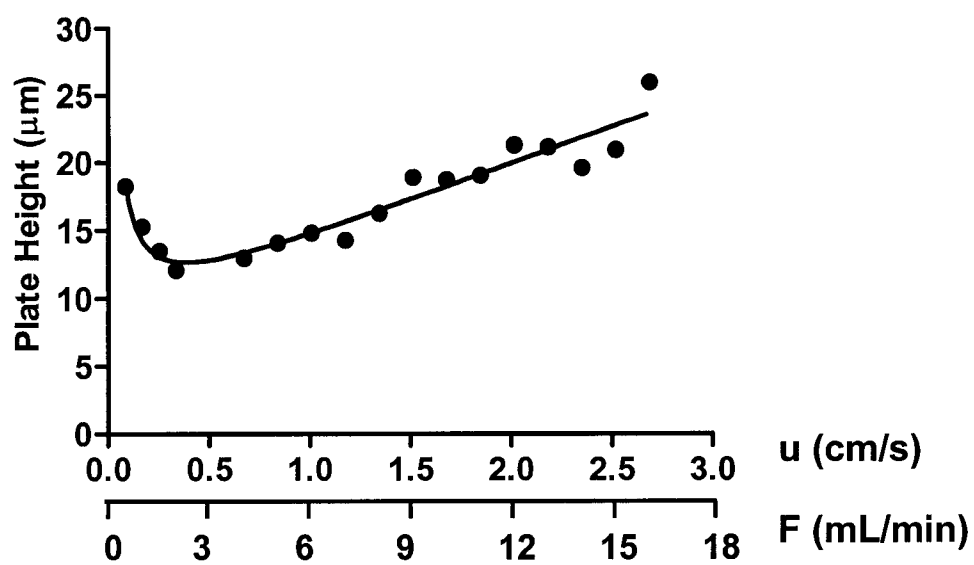


**Figure 5-5.** Plot of plate height ( $H$ ) vs. flow rate for nitrate on a monolithic column. **Experimental conditions:** Monolith, 1.5 mM TBA-1.1 mM phthalate with 5% (v/v) acetonitrile, 20  $\mu\text{L}$  injection.

the system peak associated with the eluent anion did not overlap with any of the analyte peaks. System peaks result from the displacement of eluent ions from the stationary phase upon injection of the sample<sup>12</sup>. The displaced eluent ions elute from the column with a retention time characteristic of the eluent. This results in a positive or negative peak, which can co-elute with analyte peaks. The size of system peaks is dependent on the eluent concentration and pH as well as the sample concentration, volume and pH.<sup>12</sup> A number of eluent anions (*e.g.*, benzoic acid, salicylic acid, *p*-aminobenzoic acid, *o*-phthalic acid) were tested. *o*-Phthalic acid at pH 5.5 was found to be optimum and so was used in all further work. All of the other eluents that were tried caused co-elution of sulfate with the system peak and were not examined any further.

Eluents were prepared by titrating tetrabutylammonium hydroxide with *o*-phthalic acid as is described in Section 5.2.3. This also served as the buffer. Ideally the pH of the solution should be controlled with a separate buffer. However, the conductivity of the eluent has to be minimized when employing direct conductivity detection. Thus, the pH was controlled through the concentration of tetrabutylammonium-phthalate. This did not allow independent control of the concentration of tetrabutylammonium from that of *o*-phthalic acid, thus making method development extremely difficult. The optimum eluent composition was 1.5 mM tetrabutylammonium-1.1 mM phthalate, which resulted in a pH of 5.5. Lower concentrations of tetrabutylammonium-phthalate resulted in excessive retention of sulfate and higher concentrations resulted in insufficient retention of phosphate, such that it fell into the “water dip” at the beginning of the chromatogram. Thus the choice of tetrabutylammonium-phthalate concentration was a compromise between the retention of phosphate and sulfate. Similarly, lower pH (down to pH = 4.5)

resulted in excessive retention of sulfate since the charge of the eluent ion was decreased. Although higher pH (up to pH = 6.5) bridged the gap between sulfate and earlier eluting ions, it also served to increase the charge on phosphate causing it to co-elute with chloride. A low percentage of acetonitrile was used to minimize the amount of ion-interaction reagent needed for retention of ions (Section 1.3.4). Although an aqueous eluent would have allowed use of lower concentrations of ion-interaction reagent, an improvement in efficiency was noted when at least 5% acetonitrile was added to the eluent.

### 5.3.3 Fast Anion Separations

Figure 5-6 shows a one-minute separation of common anions using the monolithic column and a TBA-phthalate eluent. Figure 5-6A is for direct conductivity detection and Figure 5-6B is for indirect absorbance detection at 255 nm. All anions are completely resolved except for phosphate-chloride and nitrite-bromide which are nearly baseline resolved (approximately a resolution of 0.9). The system peak for phthalate elutes at approximately 1.2 min, which is after all anions of interest.

Table 5-1 lists the detection limits achieved using the conditions in Figure 5-6. Detection limits for direct conductivity are in the low ppm range, which is typical for this mode of detection.<sup>13</sup> Detection limits for indirect absorbance detection are higher than those for direct conductivity. This is especially true for iodide and sulfate whose detection limits by indirect absorbance are more than 10 times higher than for direct conductivity. Bromide has the highest detection limit due to a small system peak with which it co-elutes. A typical calibration curve for sulfate using conductivity detection is shown in Figure 5-7A. Calibration curves (number of standards,  $n = 8$ ) show linearity

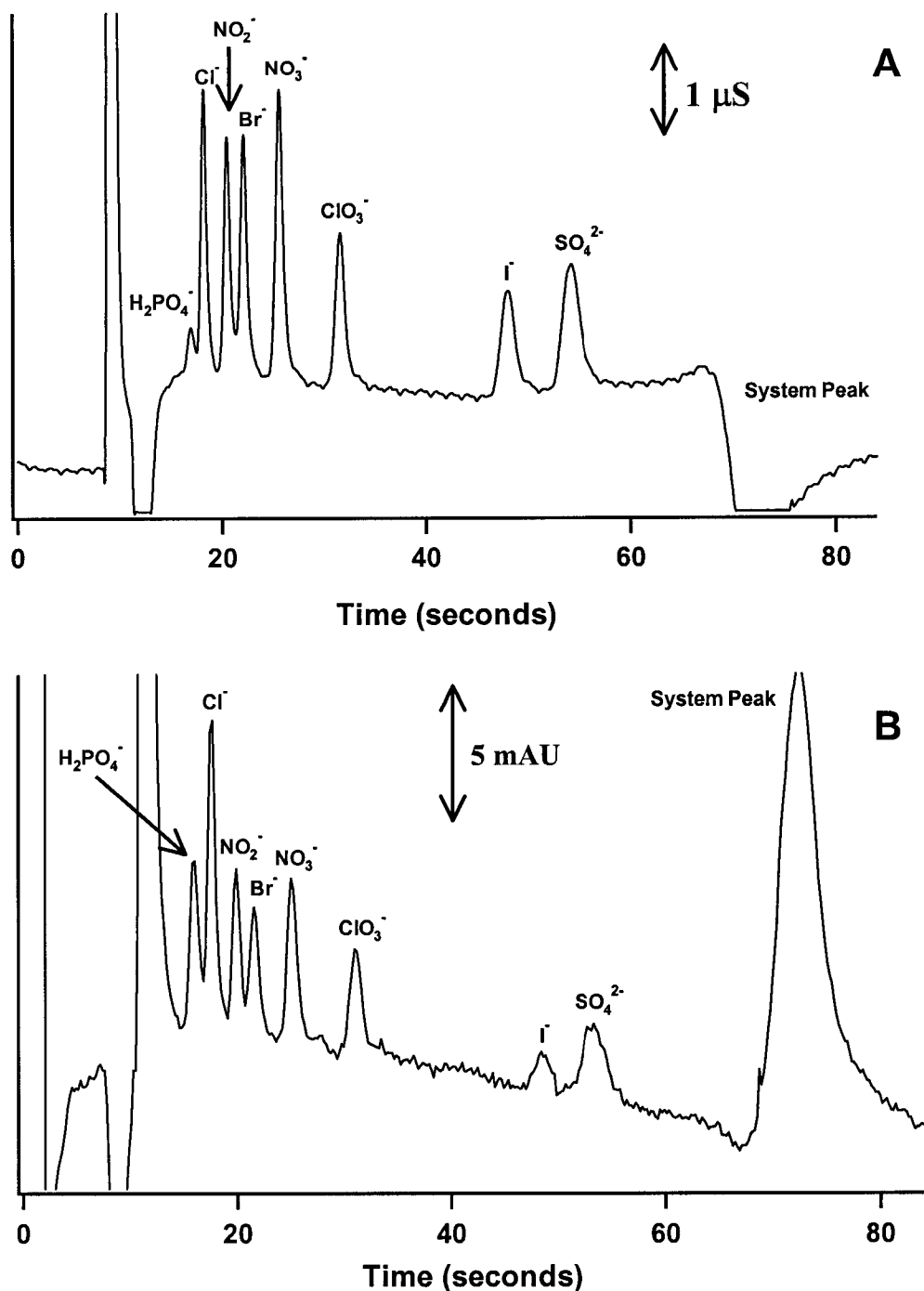


**Figure 5-6.** One-minute anion separation using, (A) conductivity detection, (B) indirect absorbance detection (255 nm). **Experimental Conditions:** Monolith, 1.5 mM TBA-1.1 mM phthalate with 5% (v/v) acetonitrile, eluent flow at 4 mL/min, 20  $\mu\text{L}$  injection. Analyte concentration approximately 25 times detection limit.

**Table 5-1.** Detection limits for common anions using direct conductivity and indirect absorbance detection.

	$\text{H}_2\text{PO}_4^-$	$\text{Cl}^-$	$\text{NO}_2^-$	$\text{Br}^-$	$\text{NO}_3^-$	$\text{ClO}_3^-$	$\text{I}^-$	$\text{SO}_4^{2-}$
Detection Limit for Conductivity (ppm)	2	0.1	0.2	4	0.1	0.2	0.9	0.2
Detection Limit for Indirect Absorbance (ppm)	1	0.4	0.7	4	0.9	2	20	8

**Experimental Conditions:** Monolith, 1.5 mM TBA-1.1 mM phthalate with 5% (v/v) acetonitrile, eluent flow at 4 mL/min, 20  $\mu\text{L}$  injection.

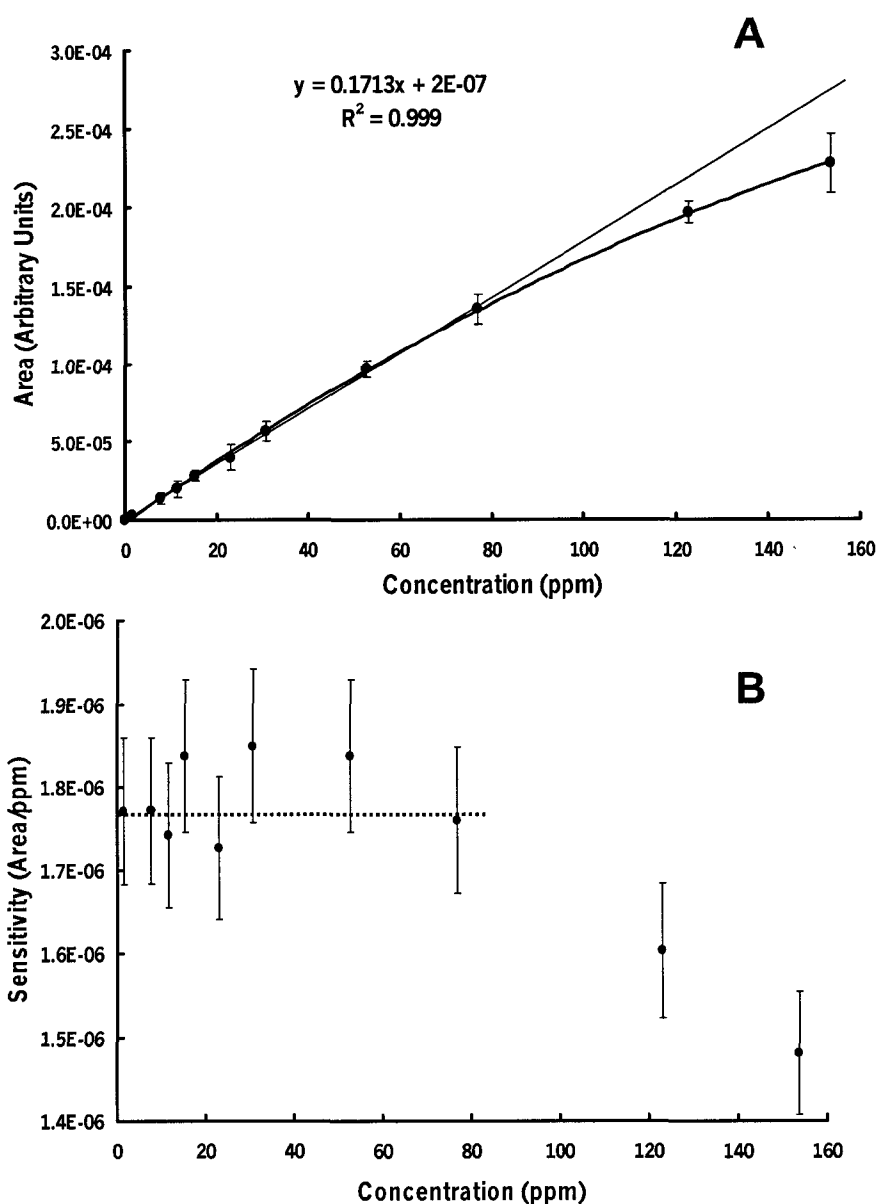


**Figure 5-7.** A) Calibration curve for sulfate using conductivity detection. B) Sensitivity plot for the calibration. Horizontal line indicates linear range. The error bars are 5% control intervals, *i.e.*, a maximum of 5% deviation from linearity. Curved line drawn by “connecting the dots”. **Experimental Conditions:** Monolith, 1.5 mM TBA-1.1 mM phthalate with 5% (v/v) acetonitrile, eluent flow at 4 mL/min, 20  $\mu$ L injection.



almost over two orders of magnitude (*e.g.*, from 1 ppm to 80 ppm for sulfate). The linearity of calibration curves was determined with a sensitivity plot, *i.e.* area/concentration vs. concentration (Figure 5-7B) as advocated by Cassidy.<sup>14</sup> There should be no relationship between sensitivity and concentration if the calibration curve is linear. Therefore, a flat region in a sensitivity plot indicates the linear range of the method. Intercepts in the calibration curve were equal to zero at the 95% confidence level.

Retention time reproducibility is necessary for reliable peak identification and quantification. The retention times of the anions separated in this work varied on average by 0.4 % ( $n = 5$ ) (relative standard deviation (RSD)) on a day-to-day basis and 0.7 % ( $n = 5$ ) on a week-to-week basis. The RSD for peak area determinations of nitrate was 2 % ( $n = 5$ ) at a concentration of 25 times the detection limit. Precision for phosphate was the poorest of all anions (RSD = 9% ( $n = 5$ ) at a concentration of 25 times the detection limit) due to its low sensitivity and only partial resolution from chloride.

#### **5.3.4 Analysis of an Industrial Water Sample**

The viability of the proposed method in real-world anion analysis was tested with an industrial water sample. The sample was diluted 20-fold and filtered before injection. Table 5-2 shows the results from the quantification of the anions present in the sample. A *t*-test<sup>15</sup> was used to compare the concentrations of anions as determined by each method. The two methods are statistically equivalent for chloride and sulfate at the 95% confidence level. Unfortunately, the phosphate in the sample could not be quantified using high-speed IC due to the limited sensitivity for phosphate using direct conductivity

**Table 5-2.** Comparison of levels of anions determined by two different methods.

	<b>Concentration by Standard Method (ppm)</b>	<b>Concentration by Proposed Method (ppm)</b>	<b>% Error</b>
Phosphate	2.4 ± 0.2	< 2	-
Chloride	72 ± 5	76 ± 4	6 %
Sulfate	410 ± 10	420 ± 10	4 %

**Experimental Conditions for Standard Method:** Dionex AS4A-SC column, 1.7 mM bicarbonate/ 1.8 mM carbonate, 1.75 mL/min, 25 µL injection. Uncertainty is 95 % confidence interval based on a relative standard deviation of 2% with three replicate measurements.

**Experimental Conditions for Proposed Method:** Monolith, 1.5 mM TBA – 1.1 mM phthalate, with 5 % (v/v) acetonitrile, 4 mL/min, 20 µL injection. Uncertainty is 95 % confidence interval based on three replicate measurements.

detection. Direct conductivity detection is about 100 times less sensitive than suppressed conductivity detection.<sup>16</sup>

### 5.3.5 Ultra-Fast Separations

The one-minute separation of common anions used a 4 mL/min flow rate with a pressure drop of only 750 psi. The monolith is rated to 3000 psi by the manufacturer. Therefore, the flow rate can be increased even further to allow for much faster separations. Figure 5-8A shows a 30-second anion separation and Figure 5-8B shows a 15-second separation of the same anions. The 30-second separation shows comparable resolution to the one-minute separation (Figure 5-6A). This is consistent with Figure 5-5, *i.e.*, the loss in efficiency is small at flow rates up to 8 mL/min. The variation in retention time has increased (1.0% RSD,  $n = 5$ ) and peak area reproducibility (3% RSD,  $n = 5$  for nitrate and 11% for phosphate) is still well preserved compared to the one-minute separation.

At 16 mL/min, a 15-second separation of the same anions is achieved (Figure 5-8B). Further, the pressure drop across the monolith is only 2500 psi., which is well within normal HPLC operating conditions. However, the peak efficiency has been adversely affected by these extreme flow rates, such that the resolution between nitrite and bromide is only 0.7. The variation in peak area is 3% RSD ( $n = 5$ ) for nitrate and 15% RSD ( $n = 5$ ) for phosphate. The variation in retention time increased to 2.8% RSD ( $n = 5$ ).

It is important to note that a number of modifications to the HPLC system were necessary to achieve the 15-second separation shown in Figure 5-8B. The column backpressure at 16 mL/min (2500 psi) was acceptable, but the pressure drop across the

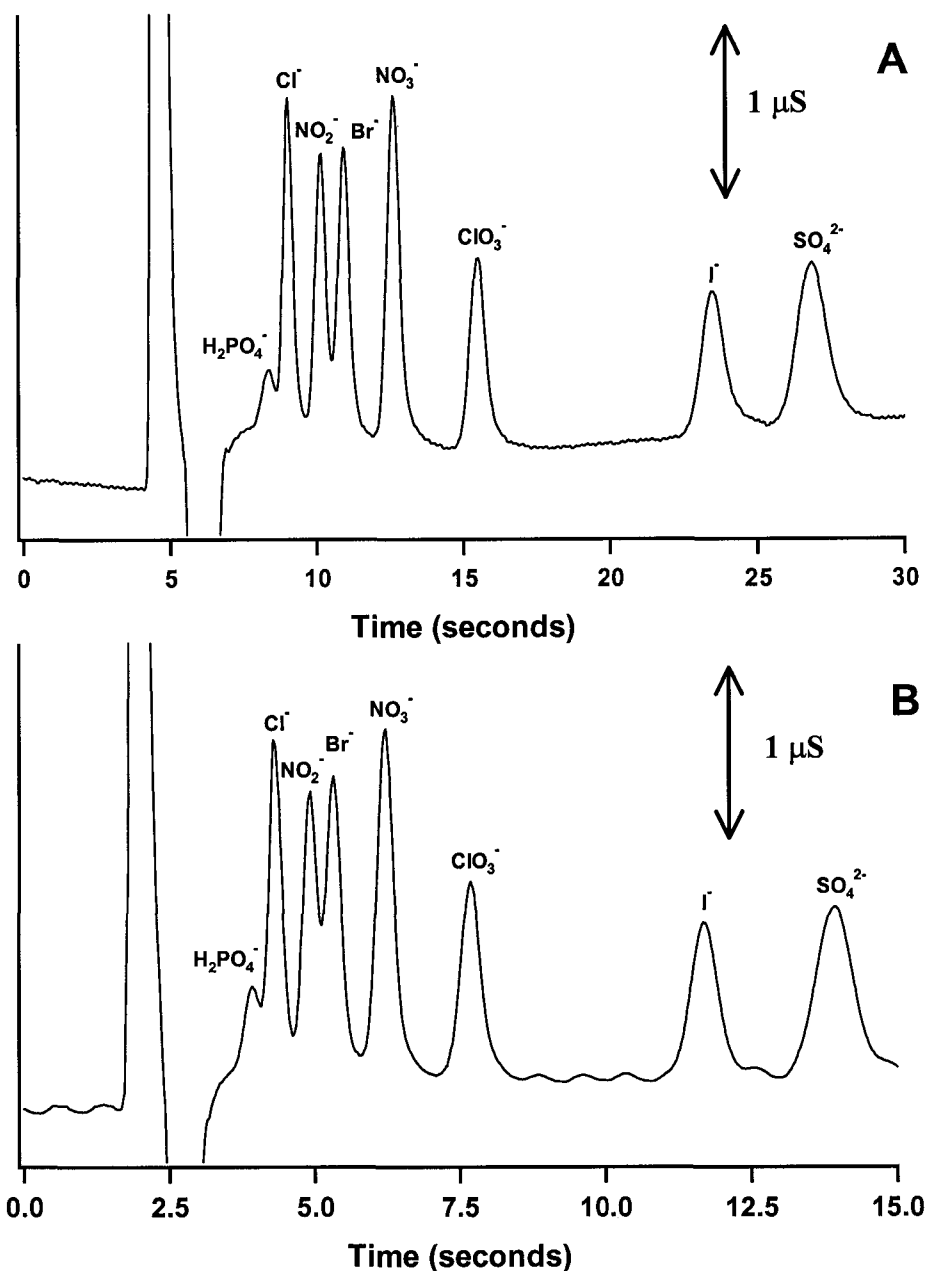


**Figure 5-8.** Separation of common anions, (A) in 30 seconds (8 mL/min – split ratio = 1), (B) in 15 seconds (16 mL/min – split ratio = 3). **Experimental Conditions:** Monolith, 1.5 mM TBA-1.1 mM phthalate with 5% (v/v) acetonitrile, 20  $\mu\text{L}$  injection. Eluent flow for 15-second separation with a Waters 590 pump. Analyte concentration approximately 25 times detection limit.

detector flow cell (300 psi) was excessive. Thus, the eluent flow was split (split ratio of 3, i.e., 12 mL/min to waste and 4 mL/min to the detector cell) before the conductivity cell to protect it from excessive backpressure. Also, the data acquisition rate of conventional conductivity detectors (*e.g.*, Dionex CDM-3, max. 5 Hz) was insufficient to monitor the peaks under the conditions used in Figure 5-8B. Therefore, the prototype ED-50A detector from Dionex was used to enable data collection at 20 Hz.

Similarly, the injection time must now be taken into consideration. The autosampler used in this work could only inject once every 30 s. Thus loading the injector requires more time than the separation. Finally at very high flow rates, eluent consumption becomes a problem as well. At 16 mL/min a normal HPLC solvent reservoir (1 L) will last for about one hour. However, approximately 60 samples have been analyzed in this time. One way to reduce eluent consumption is through recycling. A switching valve can be utilized to direct solvent back to the eluent reservoir during sample injection or column equilibration.

Nevertheless, the largest hurdle in employing the 15-second separation for routine analysis is the requirement for unconventionally high flow rates for analytical HPLC. For example, the Waters 590 pump used in this work is meant for preparative scale HPLC and even the 30-second separation requires eluent flow at 8 mL/min, which is close to the upper limit of most analytical HPLC pumps. For this reason, it is the one-minute separation that is presently the most accessible for routine analysis. At 4 mL/min, this separation requires a flow rate only marginally higher than those typically used in everyday HPLC. This is not to say that the 15-second separation should be forgotten. All this means is that the chemistry for achieving fast separations is no longer the

bottleneck, and the separation process needs to be re-evaluated to identify other areas that restrict higher sample throughput.

#### 5.4 Conclusion

This work has demonstrated that ultra-fast separations of anions can be performed using ion-interaction chromatography on a monolithic stationary phase. This approach resulted in a separation of eight anions in 15 seconds. To the best of the author's knowledge, such rapid separations of inorganic anions are unprecedented. The use of phthalate as an eluent ion allowed the use of either conductivity or indirect absorbance detection of anions. Detection limits for direct conductivity were in the low ppm range and those for indirect absorbance detection were up to an order of magnitude higher. For the most part, the detection limits for conductivity detection were adequate for the analysis of an industrial water sample. Good agreement was seen between the levels of anions determined by the proposed method and by standard IC with suppressed conductivity detection. However, the phosphate in the water sample could not be quantified due to it being present at levels right at the detection limit. The lack of sensitivity of the present method will be addressed in the next chapter.

#### 5.5 References

- (1) Martin, M.; Eon, C.; Guiochon, G. *J. Chromatogr.* **1974**, *99*, 357.
- (2) Martin, M.; Eon, C.; Guiochon, G. *J. Chromatogr.* **1975**, *108*, 229.
- (3) Martin, M.; Eon, C.; Guiochon, G. *J. Chromatogr.* **1975**, *110*, 213.
- (4) Xie, S. F.; Svec, F.; Frechet, J. M. J. *J. Chromatogr. A* **1997**, *775*, 65-72.

- (5) Wang, Q. C.; Svec, F.; Frechet, J. M. J. *Anal. Chem.* **1993**, *65*, 2243-2248.
- (6) Svec, F.; Frechet, J. M. J. *Anal. Chem.* **1992**, *64*, 820-822.
- (7) Tanaka, N.; Kobayashi, H.; Nakanishi, K.; Minakuchi, H.; Ishizuka, N. *Anal. Chem.* **2001**, *73*, 420A-429A.
- (8) Cabrera, K.; Lubda, D.; Eggenweiler, H. M.; Minakuchi, H.; Nakanishi, K. *J. High Resolut. Chromatogr.* **2000**, *23*, 93-99.
- (9) Leinweber, F. C.; Lubda, D.; Cabrera, K.; Tallarek, U. *Anal. Chem.* **2002**, *74*, 2470-2477.
- (10) Grant, C. L.; Hewitt, A. D.; Jenkins, T. F. *Am. Lab.* **1991**, *23*, 15-33.
- (11) Cantwell, F. F. *Analytical Separations Class Notes*; University of Alberta: Edmonton, 1998.
- (12) Jackson, P. E.; Haddad, P. R. *J. Chromatogr.* **1985**, *346*, 125-137.
- (13) Jupille, T. In *Ion Chromatography*; Tarter, J. G., Ed.; Marcel Dekker, Inc.: New York, 1987, pp 36-37.
- (14) Lu, W.; Cassidy, R. M. *Anal. Chem.* **1993**, *65*, 1649-1653.
- (15) Devore, J. L. *Probability and Statistics for Engineering and the Sciences, 4th Ed.*; Duxbury: New York, 1995.
- (16) Johnson, E. L. In *Ion Chromatography*; Tarter, J. G., Ed.; Marcel Dekker, Inc.: New York, 1987, pp 12.

## CHAPTER SIX. Improved Sensitivity and Characterization of High-Speed Ion Chromatography of Anions\*

### 6.1 Introduction

Chapter Five introduced the use of monolithic separation media to achieve ultra-fast separations of inorganic anions. Although significant reductions in analysis time were demonstrated, the approach in Chapter Five had a number of drawbacks. First and foremost, direct conductivity detection resulted in a high background, and the presence of system peaks. System peaks made method optimization incredibly difficult since it was necessary to move system peaks around the analyte peaks. Secondly, detection limits were only in the low ppm range using direct conductivity. This is not adequate for many real-world samples.

This chapter presents improvements to the high-speed separations shown in Chapter Five. In particular, the successful implementation of suppressed conductivity detection with high-speed IC (*i.e.*, sub-minute separations) is demonstrated for the first time. The use of suppressed conductivity detection offers significant improvements in sensitivity (Section 1.3.2.2). Also, the elimination of system peaks, greatly simplifies method development. Finally, issues associated with band broadening in high-speed IC are discussed.

---

\* A version of this chapter has been accepted for publication. Hatsis, P.; Lucy, C.A. *Analytical Chemistry*, accepted December 5, 2002, 31 pages.



## 6.2 Experimental

### 6.2.1 Apparatus

Separations were performed with a Metrohm chromatography system (Metrohm, Herisau, Switzerland) consisting of a 709 serial dual piston pump, 732 conductivity detector, Metrohm MSM suppressor module and a 752 peristaltic pump for the on-line regeneration of suppressors. A Waters 590 pump (Waters, Milford, MA, USA) was used for separations requiring flow rates in excess of 5 mL/min. Injection was performed manually using a Cheminert CCP0140 injection valve (Valco Instruments, Houston, TX) fit with a 20  $\mu$ L loop. All separations were performed on a Chromolith<sup>®</sup> Speed ROD RP-18e column (4.6 mm i.d. x 50 mm) (Merck KGaA, Darmstadt, Germany) permanently coated with didodecyldimethylammonium bromide (DDAB) as is described in Section 6.2.3. Connecting tubing was 0.005" i.d. PEEK (Upchurch Scientific, Oak Harbor, WA, USA).

The primary detection scheme used in this work was suppressed conductivity detection. This was accomplished with a Dionex ED-50A electrochemical detector (unless otherwise stated) coupled to the Metrohm MSM suppressor module. The rise time was set to 0.05 s and data collection was at 20 Hz. Direct conductivity detection was also used in this work with the same detector settings as with suppressed conductivity detection. Data was collected using a Metrohm 762 data acquisition system interfaced to a Pentium II computer running IC Net 2.1 software (Metrohm).

### 6.2.2 Reagents

All reagent solutions were prepared using distilled deionized water (Nanopure Water System, Barnstead, Chicago, IL, USA). All chemicals were reagent grade or

better. Iodate (ACP Inc., Montreal, Canada), chloride (BDH, Toronto, Canada), nitrite (BDH), sulfate (BDH), and phosphate (Fisher, Nepean, Canada) were used as their sodium salts. Bromide (Fisher) and nitrate (BDH) were used as their potassium salts. Elution was accomplished with *o*-cyanophenol (99%, Aldrich, Milwaukee, WI, USA) titrated to the desired pH with sodium hydroxide (BDH). Eluents were filtered with a 0.22  $\mu\text{m}$  GP Express Membrane Filter (Millipore, Bedford, MA, USA). As is good practice in HPLC method development, eluents were not allowed to sit for extended periods of time (*i.e.*, generally no more than two days) to avoid decomposition, bacterial growth, contamination, etc.<sup>1</sup> Acetonitrile was obtained from Fisher (HPLC grade).

A water sample from an industrial source was used in a blind test of the method described in this work. The sample was injected as received. The results are compared with those obtained using a standard IC procedure on a Dionex AS4A-SC anion-exchange column with a Dionex Atlas suppressor, 1.7 mM sodium bicarbonate/1.8 mM sodium carbonate eluent, 1.75 ml/min eluent flow rate and a 25  $\mu\text{L}$  injection volume.

### 6.2.3 Coating Procedure

The required amount of DDAB was weighed and added to a plastic volumetric flask partially filled with water. The resultant mixture was stirred gently with a magnetic stirrer and was then sonicated for 30 minutes until the solution became clear. The required volume of acetonitrile was added to this solution and the remainder of the volume was made up with water. The solution was filtered with a 0.22  $\mu\text{m}$  GP Express Membrane Filter Unit. Meanwhile, the monolith was equilibrated with an aqueous eluent containing the same amount of acetonitrile as the coating solution. The optimized column coating for this work was obtained by flowing a 1 mM DDAB solution (5 %

ACN) at 5 mL/min until complete breakthrough occurred, as indicated by a rapid increase in the conductivity (direct conductivity). Under these conditions breakthrough occurred in about 20 min. The column was then flushed with water for 30 min at 5 mL/min to remove excess DDAB, and then equilibrated with eluent for 15 min at 5 mL/min.

The capacity of the coated column was roughly estimated through the breakthrough curve<sup>2,3</sup> and the following equation<sup>3</sup>:

$$Cap = C_{DDAB} F (t_b - t_o) \quad (6-1)$$

where  $Cap$  is the capacity of the coated column ( $\mu\text{eq}/\text{column}$ ),  $C_{DDAB}$  is the concentration of DDAB in the coating solution ( $\mu\text{eq}/\text{mL}$  or  $\mu\text{mol}/\text{mL}$  assuming one ion exchange site for every DDAB),  $F$  is the flow rate ( $\text{mL}/\text{min}$ ),  $t_b$  is the time for complete breakthrough of DDAB (min) and  $t_o$  is the void time of the column (min).

The stability of the DDAB-coated column was determined by continually flowing 6 mM *o*-cyanophenol (pH 7.0) through the column at 1 mL/min. A chromatogram was acquired every hour until the separation of the test anions was compromised, *i.e.*, a 10 % change in retention time was observed.

#### 6.2.4 Band Broadening Studies

Band broadening was studied by separating iodate, phosphate and sulfate on the DDAB-coated column at flow rates ranging from 0.25 mL/min to 10 mL/min. Extra-column effects were measured over the same flow rate range by removing the column and replacing it with a zero dead volume union (UpChurch)<sup>4</sup>.

#### 6.2.5 Calculations

Integration was performed with IC Net 2.1 software. Detection limits were calculated as the minimum concentration of an anion that can be reported with 99%

confidence to be greater than the blank.<sup>5</sup> The area of  $n$  (usually  $n = 10$ ) samples with a concentration 1 – 5 times the detection limit were measured and the standard deviation was calculated. The detection limit is the product of the standard deviation and the value of Student's  $t$  for 98% confidence (two-sided) and  $n-1$  degrees of freedom. Data analysis was performed with Microsoft Excel 97 software (Microsoft Corporation, Seattle, WA) unless otherwise stated.

Peaks were fit to an exponentially modified Gaussian (EMG) function:<sup>6,7</sup>

$$EMG(t) = \frac{1}{2\tau} \exp\left[\frac{1}{2}\left(\frac{\sigma}{\tau}\right)^2 - \frac{t-t_g}{\tau}\right] \left\{1 + \operatorname{erf}\left[\frac{1}{\sqrt{2}}\left(\frac{t-t_g}{\sigma} - \frac{\sigma}{\tau}\right)\right]\right\} \quad (4-1)$$

using an in-house routine for Matlab 6 (Mathworks Inc., Natick, MA, USA) to determine the second statistical moment (*i.e.*, the variance) and subsequently the plate height. In Equation 4-1,  $t$  is time,  $t_g$  is the centroid of the Gaussian component,  $\sigma$  is the standard deviation,  $\tau$  is the time constant of the exponential function and  $\operatorname{erf}()$  is the error function. The software routine is included as Appendix One. The variance ( $\sigma_p^2$ ) retention time ( $t_R$ ) and plate height of peaks was calculated as:

$$\sigma_p^2 = \sigma^2 + \tau^2 \quad (4-2a)$$

$$t_R = t_g + \tau \quad (4-2b)$$

$$H = (\sigma_p^2 L_c)/t_R^2 \quad (4-2c)$$

where  $L_c$  is the length of the column. Plate height vs. linear velocity data were fit to the van Deemter equation (Equation 1-10) using GraphPad Prism 3.02 (GraphPad Software Inc., San Diego, CA, USA).

Plate heights corrected for extra-column effects were calculated with the equation:

$$H_{\text{corr}} = (\sigma_p^2 - \sigma_{\text{xc}}^2) L / (t_R^2) \quad (6-2)$$

where  $H_{corr}$  is the corrected plate height,  $\sigma_{xc}^2$  is the variance of the peak obtained without the column in place and  $t_R$  is the retention of the peak with the column in place. The retention time of the peak without the column in place was ignored in the calculation since it was much smaller than the column retention time (< 5 %).

Linear velocity was calculated with the equation:

$$u = \frac{F}{\pi \varepsilon_b r_C^2} \quad (5-3)$$

where  $u$  is linear velocity (cm/s),  $F$  is flow rate (cm<sup>3</sup>/s),  $\varepsilon_b$  is the external porosity of the monolithic bed and  $r_C$  is the radius of the column (cm). The external porosity of the bed was taken as 0.597 based on the work of Leinweber *et al.*<sup>8</sup>

## 6.3 Results and Discussion

### 6.3.1 Preparation of the DDAB-Coated Column

The Chromolith Speed ROD RP-18e used in this work is a reversed-phase column, and as such is not well suited to the separation of inorganic anions. One approach routinely used for the separation of ionizable species on reversed-phase stationary phases is ion-interaction chromatography, which was used in Chapter Five. Alternatively, a reversed-phase column can be permanently coated with a long chain surfactant (*e.g.*, cetylpyridinium chloride) to convert it into an ion exchanger. This approach was pioneered by Cassidy and Elchuk 20 years ago.<sup>9, 10</sup> They achieved highly efficient separations of inorganic ions on coated reversed-phase columns, with the added benefit of control of column capacity through the addition of an organic modifier (*e.g.*, methanol or acetonitrile) to the coating solution.

Connolly and Paull used didodecyldimethylammonium bromide (DDAB) to coat 3 cm long reversed-phase columns for fast ion exchange separations.<sup>2</sup> Columns prepared in this manner were said to be extremely stable, although no evidence was offered to support this claim. However, in preliminary experiments in this lab, DDAB was found to give the best coatings (*i.e.*, high capacity and good stability) compared to the C<sub>14</sub>, C<sub>16</sub>, C<sub>18</sub> analogues of DDAB or cetylpyridinium chloride. Therefore, DDAB was used to coat the monolithic column with the procedure outlined in Section 6.2.3. A typical breakthrough curve for DDAB is shown in Figure 6-1. Table 6-1 presents data on the capacity of the DDAB-coated column as a function of the acetonitrile concentration in the 1 mM DDAB coating solution. Percentages of acetonitrile higher than 30% were not examined as they resulted in inadequate retention of anions. Table 6-1 shows capacities ranging from 113 to 32  $\mu\text{eq}/\text{column}$ . For comparison, 113  $\mu\text{eq}/\text{column}$  represents a rather high capacity compared to many commercially available IC columns.<sup>11</sup> These capacities are lower than the 120  $\mu\text{eq}/\text{column}$  (30 x 4.6 mm) obtained by Connolly and Paull<sup>2</sup>, due possibly to the lower total surface area of monolithic columns compared to particulate columns.<sup>8</sup>

Optimal separations were obtained when 5% acetonitrile was present in the 1 mM DDAB coating solution, as is shown in Figure 6-2B. Above 5% acetonitrile, the resolution between the critical pair of bromide and nitrate was unacceptable ( $R_s = 0.75$  at 15% acetonitrile, Figure 6-2A). Below 5% acetonitrile there was no significant improvement in resolution between bromide and nitrate ( $R_s = 1$ ).

### 6.3.2 Band Broadening from the Column

The effect of linear velocity on plate height can be conveniently expressed with the van Deemter equation (Section 1.2.4):

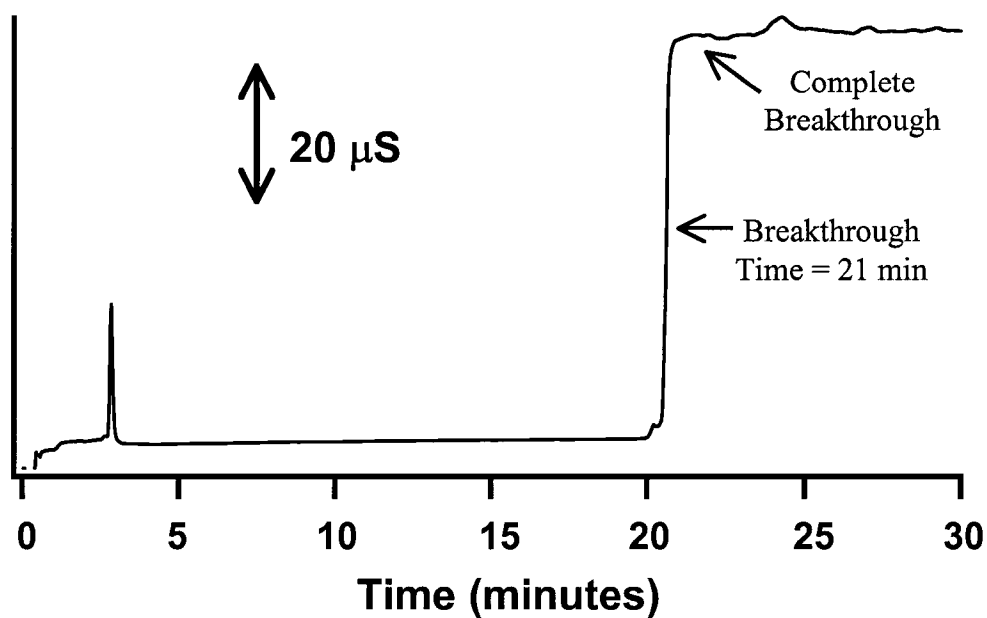


**Figure 6-1.** Breakthrough curve of DDAB on the monolith.

**Experimental Conditions:** 1 mM DDAB in 95/5 water/acetonitrile, flow at 5 mL/min, Detection was by conductivity. The column void time is 0.1 min.

**Table 6-1.** Capacity of the DDAB-coated column as a function of the amount of acetonitrile present in the coating solution.

<b>% Acetonitrile</b>	<b>Capacity (<math>\mu\text{eq}/\text{column}</math>)</b>
30	$32 \pm 1$
15	$74 \pm 2$
10	$87 \pm 1$
5	$99 \pm 2$
0	$113 \pm 2$

**Experimental Conditions:** Monolithic column coated with 1 mM solution of DDAB (% acetonitrile varied) at 5 mL/min until complete breakthrough was seen. Standard deviation based on three replicate measurements.



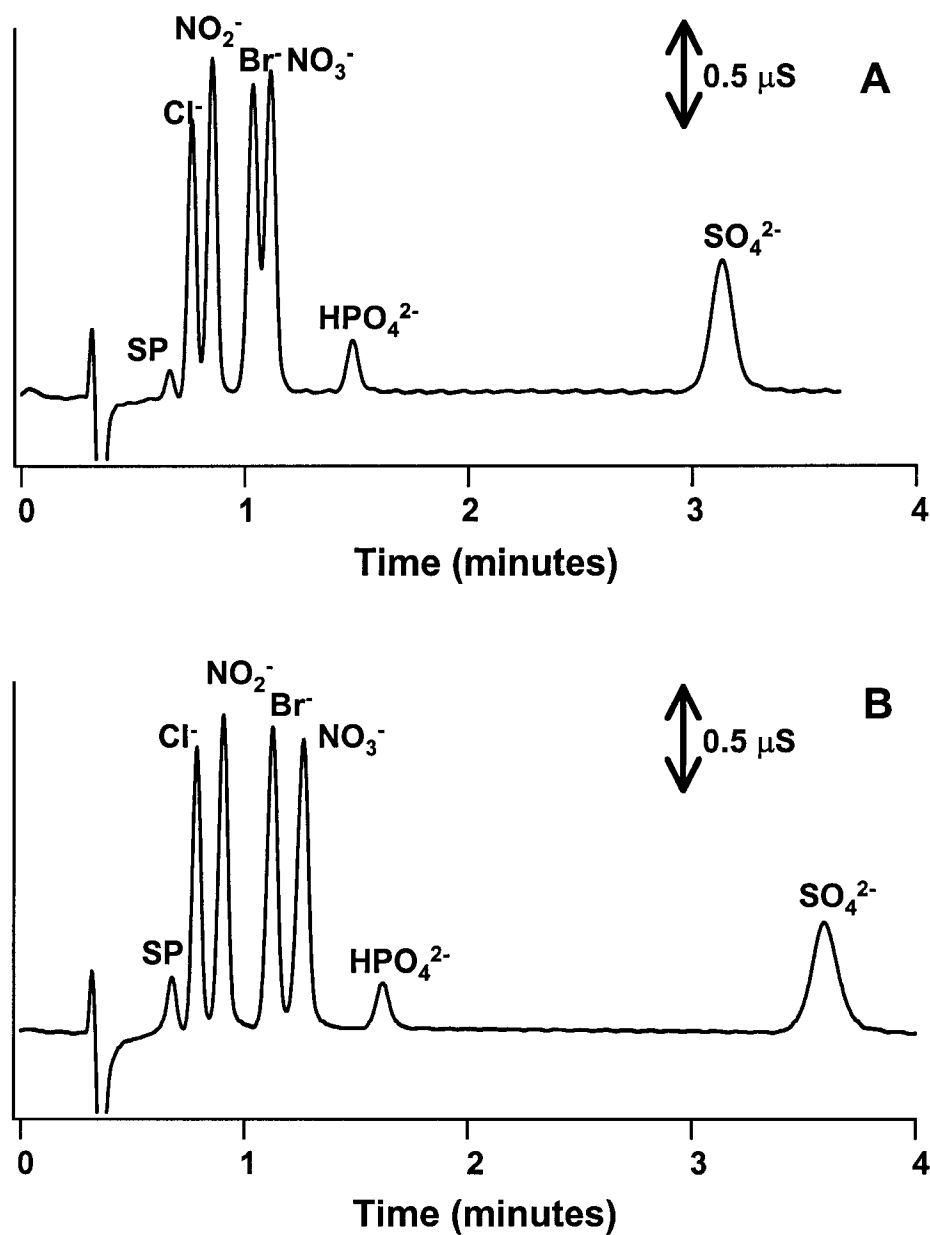


**Figure 6-2.** Effect of column capacity on the separation of anions. A) 15% acetonitrile in coating solution, B) 5% acetonitrile in coating solution. SP = system peak. **Experimental Conditions:** DDAB-coated monolith, 5.5 mM o-cyanophenol (pH 7.0) at 2 mL/min, 20  $\mu\text{L}$  injection, direct conductivity detection. Approximately 50  $\mu\text{M}$  concentration of analytes.

$$H = A + B/u + Cu \quad (1-10)$$

where  $H$  is the plate height,  $u$  is the linear velocity and  $A$ ,  $B$  and  $C$  represent the various processes within the column that give rise to band broadening. In terms of high-speed separations, the  $C$ -term is of most importance because it is dominant at high linear velocities. Therefore, high-speed separations require that the  $C$ -term be as small as possible.

The band broadening behaviour of the DDAB-coated column was studied for three inorganic anions, as shown in Figure 6-3. The corresponding coefficients are given in Table 6-2. The anions that were chosen represent a wide range of retention factors, *e.g.*,  $k = 0.5$  for iodate,  $k = 2$  for phosphate and  $k = 5$  for sulfate, so that an accurate picture of the band broadening in the separation is obtained. The top curve in each plot (A) is the overall broadening behaviour observed, while the bottom curve (B) is the band broadening due to the column alone, *i.e.*, extra column effects were subtracted as described in Section 6.2.4. Figure 6-3 reveals that extra-column band broadening is most pronounced for the early eluting peaks, as is always the case in HPLC.<sup>1</sup> Therefore, the efficiency of early eluting peaks is drastically affected compared to later eluting peaks.

Figure 6-3 shows that plate height does not increase appreciably with increasing linear velocity for any of the anions studied. For example, for sulfate the optimum plate height is 15  $\mu\text{m}$ , which increases to only 27  $\mu\text{m}$  at 1.7 cm/s (10 mL/min). This represents an increase in plate height by 1.8, or a loss in resolution of less than  $\sqrt{2}$ . This means that separations can be performed at relatively high linear velocities while preserving most of the efficiency.

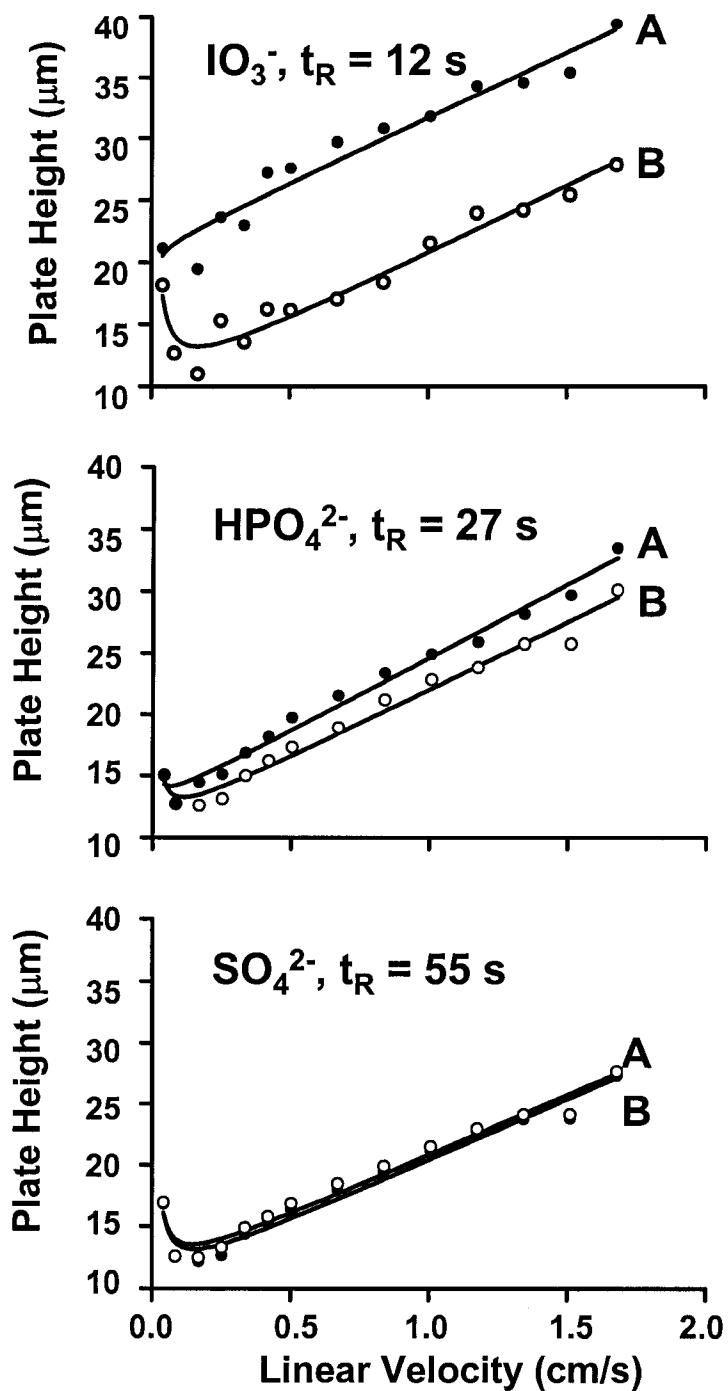


**Figure 6-3.** van Deemter curves for iodate, phosphate and sulfate. A = not corrected for extra-column effects, B = corrected for extra-column effects.

**Experimental Conditions:** DDAB-coated column, 6 mM o-cyanophenol (pH 7.0), flow 0.25 - 10 mL/min, 20  $\mu\text{L}$  injection. Suppressed conductivity detection.

**Table 6-2.** van Deemter equation coefficients for iodate, phosphate and sulfate.

	<b>A</b> ( $10^{-6}$ m)	<b>B</b> ( $10^{-8}$ m <sup>2</sup> s <sup>-1</sup> )	<b>C</b> ( $10^{-4}$ s)	<b>A</b> ( $10^{-6}$ m) <b>Corrected</b>	<b>B</b> ( $10^{-8}$ m <sup>2</sup> s <sup>-1</sup> ) <b>Corrected</b>	<b>C</b> ( $10^{-4}$ s) <b>Corrected</b>
Iodate	28 ± 2	-0.1 ± 0.1	9.7 ± 0.7	9.5 ± 0.9	0.31 ± 0.07	9.3 ± 0.6
Phosphate	16.8 ± 0.9	0.02 ± 0.07	11.0 ± 0.7	10.3 ± 0.7	0.15 ± 0.06	9.9 ± 0.7
Sulfate	11.7 ± 0.7	0.21 ± 0.05	8.6 ± 0.5	10.1 ± 0.6	0.23 ± 0.05	8.7 ± 0.5

**Experimental Conditions:** DDAB-coated column, 6 mM o-cyanophenol (pH 7.0), eluent flow from 0.25 to 10 mL/min, 20 µL injection. Detection was by suppressed conductivity.

The corrected  $A$ -terms shown in Table 6-2 are about three times the equivalent particle diameter of the monolithic column, and are comparable to the  $A$ -terms determined by Leinweber *et al.*<sup>8</sup>. Ideally  $A$  should be about one to two times the particle diameter. The large  $A$ -term is in contradiction to the relatively homogeneous structure of monolithic columns compared to particulate columns. However, the seemingly large  $A$ -term may not be an accurate depiction of what is actually happening in the column. Knox has recently proposed a new equation to account for the effect of the mobile zone on band broadening, and used this equation to show that monoliths exhibit superior performance compared to particulate columns due to the regularity of their structure.<sup>12</sup> However, such an analysis is outside the scope of this thesis. The  $B$ -terms will not be discussed since insufficient data was taken at low linear velocities (exemplified in the statistically insignificant  $B$ -terms in Table 6-2 for iodate and phosphate) and are not of any concern at the high linear velocities used in this work. Finally, the  $C$ -terms obtained in this work for inorganic anions are about an order of magnitude lower than those obtained by Leinweber *et al.* for proteins.<sup>8</sup> This is consistent with the much higher diffusion coefficients of inorganic anions than proteins.

### 6.3.3 Band Broadening from Extra-Column Effects

Extra-column band broadening can significantly affect the efficiency of a separation. In particular, components of the chromatographic system, *e.g.*, connecting tubing and detector response time<sup>1, 13</sup>, that exhibit flow rate dependencies on the amount of band broadening they produce must be given the most attention in high-speed separations<sup>14</sup>.

The effect of connecting tubing was discussed in Section 1.2.4.6, where it was mentioned that Equation 1-19:

$$\sigma_{v,T}^2 = \frac{\pi F L_T r_T^4}{24 D_M} \quad (1-19)$$

does not provide a good estimate of broadening due to connecting tubing under certain circumstances. For example, Atwood and Golay found that even slight curvature in connecting tubing results in significantly smaller variances than predicted by Equation 1-19, especially at flow rates  $> 0.5$  mL/min.<sup>17</sup> Furthermore, connecting tubing may be tightly coiled in a helix, as is commonly done in conductivity detectors to ensure thermal equilibration of the eluent before detection. The helical configuration of the tubing generates a secondary flow pattern, which is especially pronounced at the flow rates used in high-speed HPLC.<sup>18</sup> The secondary flow pattern would serve to relax the non-uniform flow profile and therefore decrease the variance due to connecting tubing below what is predicted by Equation 1-19.<sup>18</sup> The onset of secondary flow within connecting tubing occurs when  $De^2 Sc > 10$  and is fully developed at  $De^2 Sc > 10^4$ , where:

$$De = \frac{2ur_T \rho \chi^{1/2}}{\eta} \quad (6-3a)$$

$$Sc = \frac{\eta}{D\rho} \quad (6-3b)$$

$De$  is known as the Dean number,  $Sc$  is the Schmidt number,  $u$  is linear velocity,  $\rho$  is density,  $\eta$  is viscosity and  $\chi$  is the ratio of the tubing inner radius to the coil radius. The plate height,  $H$ , for the coiled tubing can be calculated with the equation:

$$H = \frac{968r_T}{Re Sc^{0.14} \chi} f(k_T) \quad (6-4a)$$

$$\text{Re} = \frac{2ur_T\rho}{\eta} \quad (6-4b)$$

$$f(k_T) = \frac{1 + 6k_T + 11k_T^2}{(1 + k_T)^2} \quad (6-4c)$$

where  $Re$  is the Reynolds number and  $k_T$  is the retention factor in the connecting tubing. For example, if a conductivity detector cell (*e.g.*, the Metrohm 732 conductivity detector) is used with 100 cm of 0.01" i.d. tubing coiled in a helix of 1 cm diameter, at a flow rate of 5 mL/min, and the diffusion coefficient of iodate is  $1.2 \times 10^{-5}$  cm<sup>2</sup>/s, then  $De^2Sc = 4 \times 10^6$ , which means that secondary flow is fully developed and a relaxation of the band broadening within the tubing is occurring. Substitution of the appropriate values into Equation 6-4a (assuming  $k_t = 0$ ) results in a plate height of 0.5 cm. Therefore, the tubing results in  $1 \times 10^{-5}$  mL<sup>2</sup> in terms of volume variance and is only 2 % of the column variance of iodate ( $6 \times 10^{-4}$  mL<sup>2</sup>, based on an efficiency of 2600 plates for iodate at 5 mL/min obtained from Figure 6-3). However, Equation 1-19 predicts a variance of  $2 \times 10^{-3}$  mL<sup>2</sup> due to the connecting tubing. In other words, the connecting tubing represents 400 % of the column variance, and dominates the broadening of iodate at high flow rates. In practice, no difference in peak broadening was seen when a conductivity cell was used with or without the connecting tubing in question, *i.e.*, a separation identical to the one in Figure 6-5 was always obtained. Therefore, Equation 1-19 has a tendency to overestimate the band broadening imparted to chromatographic peak in high-speed HPLC, and should always be used with caution when modeling the effect of connecting tubing on peak variance.

Thompson and Carr have shown that detector response times must be kept to a minimum when performing high-speed separations.<sup>19</sup> According to Equation 1-20:

$$\sigma_{V,R}^2 = (F\tau)^2 \quad (1-20)$$

a response time of 0.05 seconds would result in negligible band broadening (less than 10 % of the column variance) for the separations in this work assuming a variance of  $6 \times 10^{-4}$  mL<sup>2</sup> (based on an efficiency of 2600 plates for iodate at 5 mL/min obtained from Figure 6-3).

#### 6.3.4 High Speed Separations

Chapter Five demonstrated anion separations with analysis times as low as 15 seconds. However, the use of direct conductivity detection resulted in problematic system peaks and poor sensitivity. Therefore, the switch to suppressed conductivity detection is made in this work.

Unfortunately, the application of suppressed conductivity detection to high-speed IC presented its own hurdles. First, and foremost, as discussed in Section 1.3.2.1, suppressed conductivity detection works well only with eluents that have a  $\text{pK}_a > 7$ .<sup>20</sup> In other words, basic eluents (*e.g.*, hydroxide, carbonate and borate) are preferred, with the most basic eluent giving the lowest background conductivity (*i.e.*, dissociates the least) after suppression. However, basic eluents are not compatible with the pH stability ( $\text{pH} < 7.5$ ) of silica stationary phases. Therefore, it was necessary to find a compromise between the need for an eluent that could be suppressed, and the limited pH stability of silica. Such a compromise was found in the use of cyanophenol as an eluent ion. In particular, the only form (*i.e.*, *ortho*, *meta* or *para*) of cyanophenol that would be charged at a pH less than 7.5 was *o*-cyanophenol. It has a  $\text{pK}_a$  of 6.9, which is higher than that of carbonate ( $\text{pK}_a = 6.6$ ). Furthermore, since *o*-cyanophenol is an aromatic organic acid and



thus has a low equivalent conductivity, it can also be used in a direct conductivity detection scheme if so desired.

The second problem complicating the use of suppressed conductivity detection with high-speed separations is the use of high flow rates. The most widely used suppressors are membrane suppressors.<sup>11</sup> The membranes within these suppressors are thin so as to maximize mass transfer and thus suppression capacity. However this also makes the membranes fragile, resulting in limited capability of withstanding pressure. Therefore, separations using commercially available membrane suppressors are limited to flow rates of less than 3 mL/min. This severely restricts the speed of separation that can be achieved. Nevertheless, Figure 6-4A demonstrates the use of a splitter before the suppressor as a means to reduce the flow rate of the eluent through the suppressor. Significant band broadening was observed upon combined use of a Dionex CSRS-Ultra membrane suppressor (50  $\mu$ L internal volume) and a splitter (split ratio = 2.5, *i.e.*, 5 mL/min to waste and 2 mL/min through the suppressor) at an eluent flow of 7 mL/min. No significant band broadening was observed when the suppressor was used below 3 mL/min without the splitter (Figure 6-4B), or when a suppressor was not used but the splitter was still in place (2.25: 1 split ratio, *i.e.*, 4.5 mL/min to waste and 2 mL/min to the detector), as shown in Figure 6-4C. When a splitter is used, the volume of a peak decreases in proportion to the split ratio. Therefore, the peak becomes more susceptible to the effects of band broadening from the other components of the system (*e.g.*, suppressor, detector cell etc.) past the splitter. Thus, a packed bed suppressor (Metrohm MSM) was used in this work. This suppressor can withstand pressures up to 300 psi and flow rates as high as 10 mL/min so there was no need to split the flow prior to the

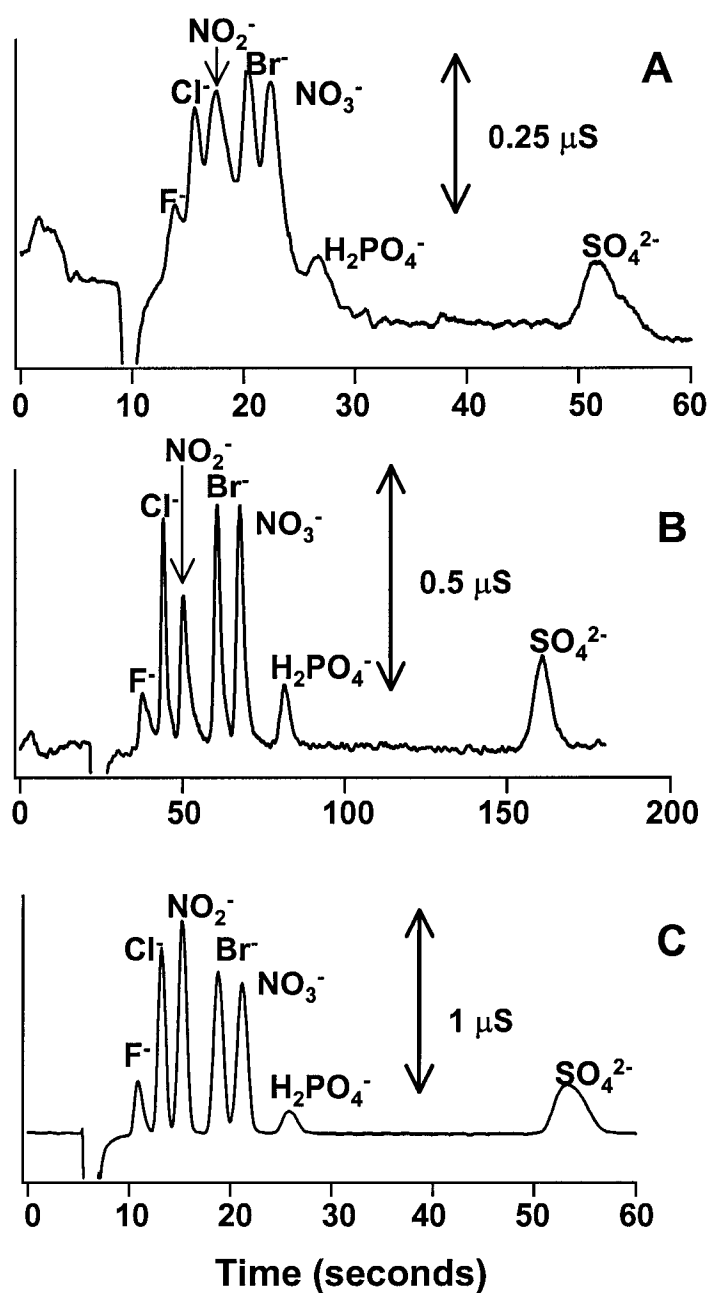


**Figure 6-4.** Effect of splitting on efficiency. A) 2.5: 1 split before suppressor. Flow at 7 mL/min. B) With suppressor but no splitter. Flow at 3 mL/min. C) No suppressor, but 2.25: 1 split before detection cell. Flow at 6.5 mL/min. **Experimental Conditions:** DDAB-coated column, 5.5 mM o-cyanophenol (pH 7.0), 20  $\mu$ L injection. 50  $\mu$ m analytes.

suppressor. Further, if this pressure limit is exceeded, the suppressor simply leaks, and then reseals when the pressure is reduced. Regardless, no difficulties were experienced with this packed bed suppressor, even at the maximum flow rate studied herein (10 mL/min).

Separations of seven anions are shown in Figure 6-5. Figure 6-5A was acquired using suppressed conductivity detection and Figure 6-5B was acquired using direct conductivity. Examination of Figure 6-5A reveals that major system peaks have been eliminated such that they are no longer a problem during method development. There is a rather small system peak ( $t_r = 12$  s) in Figure 6-5B (non-suppressed) on the left shoulder of iodate, which can be problematic if direct conductivity detection is being used. However, suppression virtually eliminates this system peak. Figure 6-5 also shows that weakly retained ions (*e.g.*, iodate) are adequately resolved from the water dip on the DDAB-coated column. Fluoride elutes slightly after iodate, but was not included in Figure 6-5 because of its potential loss to the silica support.<sup>9</sup> Thus, this method is not suitable for the determination of low levels of fluoride. Finally, a resolution of at least 1 is seen between all ions in Figure 6-5A. The use of a suppressor imparted very little extra-column band broadening to the separation, *e.g.*, the efficiency of iodate only decreases from 1700 plates to 1400 plates upon introduction of the suppressor.

There is a large gap between phosphate and sulfate in Figure 6-5. Clearly, separation speed could be further increased if the retention of sulfate were decreased relative to the other anions. A change in eluent strength affects the retention of ions in direct proportion to their charge (Section 1.3.3.3). Therefore, the gap between sulfate and the singly charged ions could be reduced by increasing the eluent strength (*i.e.*, increasing

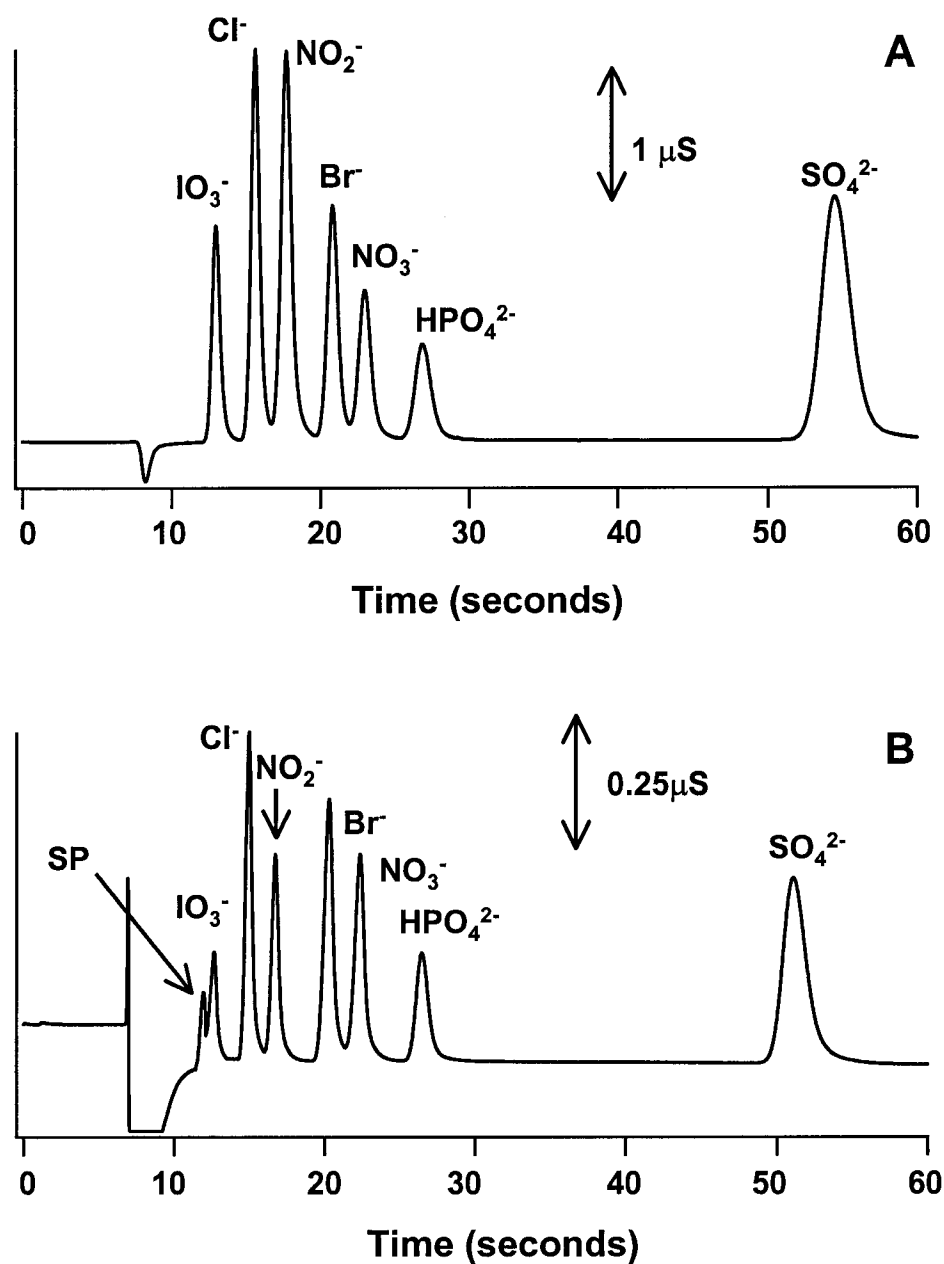


**Figure 6-5.** High-speed separation of 7 anions. A) Using suppressed conductivity detection, B) Using direct (non-suppressed) conductivity detection. SP = system peak. **Experimental Conditions:** DDAB-coated column, 6 mM o-cyanophenol (pH 7.0) at 5 mL/min, 20  $\mu\text{L}$  injection. Approximately 50  $\mu\text{M}$  concentration of analytes.

concentration of *o*-cyanophenol). However in the present case, this approach was limited by the potential co-elution of phosphate (which has a charge of 1.5 at the eluent pH = 7) with nitrate. As a consequence, 6 mM *o*-cyanophenol was chosen as the optimum eluent concentration. Furthermore, pH 7.0 was chosen as the optimum since a lower pH would reduce the charge on phosphate ( $pK_{a2} = 7.2$ ) and cause it to co-elute with the singly charged anions. A higher pH was not used due to concern about the limited pH stability (pH < 7.5) of silica.

There is a substantial increase in the sensitivity upon suppression in Figure 6-5. As shown in Table 6-3, the detection limits obtained with suppressed conductivity are about 10 times lower than those obtained with direct conductivity detection. Iodate has one of the highest detection limits in the direct conductivity scheme due to the system peak that was mentioned earlier. Phosphate has a relatively high detection limit in both detection schemes. Typical detection limits when employing a conventional IC column with a carbonate eluent and suppressed conductivity detection at 2 mL/min range from 2 ppb for chloride to 20 ppb for phosphate.<sup>21</sup>

A calibration curve for chloride using suppressed conductivity detection is shown in Figure 6-6A. All calibration curves (number of standards,  $n = 6$ ) are linear over two orders of magnitude (*e.g.*, from 0.05 ppm to 5 ppm for chloride) with correlation coefficients ( $r^2$ )  $\geq 0.999$  and intercepts equal to zero at the 95 % confidence level. A typical linear range for an IC method that uses a carbonate eluent is approximately three orders of magnitude.<sup>21</sup> The linear working range of high-speed IC was determined with the help of sensitivity plots (Figure 6-6B, peak area/concentration vs. concentration).<sup>22</sup> The linear range of this method is restricted by the protonation of dissociated eluent ions

**Table 6-3.** Detection limits achieved with suppressed and direct (non-suppressed) conductivity detection.

	$\text{IO}_3^-$	$\text{Cl}^-$	$\text{NO}_2^-$	$\text{Br}^-$	$\text{NO}_3^-$	$\text{HPO}_4^{2-}$	$\text{SO}_4^{2-}$
Suppressed Conductivity (ppb)	9	7	4	4	6	30	4
Direct Conductivity (ppb)	200	30	50	80	100	500	100

**Experimental Conditions:** DDAB-coated column, 6 mM o-cyanophenol (pH 7.0), eluent flow at 5 mL/min, 20  $\mu\text{L}$  injection.

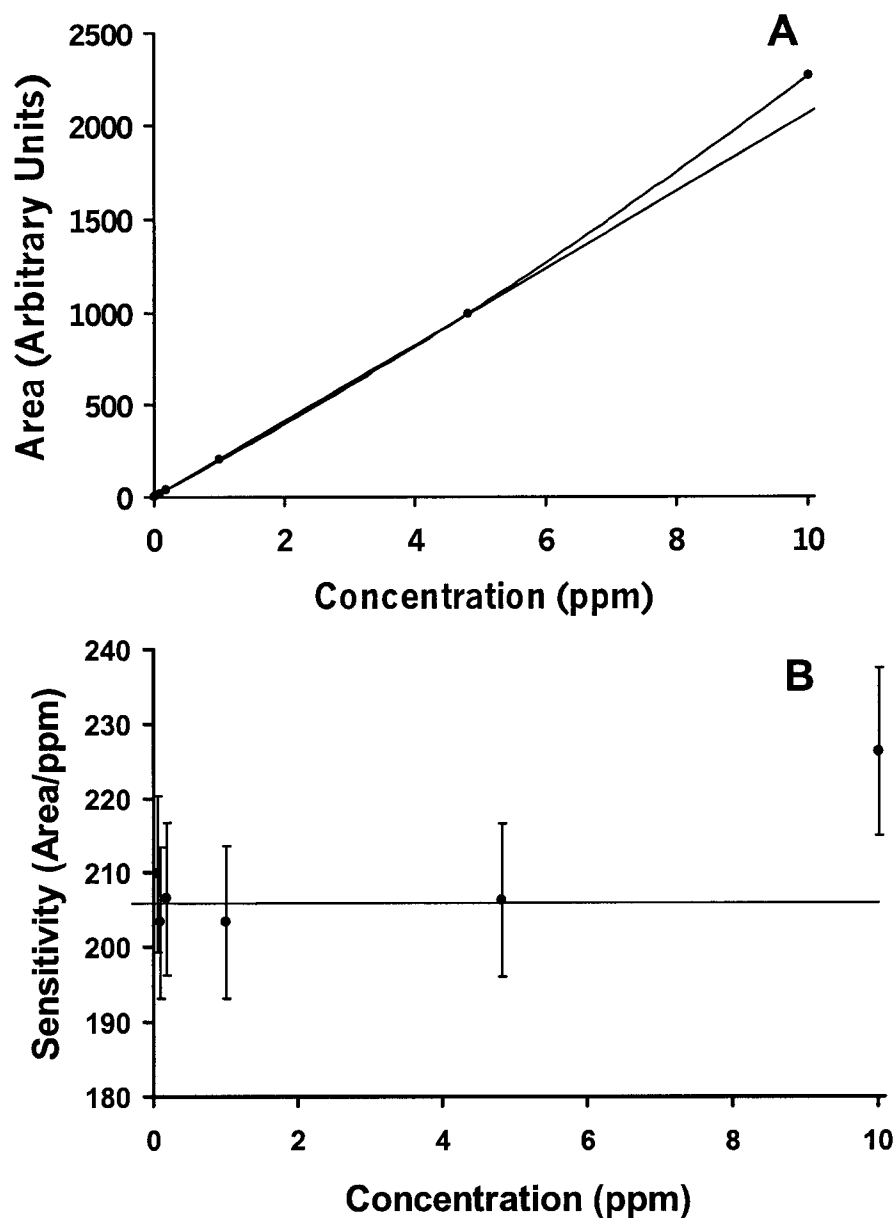


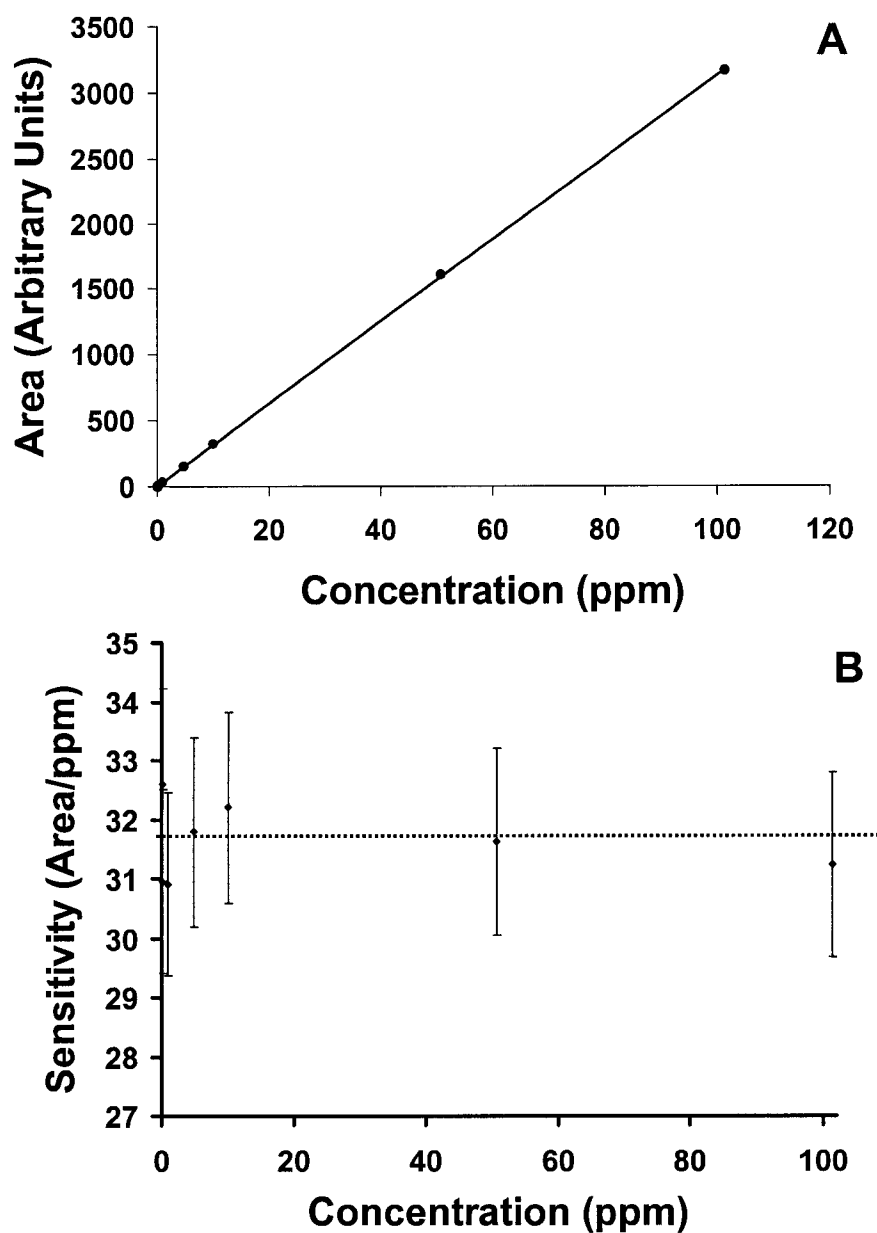
**Figure 6-6.** A) Calibration curve for chloride using suppressed conductivity detection. B) Sensitivity plot for chloride indicating linear range. Horizontal line indicates linear range. The error bars are 5% control intervals, *i.e.*, a maximum of 5% deviation from linearity. **Experimental Conditions:** DDAB-coated column, 6 mM o-cyanophenol (pH 7.0) at 5 mL/min, 20  $\mu$ L injection. Approximately 50  $\mu$ m concentration of analytes.

by analyte ions after the suppressor.<sup>20, 23</sup> Therefore, the background conductivity will be slightly lower in the presence of an analyte ion than when the eluent alone is flowing through the detector cell. This results in a lower slope of the calibration curve on the low end compared to the high end. This non-linearity effect is most pronounced with eluents that do not have their first  $pK_a$  well into the basic end of the pH scale, *e.g.*, carbonate and *o*-cyanophenol, and therefore, partially dissociate after suppression. This effect is negligible when hydroxide ( $pK_a = 14$  of conjugate acid) is used as an eluent ion. In contrast, this effect is not present when using direct conductivity detection. As is shown in Figure 6-7, the linear range when direct conductivity detection is used is over three orders of magnitude (*e.g.*, from 0.1 ppm to 100 ppm for chloride) with correlation coefficients ( $r^2$ ) of at least 0.999 and intercepts equal to zero at the 95% confidence level.

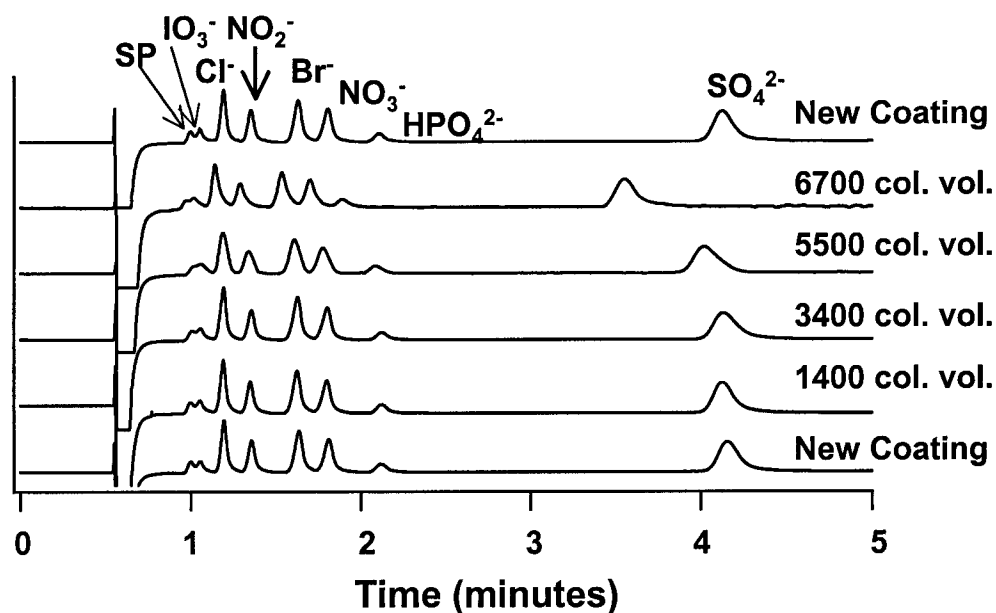
### 6.3.5 Stability and Reproducibility of the Coated Column

Figure 6-8 illustrates the long-term stability of the DDAB coated column. Column performance had degraded (*i.e.*, 10% decrease in retention time for sulfate) by 5500 column volumes of eluent. In addition, a 25% increase in system back pressure was noted by the time the performance of the coated column had failed. This represents over 12 hours of continuous operation at 5 mL/min. Removal of the old coating with 100% acetonitrile (30 min at 5 mL/min) and recoating of the monolithic column regenerated the performance of the column and the system back pressure was back to normal. Less than 4 % RSD ( $n = 3$ ) variation in the retention time of sulfate was observed upon recoating the column. Column lifetime could be extended by placing a DDAB-coated guard column upstream from the injector to prevent a loss of surfactant from the analytical column. In this manner, Cassidy and Elchuk were able to extend the lifetime of their





**Figure 6-7.** A) Calibration curve for chloride using non-suppressed conductivity detection. B) Sensitivity plot for chloride. Horizontal line indicates linear range. The error bars are 5% control intervals, *i.e.*, a maximum of 5% deviation from linearity. **Experimental Conditions:** DDAB-coated column, 6 mM *o*-cyanophenol (pH 7.0) at 5 mL/min, 20  $\mu$ L injection. 50  $\mu$ m analytes.



**Figure 6-8.** Long-term stability of DDAB-coated column. SP = system peak.

**Experimental Conditions:** DDAB-coated column, 6 mM o-cyanophenol (pH 7.0) at 1mL/min, 20  $\mu$ L injection, direct conductivity detection. Approximately 50  $\mu$ m concentration of analytes.

cetylpyridinium chloride-coated columns to over 80 days of continuous use at 1 mL/min.<sup>9</sup> However, this was not done in the present study since monolithic guard columns were not available.

The reproducibility of separations performed at 5 mL/min were 0.7 % RSD on a run-to-run basis (n = 5), 1.7 % on a day-to-day basis (n = 5) and 2.5 % on a week-to-week basis (n = 4) for nitrate. Comparable reproducibility was observed for the other anions except for phosphate and sulfate. Phosphate and sulfate exhibited the worst reproducibility (0.7 % on a run-to-run basis, 3.1 % on a day-to-day basis and 5.5 % on a week-to-week basis for sulfate) due to their retention being very sensitive to slight changes in eluent concentration. This is a direct result of phosphate and sulfate being multiply charged ions and as such their retention shows a stronger dependence on eluent strength than singly charged anions (Section 1.3.3.3). Peak area showed a variation of 0.4 % for nitrate (n = 5) at a concentration of 50 times the detection limit.

### **6.3.6 Validation of High-Speed IC**

The applicability of high-speed IC to real-world anion analysis was evaluated using a blind test with an industrial water sample. Table 6-4 shows general agreement between the high-speed analysis and a standard IC method. However the analyses are statistically different at the 95 % confidence level for all anions studied

### **6.3.7 Considerations in High-Speed IC**

The one-minute separation of the seven anions is performed at 5 mL/min, which is a flow rate accessible by most conventional HPLC pumps, and at a relatively modest pressure drop of 1000 psi. Hence, the flow rate was increased even further to 10 mL/min such that a 30 second separation of the same seven anions is achieved. This is shown in

**Table 6-4.** Comparison of concentrations of anions determined by conventional and high-speed IC.

	<b>Concentration by Standard Method (ppm)</b>	<b>Concentration by High-Speed IC (ppm)</b>
Chloride	2.9 ± 0.2	3.4 ± 0.2
Phosphate	5.1 ± 0.3	4.2 ± 0.3
Sulfate	46 ± 2	41 ± 2

**Experimental Conditions for Standard Method:** Dionex AS4A-SC column, 1.7 mM bicarbonate/ 1.8 mM carbonate, 1.75 mL/min, 25 µL injection. Uncertainty is 95 % confidence interval based on a relative standard deviation of 2% with three replicate measurements.

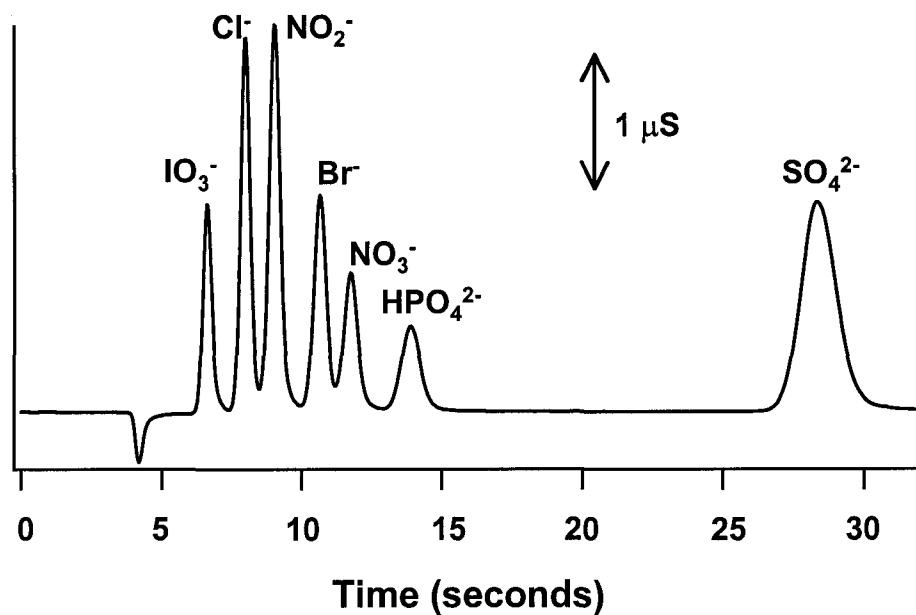
**Experimental Conditions for High-Speed IC:** DDAB-coated column, 6 mM *o*-cyanophenol (pH 7.0), 5 mL/min, 20 µL injection. Detection by suppressed conductivity. Standard deviation is based on five replicate injections. Uncertainty is 95 % confidence interval based on three replicate measurements.

Figure 6-9. Even at 10 mL/min the resolution of the separation has not been significantly compromised. This is consistent with the van Deemter curves shown in Figure 6-3. Since the pressure drop at 10 mL/min is only 1660 psi (achieved with a different pump than above), and the manufacturer rates the monolithic column to 3000 psi, even faster separations are possible. However, this was not attempted since the flow rates required fall outside the range of analytical HPLC.

Apart from the inconvenience, the high flow rates necessary for high-speed IC is not a true limitation of the technology since there are dramatic improvements in speed that are concomitant with the increased eluent flow. Therefore, the price per analysis remains the same and there is no additional cost in operating at the higher flow rates. Nevertheless, there would be tremendous benefits in terms of convenience and cost per analysis if smaller bore columns were used. For example, the flow rates with a 2 mm i.d. column would be 5.3 times less or at just under 1 mL/min for a one-minute separation and 2 mL/min for a 30 second separation, thus maintaining the speed of the separations but with routine analytical HPLC flow rates. Unfortunately, monolithic columns with smaller internal diameters were not available before completion of this work.

#### **6.4 Conclusion**

This work has demonstrated the successful implementation of suppressed conductivity detection with high-speed IC. This approach resulted in a separation of seven anions in as little as 30 seconds with detection limits in the ppb range. Careful control of band broadening was found to be imperative to the successful implementation of high-speed IC. Further, it was shown that the effect of connecting tubing is not as



**Figure 6-9.** Thirty-second separation of seven anions. **Experimental Conditions:** DDAB-coated column, 6 mM o-cyanophenol (pH 7.0) at 10 mL/min, 20 μL injection, suppressed conductivity detection. Eluent flow with Waters 590 pump. Approximately 50 μM concentration of analytes.

severe as it is often thought to be when employing the flow rates typically used in high-speed HPLC.

## 6.5 References

- (1) Snyder, L. R.; Glajch, J. L.; Kirkland, J. J. *Practical HPLC Method Development*, 2nd ed.; Wiley-Interscience: New York, 1996.
- (2) Connolly, D.; Paull, B. *J. Chromatogr. A* **2002**, *953*, 299-303.
- (3) Conder, J. R.; Young, C. L. *Physicochemical Measurement by Gas Chromatography*; John Wiley & Sons: Toronto, 1979.
- (4) Cantwell, F. F. *Analytical Separations Class Notes*; University of Alberta: Edmonton, 1998.
- (5) Grant, C. L.; Hewitt, A. D.; Jenkins, T. F. *Am. Lab.* **1991**, *23*, 15-33.
- (6) Foley, J. P.; Dorsey, J. G. *Anal. Chem.* **1983**, *55*, 730-737.
- (7) Grushka, E.; Meyers, M. N.; Schettler, P. D.; Giddings, J. C. *Anal. Chem.* **1969**, *41*, 889-892.
- (8) Leinweber, F. C.; Lubda, D.; Cabrera, K.; Tallarek, U. *Anal. Chem.* **2002**, *74*, 2470-2477.
- (9) Cassidy, R. M.; Elchuk, S. *J. Chromatogr. Sci.* **1983**, *21*, 454-459.
- (10) Cassidy, R. M.; Elchuk, S. *Anal. Chem.* **1982**, *54*, 1558-1563.
- (11) *Dionex Product Selection Guide*; Dionex: Sunnyvale, 1997.
- (12) Knox, J. H. *J. Chromatogr. A* **2002**, *960*, 7-18.
- (13) Kirkland, J. J.; Yau, W. W.; Stoklosa, H. J.; Dilks Jr., C. H. *J. Chromatogr. Sci.* **1977**, *15*, 303-316.

- (14) Yan, B.; Zhao, J.; Brown, J. S.; Blackwell, J.; Carr, P. W. *Anal. Chem.* **2000**, *72*, 1253-1262.
- (15) Taylor, G. I. *Proc. Roy. Soc. (London)* **1953**, *A219*, 186-203.
- (16) Aris, R. *Proc. Roy. Soc. (London)* **1965**, *A235*, 67-77.
- (17) Atwood, J. G.; Golay, M. J. E. *J. Chromatogr.* **1981**, *218*, 97-122.
- (18) Tijssen, R. *Sep. Sci. Technol.* **1978**, *13*, 681-722.
- (19) Thompson, J. D.; Carr, P. W. *Anal. Chem.* **2002**, *74*, 4150-4159.
- (20) Haddad, P. R.; Jackson, P. E. *Ion Chromatography: Principles and Applications*; Elsevier: New York, 1990.
- (21) *Application Note 133*; Dionex Corporation: Sunnyvale, 1999.
- (22) Lu, W.; Cassidy, R. M. *Anal. Chem.* **1993**, *65*, 1649-1653.
- (23) Midgley, D.; Parker, R. L. *Talanta* **1989**, *36*, 1277-1283.



## CHAPTER SEVEN. Conclusions and Future Work

### 7.1 Conclusions

This thesis explored two approaches for reducing analysis time in IC: high-temperature high-speed separations, and the use of monolithic separation media. It was found that high-speed IC is most easily and most effectively accomplished with monolithic columns. This approach resulted in the separation of anions in less than one minute with detection limits in the ppb range. On the other hand, the maximum separation speed achievable in high-temperature separations was restricted by the thermal instability of PEEK column materials and selectivity changes at elevated temperatures that result in a loss of resolution. Consequently, only modest improvements (35%) in analysis time were obtained with high-temperature IC.

Regardless of which approach is used, careful control of band broadening was found to be imperative to the realization of high-speed separations. Firstly, highly efficient columns are needed that are able to maintain efficiency at flow rates well past the optimum in the van Deemter curve. Secondly, and just as important, was the need to minimize extra-column band broadening, *e.g.*, from splitters, detector response time and connecting tubing, which becomes significant at high flow rates. However, this thesis also showed that the effect of connecting tubing is not as severe as it is often thought to be when employing the flow rates typically used in high-speed HPLC.

Although elevated temperature was not as promising as monolithic columns for achieving high-speed separations, it had an effect on the selectivity of IC separations. This thesis showed that elevated temperatures cause retention to increase, decrease or even stay the same depending on the analyte, stationary phase and eluent. However,

selectivity changes were limited to analytes belonging to different groups of temperature behaviour. Consequently, elevated temperatures did not affect the selectivity between analytes in the same group. Therefore, column temperature can be an effective variable to alter IC selectivity in selected cases.

## 7.2 Future Work

### 7.2.1 Ultra-Fast Anion Separations with Polymeric Monoliths

The suitability of monolithic separation media for high-speed IC was shown in Chapters Five and Six. However, the major drawback of the approach for high-speed IC outlined in this thesis is the requirement to periodically coat columns and the use of silica monoliths. Silica has limited pH stability ( $\text{pH} < 7.5$ ) and as such cannot be used with the eluents that are typically used in suppressed IC (*e.g.*, carbonate and hydroxide).

In recent years, there has been a considerable amount of work on the synthesis of polymeric monoliths for use in conventional liquid chromatography, micro-LC and capillary electrochromatography.<sup>1-5</sup> These monoliths have been successfully used for high-speed separations of neutral molecules and proteins. In particular, polystyrene-divinylbenzene monoliths exhibit higher rigidity than most polymer monoliths.<sup>3, 5</sup> Further, the pore size is readily controlled so that columns can be tailored to have the desired permeability while having adequate surface area for retention.<sup>1-3, 5</sup> However, for the purposes of this work, a non-mesoporous monolith will be prepared so that it is compatible with the latex-agglomeration procedure described below.

A polystyrene-divinylbenzene monolith should be prepared inside a PEEK column blank (0.5 – 1.5 mm i.d.). The 0.5 – 1.5 mm i.d. column format will allow fast

separations to be achieved with flow rates on the order of 0.5 – 2 mL/min. This would reduce solvent consumption and dramatically lower the cost per analysis compared to a 4.6 mm i.d. column. The monolith can be sulfonated by flowing fuming sulfuric acid through the capillary.<sup>6</sup> This treatment creates sulfonate groups on the surface of the monolith, *i.e.*, a cation exchanger. The capillary should then be flushed with a suspension of 75 nm Dionex anion-exchange latex particles (*i.e.*, the same particles used in the Dionex Ion Pac columns). These positively charged particles will agglomerate onto the negative surface of the monolith leaving it ready for anion-exchange chromatography. Further, agglomerated stationary phases are extremely stable, *i.e.*, no appreciable loss of the latex will occur over time. Breadmore *et al.* have established the feasibility of the agglomeration process in the case of open-tubular ion-exchange capillary electrochromatography.<sup>7</sup>

The advantage of agglomerating ion chromatographic latex particles onto polymeric monoliths is that ultra-fast separations will be possible with the same stationary phase chemistry and eluents used presently for ion analysis. Control of capacity, selectivity and retention is built in to the latex particles. Further, a monolith coated with this latex would not exhibit significant problems with micropores in the polymeric support<sup>8-10</sup>. In essence, a pellicular monolith is prepared in the same manner as Dionex has for over twenty years. Direct functionalization of the polymer backbone, however would not eliminate the problem of micropores. Even if the efficiency of the polymeric monolith is insufficient for complex separations, the following idea will make use of the monolith.

### 7.2.2 Ultra-Fast Sample Preconcentration

The most popular means of performing preconcentration in IC is to use a precolumn designed to retain trace level analytes from a large volume (50 mL) of sample.<sup>11</sup> This enables performing routine analysis for ions at ppb to ppt levels. For preconcentration, an accurately known volume of sample is passed through a small ion exchange column (*e.g.* 2 x 15 mm) using a syringe or a sample pump. A suitable stationary phase is chosen that will retain analyte ions but will not retain matrix components. For example, an ion exchanger can be used to separate ionic analytes from neutral matrix components. A valve then switches the concentrator column in-line with the separation column and the analyte is eluted off the preconcentrator and onto the analytical column by the eluent.

Unfortunately, this process requires as much or even more time than the separation since the loading of sample onto the preconcentrator is done at low flow rates (< 3mL/min) so as not to exceed the pressure limitation of the preconcentration equipment (approximately 300 psi) (column and/or pump). Therefore, for analyses that require sample preconcentration, it is the preconcentration step that limits high sample throughput and not the separation. Clearly, this is an area where monoliths possess a distinct advantage. The high permeability of monoliths can be exploited to preconcentrate samples at very high flow rates (10 mL/min) with only modest pressure drops.

A DDAB-coated column can be used as a preconcentrator column for anion exchange. One concern in making a preconcentrator column is that its capacity is smaller than the capacity of the analytical column. Otherwise a strong eluent will be needed to

elute analytes off the preconcentrator, which will result in insufficient retention on the analytical column. As was demonstrated in Chapter Six, the capacity of DDAB coated monoliths can be easily moderated through the acetonitrile that is present in the coating solution. Further, these columns are stable for up to 6 hours of use at flow rates as high as 10 mL/min. Alternatively, a polymeric monolith can be prepared as outlined in Section 7.2.1.

### **7.2.3 Improved Implementation of Elevated Temperature for Selectivity Control in Anion Exchange**

Chapter Two showed that the use of elevated temperature for selectivity control in anion exchange is limited by the thermal instability of quaternary ammonium sites. Elevated temperatures cause the degradation of the site to a tertiary amine and an alcohol, resulting in a loss of strong base capacity. However, tertiary amines are thermally stable and would not degrade at elevated temperatures.

The utility of elevated temperature to control the selectivity of separations performed with tertiary amine (*i.e.*, weak base) anion exchangers in IC can be evaluated. Tertiary amine anion exchangers are commercially available from Alltech (Deerfield, IL, USA)<sup>12</sup>. Temperatures as high as 90 °C can be examined and the resulting selectivity changes studied as was done in Chapter Two. Temperature will affect the capacity of the stationary phase through changes in the  $pK_a$  of the tertiary amine functional groups. The  $pK_a$  will decrease, resulting in more protonation and a higher capacity. Provided that the implementation of elevated temperatures with tertiary amine anion exchangers is successful, computer-aided optimization routines can be constructed.<sup>13-15</sup> This would

allow the user to find the optimum temperature and eluent concentration based on a minimal amount of runs (*e.g.*, two runs at extremes of eluent concentration and two runs at extremes of temperature). However, one disadvantage of using tertiary amine anion exchangers is that they are incompatible with suppressed conductivity detection. The amines in these stationary phases have a pKa around 9, which means that useful anion exchange capacities would be obtained at a pH of less than 8.5. Therefore, these stationary phases would be restricted to non-suppressed conductivity detection.

One way to circumvent this problem is to prepare a tertiary amine anion exchanger with an incredibly large amount of tertiary amine sites (*e.g.*, meq/column instead of the more usual  $\mu\text{eq/column}$ ). Even if an anion exchanger such as this is operated at a pH greater than 10, considerable anion exchange capacity is still obtained, due to the large amount of partially ionized anion exchange sites. Therefore, suppressed conductivity detection with carbonate eluents could be employed. The principle behind this idea is exploited in the Dionex CS12A cation exchanger used in Chapters Three and Four.<sup>16</sup> The CS12A (2.8 meq/column capacity) is a carboxylated cation exchanger operated at pH 1.5. At this pH, the vast majority of carboxylate groups (pKa  $\Psi$  4) are protonated, however excellent separations of cations are still obtained.

#### **7.2.4 High Efficiency and Mass Spectrometric Compatible Separation of Amines**

A possible extension of the work presented in Chapter Three would be to examine the separation of pharmaceuticals containing amine functionality. Currently, the most popular method for separating pharmaceuticals is RPLC.<sup>17</sup> This method is limited to relatively non-polar pharmaceuticals. However charged species can be separated with an ion-interaction reagent in the mobile phase (Chapter Five). Unfortunately, ion-interaction

reagents are not compatible with electrospray ionization mass spectrometric detection (ESI-MS), which is the most popular mode of detection in the drug discovery process. Buffer salts/surfactants lead to suppression of the analyte signal in ESI.

A polymeric cation exchanger operated at elevated temperature would offer a number of advantages over RPLC. Firstly, polymeric cation exchangers exhibit mixed-mode retention, *i.e.*, reversed phase and cation exchange interactions (Chapter Three). Mixed mode retention offers the possibility of separating compounds based on hydrophobic and cationic character. This would allow the separation of more complex samples. Each mode of retention can be moderated independently of the other. Hydrophobic interactions would be controlled through the addition of an organic modifier (*e.g.*, acetonitrile) and cation exchange interactions would be controlled through the concentration of competing ion (*e.g.*, hydronium ion). Elevated temperature can be used as an additional variable to moderate both cation exchange and hydrophobic interactions. Further, by operating the stationary phase at elevated temperature, the inherently low efficiency of polymeric stationary phases<sup>8-10</sup> will be partially offset. Preliminary results revealed improvements in efficiency of more than 50% for aromatic amines at 60 °C compared to room temperature.

This technique would be compatible with mass spectrometric detection since buffer salts/surfactants are not present in the mobile phase. Compatibility can be further enhanced through the addition of a suppressor before the mass spectrometer to convert the acidic eluent into water.

### 7.3 Future Directions

IC is considered to be a mature technique, and really the whole field of HPLC is coming of age. However, this does not mean that IC will become obsolete. The truth of the matter is that few techniques can compete with IC in terms of reproducible and dependable analysis of ions in a wide range of “nasty” matrices, *e.g.*, caustics, high salt concentrations, and disproportionate concentration ratios of ions. Thus, IC will be around for quite some time.

There remain a number of areas where significant contributions can be made to IC. These advances can potentially redefine the technique and push it into a new era. The introduction of this thesis mentioned that IC is most widely used for the separation of the seven common anions. It should strike the reader that this is a very narrow area of specialization for a technique as powerful and refined as IC. Ions exist in many forms (*e.g.*, proteins, carbohydrates, pharmaceuticals, to name a few), but yet IC has found widespread use for only inorganic ions. Why not analyze other ions by IC? Why not “analyze ions as ions”? This is a phrase coined at the 2001 International Ion Chromatography Symposium. The reasoning behind it is to exploit the ionic character of analytes along with their hydrophobicity/hydrophilicity to achieve better separations. Currently, pharmaceuticals and proteins are most frequently separated by RPLC. Carbohydrates have been routinely analyzed for many years by normal-phase liquid chromatography, *i.e.*, polar stationary phase and non-polar mobile phase. However, IC would offer a second dimension of separation that would be of tremendous use in the separation of complex samples. This is the motivation behind the idea proposed in Section 7.2.4. Therefore, one area where advances will be made in IC is in the



development of new stationary phase chemistry. This will result in stationary phases with selectivity tuned toward the separation of proteins, carbohydrates and pharmaceuticals. Furthermore, the development of methods that exploit the new stationary phases will be required.

The survival of any analytical technique requires that it possess a distinct advantage over any other technique. As was mentioned earlier, the key advantage of IC is its tolerance to real-world samples. IC's main competitor is capillary electrophoresis (CE). Although CE has a very limited ability to analyze real-world ion samples, it has a considerable advantage in terms of speed. In today's world, speed is quickly becoming the most important attribute of any analytical technique. Lab managers are constantly on the lookout at conferences for new techniques that offer improvements in analysis time. Many times they are willing to sacrifice some accuracy and precision for the increased speed. Therefore, if IC is to remain competitive, significant reductions in analysis time, even beyond what was presented in this thesis, will have to be made. The situation is encouraging. Manufacturers are reducing particle sizes and shortening columns, which will lead to decreased analysis times. However, the most significant reductions in analysis time will be made with monolithic columns. Indeed, monolithic columns, in spite of their turbulent beginnings, will be the stationary phase of choice in IC and in HPLC in general. In particular, the key to ultra-fast IC will be the construction of an efficient polymeric monolith. The idea proposed in Section 7.2.1 was aimed toward this goal.

Finally, the one area where IC research (as well as the rest of analytical chemistry) will flourish is in real-time monitoring. This represents the ultimate in

chemical analysis since chemical information on the system of interest is obtained instantaneously. IC is well poised for real-time monitoring in industrial plants. Two IC manufacturers sell instruments for real-time monitoring. Advances in instrumentation will continue to make these instruments even more robust. However, IC manufacturers have not embraced the miniaturization of IC, which would increase the portability of analysis. This is an area ripe for academic research.

In summary, although IC is no longer enjoying the period of intense research and growth that it experienced in the 1980s and early 1990s, there still exist opportunities for research, thus expanding the applicability of IC to new areas.

#### 7.4 References

- (1) Meyer, U.; Svec, F.; Frechet, J. M. J.; Hawker, C. J.; Irgum, K. *Macromolecules* **2000**, *33*, 7769-7775.
- (2) Viklund, C.; Nordstrom, A.; Irgum, K.; Svec, F.; Frechet, J. M. J. *Macromolecules* **2001**, *34*, 4361-4369.
- (3) Wang, Q. C.; Svec, F.; Frechet, J. M. J. *Anal. Chem.* **1993**, *65*, 2243-2248.
- (4) Svec, F.; Frechet, J. M. J. *Anal. Chem.* **1992**, *64*, 820-822.
- (5) Chirica, G. S.; Remcho, V. T. *J. Chromatogr. A* **2001**, *924*, 223-232.
- (6) Helfferich, F. *Ion Exchange*; Dover: Mineola, 1995.
- (7) Breadmore, M. C.; Macka, M.; Avdalovic, N.; Haddad, P. R. *Analyst* **2000**, *125*, 1235-1241.
- (8) Ells, B.; Wang, Y.; Cantwell, F. F. *J. Chromatogr. A* **1999**, *835*, 3-18.
- (9) Li, J. Y.; Litwinson, L. M.; Cantwell, F. F. *J. Chromatogr. A* **1996**, *726*, 25-36.

- (10) Li, J. Y.; Cantwell, F. F. *J. Chromatogr. A* **1996**, 726, 37-44.
- (11) Haddad, P. R.; Doble, P.; Macka, M. *J. Chromatogr. A* **1999**, 856, 145-177.
- (12) *Alltech Chromatography Source Book*; Alltech: Deerfield, 2001.
- (13) Madden, J. E.; Haddad, P. R. *J. Chromatogr. A* **1998**, 829, 65-80.
- (14) Madden, J. E.; Avdalovic, N.; Jackson, P. E.; Haddad, P. R. *J. Chromatogr. A* **1999**, 837, 65-74.
- (15) Madden, J. E.; Haddad, P. R. *J. Chromatogr. A* **1999**, 850, 29-41.
- (16) *1997-1998 Dionex Product Selection Guide*; Dionex: Sunnyvale, 1998.
- (17) Strega, M. A.; Stevenson, S.; Lawrence, S. M. *Anal. Chem.* **2000**, 72, 4629-4633.

**APPENDIX ONE**

This program was written in Matlab by David Gowanlock and subsequently modified by Eric Carpenter. It is used to fit an exponentially modified Gaussian to a chromatographic peak.

```
echo off
```

```
clc
```

```
clear
```

```
Data = ...
```

```
[
```

```
];
```

```
%numberofpoints =70;
```

```
%pause      % Strike any key for plot.
```

```
t = Data(:,1);
```

```
y = Data(:,2);
```

```
% average together data with a common time point (comment added 2002)
```

```
% l = 1;
```

```
% k = 1;
```

```
% while l < length(t)
```

```
%      counter = 1;
```

```

%           while t(l) == t(l+1)
%
%               counter = counter + 1;
%
%               l = l + 1;
%
%               if l >= length(t),break,end
%
%           end
%
%           yave(k) = mean(y((l-counter+1):l));
%
%           tave(k) = t(l);
%
%           l = l + 1;
%
%           k = k + 1;
%
% end

% [M0,M1,M2,M3] = moments([0 1 2 3 4 5 6 7 8 9 10], [1 1 1 1 1 1 1 1 1 1 1])

yave = y; % added for testing

tave = t;

[Ymax,indexYmax] = max(y);           % find maximum in y
[Ymin1,indexYmin1] = min(y(1:indexYmax)); % find minimum to left of max
[Ymin2,index] = min(y(indexYmax:length(y))); % find minimum to right of max
indexYmin2 = index + indexYmax - 1; % adjust right min to whole data set index

[M0,M1,M2,M3] = moments(tave,yave); % compute moments

```

```

M0 = M0                                % print area

M1 = M1                                % print centre of gravity time

retenttime_exp = (M3 ./ 2) .^ 0.3333

retenttime_gaus = M1 - retenttime_exp

variance_exp = retenttime_exp .^ 2

variance_gaus = M2 - variance_exp

global FitData_t FitData_y            % declare some global variables

FitData_t = t;

FitData_y = y;

axis([t(1) t(length(t)) 0 (Ymax .* 1.05)]); % draw a plot

plot(t,y,FitData_t,FitData_y,'o');

lam = [retenttime_gaus retenttime_exp (variance_gaus .^ 0.5) Ymax]';

% repeat calls to fitmy() to obtain a minimum value

lam = fminsearch ('fitmycurve', lam, [], FitData_t, FitData_y);

lin_scaling_factor = lam(4);          % testing

```

```

mintime = min(t);                % get limits on dataset

maxtime = max(t);

miny = 0;

maxy = max(y);

t_curvefit = t;

y_curvefit = lam(4) .* (exp(lam(3).^2 ./ (2 .* lam(2).^2)) .* exp((lam(1) - t) ...
    ./ lam(2)) ./ (2 .* lam(2)) .* ...
    (1 + erf((t-lam(1)-lam(3).^2 ./ lam(2)) ./ (sqrt(2) .* lam(3)))));

axis([0 (maxtime .* 1.1) miny (maxy .* 1.05)]); % plot the result

plot(t,y,'--',t_curvefit,y_curvefit,'-');

xlabel('Time [minutes]');

ylabel('Counts');

text(.65,.8,'numeric','sc')

text(.8,.8,'fit','sc')

text(.5,.7,'gaus tr','sc')

text(.5,.65,'gs sd.dv.','sc')

text(.5,.6,'exp tr','sc')

text(.65,.7,num2str(retenttime_gaus),'sc')

text(.65,.65,num2str(variance_gaus.^0.5),'sc')

text(.65,.6,num2str(retenttime_exp),'sc')

text(.8,.7,num2str(lam(1)),'sc')

```

```
text(.8,.65,num2str(lam(3)),'sc')  
text(.8,.6,num2str(lam(2)),'sc')  
text(.75,.5,num2str(lin_scaling_factor),'sc')  
text(.55,.5,'linear scaling','sc')  
z = [t_curvefit; y_curvefit].';  
save data.txt z -ascii -tabs;
```